

1 **Geological deformations in the Pannonian Basin during the neotectonic phase: new**  
2 **insights from the latest regional mapping in Hungary**

3 Balázs Koroknai<sup>a\*</sup>, Géza Wórum<sup>a</sup>, Tamás Tóth<sup>a</sup>, Zsuzsa Koroknai<sup>a</sup>, Viktória Fekete-Németh<sup>a</sup>,  
4 Gábor Kovács<sup>a,b</sup>,

5 <sup>a</sup>: Geomega Ltd., Zsil. u. 1, 1093 Budapest, Hungary

6 <sup>b</sup>: Eötvös Loránd University - Savaria University Centre, Department of Geography, Károlyi  
7 Gáspár tér 4., 9700 Szombathely, Hungary

8 \* : Corresponding author: koroknai@geomega.hu

9 E-mail: worg@geomega.hu, info@geomega.hu, zsuzsa.koroknai@geomega.hu,  
10 viktorianemeth@geomega.hu, g@geomega.hu

11 ***Abstract***

12 The present paper introduces the new 1:500 000 scale map of young geological deformations  
13 in Hungary, including all important deformation structures (faults and folds) related to the  
14 neotectonic evolutionary phase (<6–8 Ma) of the Pannonian basin.

15 The new map is based on the interpretation of nearly 2900 2D seismic profiles and 70 3D  
16 seismic volumes, as well as on the critical evaluation of the results of published neotectonic  
17 studies. An important novelty of the map is that not only the near-surface manifestations of the  
18 neotectonic faulting, but also their roots in the underlying pre-Pannonian substratum are  
19 displayed, allowing correlation between various reactivated fault segments of longer fault zones  
20 and aiding the better understanding of the regional structural context.

21 The new map provides a significantly more accurate definition (actual position, extension and  
22 geometry) of the neotectonic structures and provide more details compared to previous regional  
23 studies. The prevailing (E)NE–(W)SW striking neotectonic fault pattern clearly reflects the

24 control of identically oriented pre-Pannonian fault systems during the neotectonic  
25 deformations. Markedly different orientations in the neotectonic structures indicate important  
26 differences in the overall orientation of the underlying fault systems. These observations  
27 demonstrate that neotectonic activity is predominantly due to the reactivation of pre-existing  
28 (predominantly synrift) structures all over the Pannonian basin, as also indicated by previous  
29 studies.

30 Despite experiencing the largest Middle- to Late Miocene extension and the formation of the  
31 deepest depocenters in the whole Pannonian basin, SE Hungary practically lacks any observable  
32 neotectonic activity, which is a striking, but still poorly understood feature.

33 Detailed 3D seismic analysis of fault segment geometries indicates a consistent regional pattern:  
34 sinistral shear along (E)NE–(W)SW oriented, and dextral shear along (W)NW–(E)SE oriented  
35 fault zones, respectively. These observations — together with the E–W trending  
36 contractional/transpressional structures (folds, reverse faults, imbricates) occurring in western  
37 and southern Hungary — indicate a dominantly strike-slip stress regime with a laterally slightly  
38 rotating (from N–S to NNE–SSW) maximum horizontal stress axis ( $\sigma_1$ ) during the neotectonic  
39 phase. Lateral displacement along major root zones amounts to a maximum of 2–3km during  
40 the neotectonic phase.

41 Keywords: neotectonic phase, Hungary, Pannonian basin, seismic interpretation, faults, folds

## 42 ***1. Introduction***

43 The first GIS-based, regional neotectonic map of Hungary was published almost 15 years ago  
44 (Horváth et al., 2006a), and can be considered as a pioneering scientific achievement in the  
45 region. It was mainly based on the compilation, re-evaluation and correlation of structural

46 elements depicted on numerous published and unpublished maps (e.g., Horváth and Tari,  
47 unpubl.; Pogácsás et al., 1989; Csontos, 1995; Csontos and Nagymarosy, 1998; Wórum,  
48 unpubl.; Tóth and Horváth, 1997; Detzky Lőrincz et al., 2002; Síkhegyi, 2002, Bada et al.,  
49 2003a-b, 2006; Wórum and Hámori, unpubl.; Fodor et al., 2005a-b; Windhoffer et al., 2005).  
50 However, due to the applied scale and the limited use of seismic data this new initiative  
51 basically remained a large-scale, partly model-driven overview of the most important  
52 neotectonic structures in the Pannonian basin.

53 Later on several modified versions of this map was published (Horváth et al., 2009, Bada et al.,  
54 2007, 2010), but the concept of the map itself did not change. Apart from these maps only one  
55 regional neotectonic overview was published (Fodor et al., 1999) based on modern, although  
56 restricted amount of data.

57 Despite the numerous published, local-scale neotectonic studies (for details see Section 3.) a  
58 main deficiency of the former neotectonic research activity in Hungary was the lack of  
59 integrated databases used for the neotectonic evaluation (including extensive sets of seismic  
60 surveys) and their systematic tectonic interpretation according to a uniform methodology. The  
61 main goal of this work was to construct a completely new, detailed map of young geological  
62 deformations in Hungary considering (i) as large as possible set of 2D and 3D seismic data  
63 interpreted in a systematic and consistent manner, and structurally correlated using trends  
64 emerging from interpreted seismic time horizon and geophysical maps; (ii) the results of all  
65 previous relevant neotectonic studies based both on surface and subsurface data.

66 The resulting new map (available at <http://dx.doi.org/10.17632/dnjt9cmj87.1> and  
67 [www.geomega.hu](http://www.geomega.hu)) is significantly more detailed (1:500 000) than any of its countrywide  
68 precursors and opens up a whole range of utilization purposes ranging from (neo)tectonic and  
69 geodynamic syntheses, regional- or local scale modelling studies, through strategic  
70 infrastructure developments and construction works, to the assessment of seismotectonic risks.

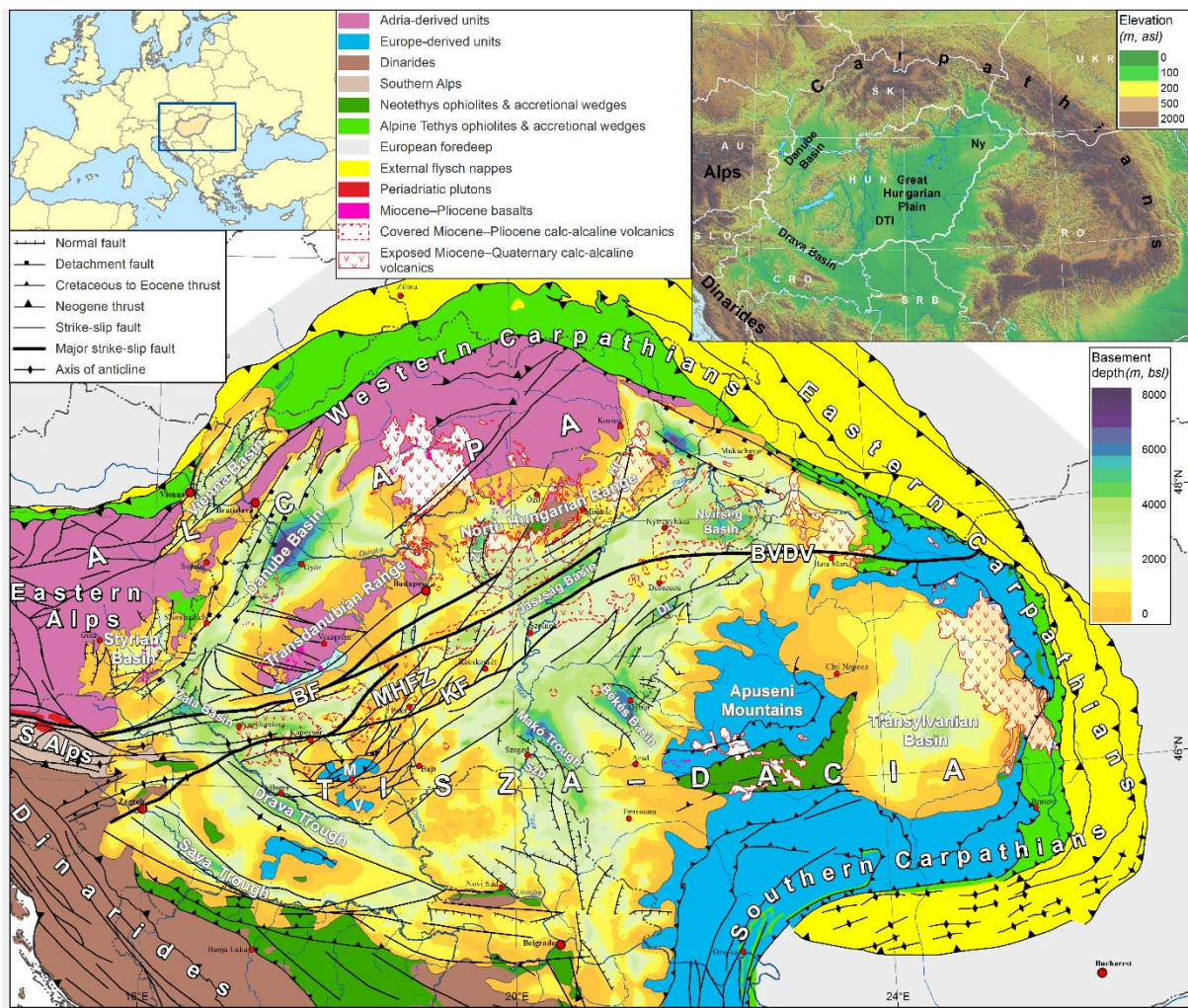
71 The main objective of this paper is to present and discuss the most important results of the new  
72 map, following the introduction of the geological background, the integrated geological-  
73 geophysical database, the key structural elements appearing on the map and the principles of  
74 the map construction.

## 75 ***2. Geological setting***

76 The Pannonian basin surrounded by the Alpine, Carpathian and Dinaric mountain chains in  
77 Central Europe (*Fig. 1*) forms a classical back-arc basin of Miocene age (Royden, 1988) within  
78 the Alpine orogenic system. The basin floor in the Hungarian part of the basin is constituted by  
79 two Alpine orogenic megaunits (Alcázar and Tisza-Dacia; Balla, 1988; Csontos and Vörös,  
80 2004; Schmid et al., 2008), showing markedly different paleogeographic affinity and geological  
81 evolution during the pre-Cenozoic times (e.g., Kovács et al., 2000; Haas and Péro, 2004 and  
82 references therein). These megaunits were juxtaposed along the Mid-Hungarian Fault Zone  
83 (MHFZ; *Fig. 1*) preceding the Miocene basin formation (Balla, 1984, 1988; Kázmér and  
84 Kovács, 1985; Csontos et al., 1992; Tari, unpubl.; Csontos and Nagymarosy, 1998; Fodor et  
85 al., 1998, 1999; Györfi et al., 1999; Tischler et al., 2007; Fodor, unpubl.).

86 In the Hungarian part, basin formation started in the Early Miocene, approximately 21 Ma ago  
87 (Horváth, 1993; Horváth et al., 2015, 2019). During the peak period of extension in the Early  
88 and Middle Miocene (the synrift phase of Royden et al., 1983) the main structural frame of the  
89 basin was established, characterized by normal and associated strike-slip faulting. Rifting took  
90 place diachronously across the basin culminating in the Early to Middle Miocene in the western  
91 and central and in the early Late Miocene in the eastern subbasins, respectively (Matenco and  
92 Radivojevic, 2012; ter Borgh et al., 2013; Balázs, et al. 2016). The continental depositional  
93 environment of the early stage (ca. 21–17 Ma, i.e., Eggenburgian–Ottományian) changed to  
94 marine conditions from the Karpatian on due to the transgression of Central Paratethys (for a  
95 detailed overview see Horváth et al., 2015, 2018). This first period of basin evolution was also

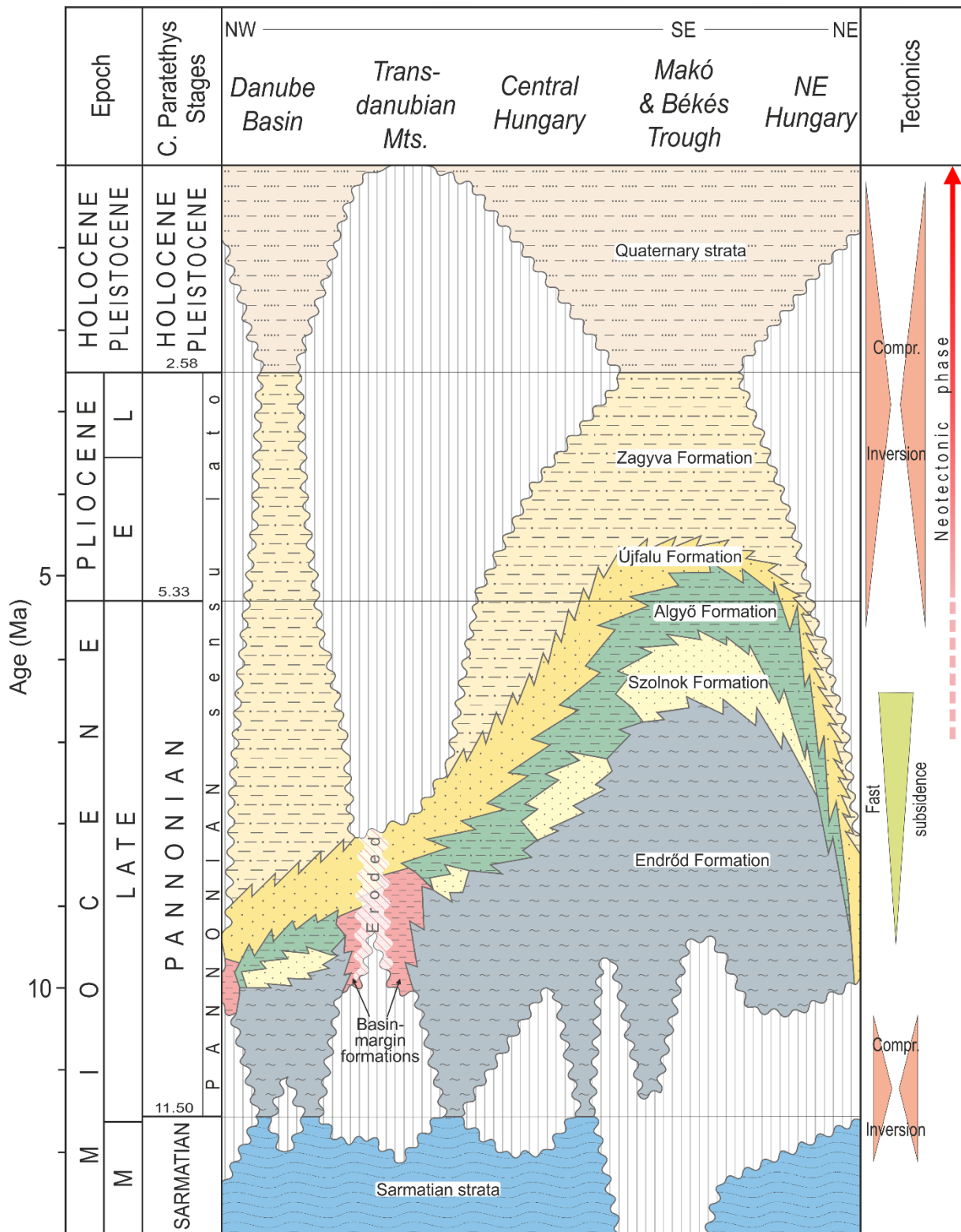
96 accompanied by a widespread silicic and subsequent calc-alkaline magmatic activity (Pécskay  
 97 et al., 2006; Harangi and Lenkey, 2007; Lukács et al., 2018; Fig. 1).



98  
 99 *Fig. 1. Simplified overview of basement units and basin morphology in the Pannonian Basin*  
 100 *and its surroundings with major tectonic units/elements and depth of the pre-Neogene*  
 101 *basement (compiled after Horváth et al., 2018 and Schmid et al., 2008). Inset map shows the*  
 102 *digital elevation model (DEM). Abbreviations: BF: Balaton fault, KF: Kapos fault, MHFZ:*  
 103 *Mid-Hungarian Fault Zone, BVDV: Bogdan Voda - Dragos Voda fault; M, V: Mecsek and*  
 104 *Villány Mts., Dt: Derecske trough, Szb: Szeged basin, Zt: Zagyva trough, Ht: Hernád trough;*  
 105 *DTI: Danube-Tisza interfluve, Ny: Nyírség*

106 From the Late Miocene on the basin became isolated due to the uplift of the surrounding  
 107 mountains as well as to the sea-level fluctuations of Paratethys (ter Borgh et al., 2013). Rifting

108 continued in the eastern subbasins in the early Late Miocene (Balázs, et al. 2016), whereas a  
109 basinwide regional thermal subsidence also occurred representing the so called post-rift phase  
110 of Horváth and Royden (1981). During the Late Miocene–Pliocene a long-lived, brackish-water  
111 lake was developed (Magyar et al., 1999) that was progressively filled up by the deposits of the  
112 Lake Pannon megasequence (Horváth et al., 2015, 2018). The boundary between the Lake  
113 Pannon megasequence and the underlying Central Paratethys megasequence is marked —  
114 except for several Transdanubian deep basins with continuous sedimentation — by a regional  
115 unconformity (*Fig. 2*) reflecting the late Middle Miocene (Sarmatian) uplift. This early  
116 inversion phase was coeval with the main collision in the East Carpathians (Horváth, 1995).  
117 The individual elements of the Lake Pannon megasequence (*Fig. 2*), playing a fundamental role  
118 in neotectonic investigations, are discussed in details by many previous lito-, bio-, and  
119 chronostratigraphic studies having paleogeographic implications (e.g., Bérczi, 1988; Juhász,  
120 1991, 1992; Magyar, 2010; Magyar et al., 1999, 2013, 2019; Sztanó et al., 2013a-b, 2016). The  
121 lithostratigraphic units displayed in Figure 2 are by definition diachronous, as the basin was  
122 gradually filled from the northwest and northeast. This process was associated with the  
123 formation of a regional shelf-margin slope system prograding, in general, to the south-southeast  
124 in the Hungarian part of the basin between ca. 10 and 5 Ma. The total thickness of the post-rift  
125 sequence together with the Quaternary strata is strongly varying: it might reach up to 6-7 km in  
126 the deepest subbasins, whereas 1–3 km thickness occurs in areas characterized by weak to  
127 moderate post-rift subsidence (*Fig. 1*).



128

129 *Fig. 2. Simplified stratigraphic overview of the post-rift basin fill (compiled after Sztanó et*  
 130 *al., 2013a-b, 2016; Balázs et al., 2018)*

131 During the most recent tectonic evolutionary stage of the basin — referred to as neotectonic  
 132 phase (Fig. 2) — inversion commenced (Tari, unpubl.; Horváth, 1995; Bada et al., 1999; Gerner

133 et al., 1999), as the prevailing tensional/transensional stress regime changed to compression  
134 (Horváth and Cloetingh, 1996; Fodor et al., 1999, 2005a; Csontos et al., 2002; Bada et al.,  
135 2007). The primary driving force of this change was, beside additional intraplate forces, the  
136 continuous northward indentation of the Adriatic microplate (“Adria-push”; Bada et al., 2007)  
137 and the consumption of subductible lithosphere along the East Carpathian arc (Horváth et al.,  
138 2015). Inversion took place diachronously across the basin: the first structures attributed to the  
139 neotectonic inversion were formed at ca. 8 Ma in SW Hungary (Zala subbasin; Uhrin et al.,  
140 2009), whereas initiation of neotectonic activity was definitely younger in the central (at ca. 4  
141 Ma) and eastern part of the basin (Tari, unpubl.; Horváth, 1995; Fodor et al., 2005a-b;  
142 Ruzsáczay-Rüdiger et al 2007; Balázs et al., 2016, 2018).

143 On a regional scale, inversion was manifested in important differential vertical movements (i.e.,  
144 subsidence of deep depocenters in the central part and uplift on the basin flanks, respectively;  
145 Rónai, 1974, 1987) interpreted as the results of large-scale folding of the lithosphere related to  
146 increased magnitude of intraplate stresses (Horváth and Cloetingh, 1996). Regional-scale  
147 folding with a wavelength being in the range of hundreds of kilometers was associated with  
148 brittle faulting in the shallow crust and intense erosion in the uplifting regions. Moreover, the  
149 basin was also interpreted as an example of irregular lithospheric folding (Cloetingh et al.,  
150 1999) with varying wavelengths being in the range from few to hundreds of kilometers. Results  
151 of analogue modelling focusing on the effect of crustal thickness variations supported this  
152 interpretation (Dombrádi et al., 2010).

153 On a local scale these processes were coupled with significant near surface deformations  
154 manifested in faulting and folding of the Lake Pannon megasequence. These deformations of  
155 tectonic origin were coexisting with faults and folds initiated by sedimentary (mainly  
156 compaction) processes, which together form the subject of the present study. In general,  
157 prominent contractional structures were formed in the southwest near the Adriatic microplate



158 boundary, whereas strike-slip deformation was dominant elsewhere (e.g., Fodor et al., 2005a,b;  
159 Bada et al., 2006, 2007; Horváth et al., 2006a, 2009). These deformations affected the  
160 uppermost post-rift sediments (i.e., Zagyva/Újfalu Formations), and in some cases the overlying  
161 Quaternary strata as well (e.g., Pogácsás et al., 1989; Detzky Lőrincz 1997; Tóth and Horváth,  
162 1997; Detzky Lőrincz et al., 2002; Magyari et al., 2005; Budai et al., 2008; Horváth et al., 2019).

### 163 ***3. Geological and geophysical database***

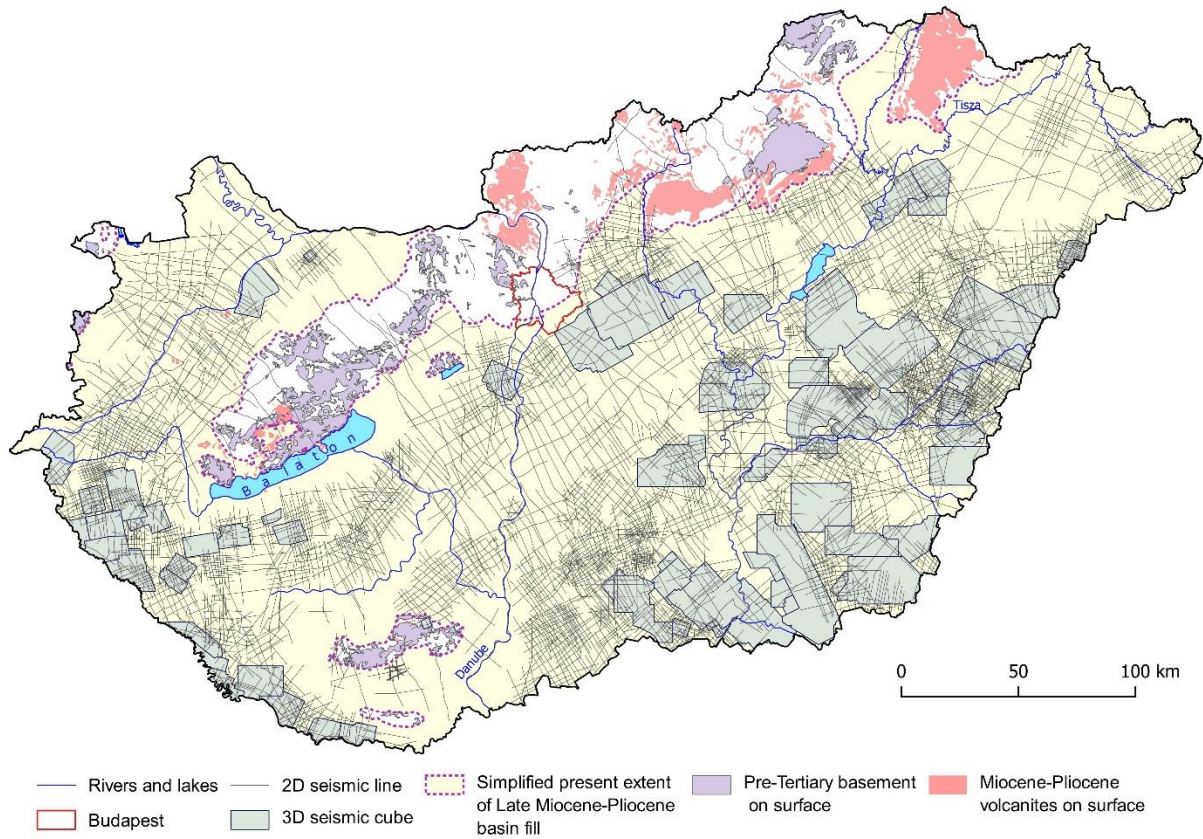
164 The integrated database used for the project has two major constituents: an extensive seismic  
165 dataset (*Fig. 3*) and a large set of surface/subsurface-geological and tectonic maps summarizing  
166 the results of various (neo)tectonic studies as well as regional geological-geophysical  
167 overviews.

168 The seismic database of the project includes nearly 2900 2D seismic profiles and 70 3D seismic  
169 volumes from the seismic database of Geomega Ltd. in digital SEG-Y format. The 2D seismic  
170 dataset contain not only land, but also multichannel and ultrahigh resolution single channel  
171 water seismic data excellently imaging the shallow subsurface making them ideal for  
172 neotectonic investigations.

173 Modern 3D seismic data volumes allowing for a particularly reliable identification and  
174 correlation of neotectonic features are mostly available in the (south)eastern and southwestern  
175 part of the country (*Fig. 3*). Coherency volumes were calculated for all 3D seismic data volumes  
176 integrated into the project, and coherency time slices were subsequently used as the primary  
177 tool for identification and correlation of neotectonic faults (See also Section 5.1.).

178 Altogether, the available seismic dataset integrated into the project ensures — except for the  
179 mountainous areas in Transdanubia and northern Hungary (*Figs. 1, 3*) — an overall good to  
180 excellent coverage in the country providing a stable basis for the identification and correlation  
181 of neotectonic structures. In the mountainous areas the low seismic coverage was only one  
182 obstacle for the mapping of neotectonic deformations, since due to the general lack of young

183 sedimentary cover the seismic imaging is rather poor. This necessitated the extensive use of  
 184 published neotectonic studies in these areas based on surface geological, geomorphological or  
 185 even remote sensing techniques.



186

187 *Fig. 3. Overview of the 2D and 3D seismic datasets integrated into the project*

188 The other main constituent of the integrated database is represented by a series of georeferenced  
 189 geological and geophysical maps aiding both the mapping of neotectonic deformations and the  
 190 final map construction. These data include published regional neotectonic maps (Fodor et al.,  
 191 1999; Horváth et al., 2006a; Horváth et al., 2009), numerous local-scale tectonic maps of  
 192 neotectonic relevance (Pogácsás et al., 1989; Cserny and Corrada, 1990; Fodor et al., 1994,  
 193 2005a-b, 2013; Csontos, 1995; Detzky Lőrincz 1997; Dudko, 1997; Tóth and Horváth, 1997;  
 194 Horváth et al., unpubl., 2019; Csontos and Nagymarosy, 1998; Halouzka et al., 1998; Wórum,  
 195 unpubl.; Sacchi et al., 1999; Detzky Lőrincz et al., 2002; Korpás et al., 2002; Kováč et al., 2002;  
 196 Lopes Cardozo et al., 2002; Sikhegyi, 2002, unpubl.; Bada et al., 2003a-b, 2006, 2010; Wórum

197 and Hámori, unpubl.; Csontos et al., 2005; Magyarai et al., 2005; Windhoffer et al., 2005; Juhász  
198 et al., 2007, 2013; Nádor et al., 2007; Ruzkiczay-Rüdiger et al., 2007, 2020; Budai et al., 2008;  
199 Székely et al., 2009; Bada et al., 2010; Konrád and Sebe, 2010; Bodor, unpubl.; Dudás, unpubl.;  
200 Nádor and Sztanó, 2011; Várkonyi, unpubl.; Várkonyi et al., 2013; Kovács et al., 2015;  
201 Visnovitz et al., 2015; Petrik, unpubl.; Loisl et al., 2018) as well as neotectonic reconstructions  
202 relying on remote sensing data (e.g., Czakó and Zelenka, 1981; Brezsnýánszky and Síkhegyi,  
203 1987).

204 These maps were complemented with a set of regional (Fülöp and Dank, 1987; Dank and Fülöp,  
205 1990; Fodor et al., 1999; Fodor, unpubl.; Gyalog and Síkhegyi, 2005; Haas et al., 2010) and  
206 local-scale geological (Némedi Varga, 1977; Hetényi et al., 1982; Matura et al., 1998; Kiss, et  
207 al., 2001; Csontos et al., 2002; Fodor et al., 2005c, 2013; Budai et al., 2008; Palotai and Csontos,  
208 2010; Tari and Horváth, 2010; Zámolyi et al., 2010; Palotai et al., 2012; Palotai, unpubl.; Oláh  
209 et al., 2014; Soós, unpubl.; Petrik et al., 2018; Héja et al., 2018) and geophysical maps (Kiss,  
210 2006; Kiss and Gulyás, 2006), which provided valuable information on (sub)surface geological  
211 relationships and structural trends largely aiding fault correlations and ultimately the final map  
212 construction. Subsurface geological and tectonic maps in publicly available hydrocarbon  
213 exploration reports were also taken into account during the model construction in this project  
214 in order to have an as wide as possible scientific basis of the new regional map.

215 The Bouguer anomaly map of Hungary (Kiss, 2006) was vectorized, and subsequently used not  
216 only as the background image of the new map (applying a different visualization,  
217 <http://dx.doi.org/10.17632/dnjt9cmj87.1>), but also for the construction of a residual Bouguer  
218 anomaly map enabling the recognition of local scale trends/structures.

#### 219 ***4. Structural elements of the new map***

220 The newly compiled map (<http://dx.doi.org/10.17632/dnjt9cmj87.1>) displays all the relevant  
221 young deformation features (both tectonic and atectonic) that were mapped using the project

222 database. The mapped structures include those faults and folds that were developed during the  
223 latest, neotectonic evolutionary phase of the Pannonian Basin (*Fig. 2*, ~ latest 6–8 Ma). From a  
224 practical, seismic interpretation point of view, those faults and folds were considered, which  
225 deform at least the Zagyva (and laterally equivalent) or younger formations (*Fig. 2*). In the  
226 oldest parts of the basin only those structures were mapped, which not only “affect”, but clearly  
227 deform the entire imaged part of the Zagyva/(Újfalu) formation ensuring that the age of the  
228 deformation is younger than the mentioned 6-8 Ma. A more precise temporal definition about  
229 the formation age of these structures cannot be given using the applied method because of the  
230 (i) intense erosion of younger Late Miocene–Pliocene strata in the uplifted parts of the basin,  
231 and (ii) the poorly imaged nature of the seismic sections in the upper 200–500ms. All things  
232 considered, most of the mapped deformations probably occurred in the last 5–6 million years,  
233 locally including deformations during the Quaternary.

234 There are three groups of structural elements displayed on the new map:

- 235 • Fault lines displaying the near surface manifestations (i.e. mapped fault traces) of  
236 faulting affecting the Late Miocene–Pliocene or younger sediments (both tectonic and  
237 atectonic)
- 238 • Neotectonic folds affecting the Late Miocene–Pliocene or younger sediments  
239 excluding folding related exclusively to sedimentary processes such as differential  
240 compaction (e.g. drape-over anticlines)
- 241 • Pre-Pannonian faults with or without near surface neotectonic manifestation that had  
242 any influence on the sedimentation and subsequent (i. e. neotectonic) deformation of  
243 the entire post-rift sequence. These include important syn- and pre-rift faults,  
244 comprising also blind faults that cannot belong to the group of neotectonic faults  
245 defined above, because the young reactivation were not strong enough to cause visible  
246 fault offsets in the Zagyva/(Újfalu) Formation. These faults are essential — regardless

247 of their tectonic activity during the neotectonic phase — in the understanding of the  
248 depicted near surface deformations.

249 Main characteristics, their schematic genetic evolution and important differences between the  
250 mapped structures are summarized in *Fig. 4* and below.

Early Late Miocene	Prior to neotectonic phase (~ Early Pliocene)	Present-day	Key features
			<p><b>Compression-related folds</b></p> <ul style="list-style-type: none"> <li>- Upward constant amplitude of folding</li> <li>- Angular unconformity/truncation of post-rift strata</li> <li>- Formed by compressional tectonic forces</li> </ul>
			<p><b>Differential vertical motion-related folds</b></p> <ul style="list-style-type: none"> <li>- Upward constant amplitude of folding</li> <li>- Angular unconformity/truncation of post-rift strata</li> <li>- Deformation related to tectonic processes</li> <li>- Abrupt upward transition from faulting to folding on the flanks</li> </ul>
			<p><b>Compaction / drape over folds</b></p> <ul style="list-style-type: none"> <li>- Upward decreasing and diminishing amplitude of folding</li> <li>- Deformation is purely compactional</li> <li>- No signs of tectonic processes</li> <li>- Identified, but excluded from regional mapping</li> </ul>
			<p><b>Monoclinical folds</b></p> <ul style="list-style-type: none"> <li>- Drag folding related to reactivation of pre-existing faults</li> <li>- Strongly asymmetric geometry</li> <li>- Blind faulting often recognisable in the lowermost post-rift sequence</li> <li>- Deformation related to tectonic processes</li> </ul>
			<p><b>Neotectonic faults and fault-related folds</b></p> <ul style="list-style-type: none"> <li>- Deformation is clearly related to tectonic reactivation of pre-existing faults</li> <li>- Local folding is related and subparallel to nearby young faults</li> <li>- Root zones of major fault zones also mapped</li> </ul>
			<p><b>Atectonic faults</b></p> <ul style="list-style-type: none"> <li>- Induced by sedimentary processes</li> <li>- Syn-sedimentary compaction faults with upward decreasing offset</li> <li>- Slump-related faults with fault terminations within the post-rift sequence</li> <li>- Simple near-surface geometry</li> </ul>

Fig. 4. Overview of the mapped structures and their schematic genetic evolution

251

252

253

254 *4.1. Faults*

255 According to origin, the brittle deformations (i.e. faulting) identified within the Late Miocene–  
256 Pliocene or younger sediments were classified into three main categories (*Fig. 4*):

- 257 • tectonic faults related to the reactivation of pre-existing faults (i.e. neotectonic faults by  
258 definition)
- 259 • atectonic faults whose formation is not (or only indirectly) associated with pre-existing  
260 fracture systems (e.g. related to atectonic sedimentary processes such as compaction  
261 and slumping).
- 262 • Several fault zones were mapped, where the tectonic or atectonic origin could not be  
263 determined unambiguously, or there exist different views in the literature on their  
264 interpretation. These faults were classified as “faults with uncertain/debated origin”.  
265 They typically occur above basement highs and disappear basinwards along strike (signs  
266 of atectonic origin), but display characteristic flower structure in seismic profiles (sign  
267 of tectonic origin).

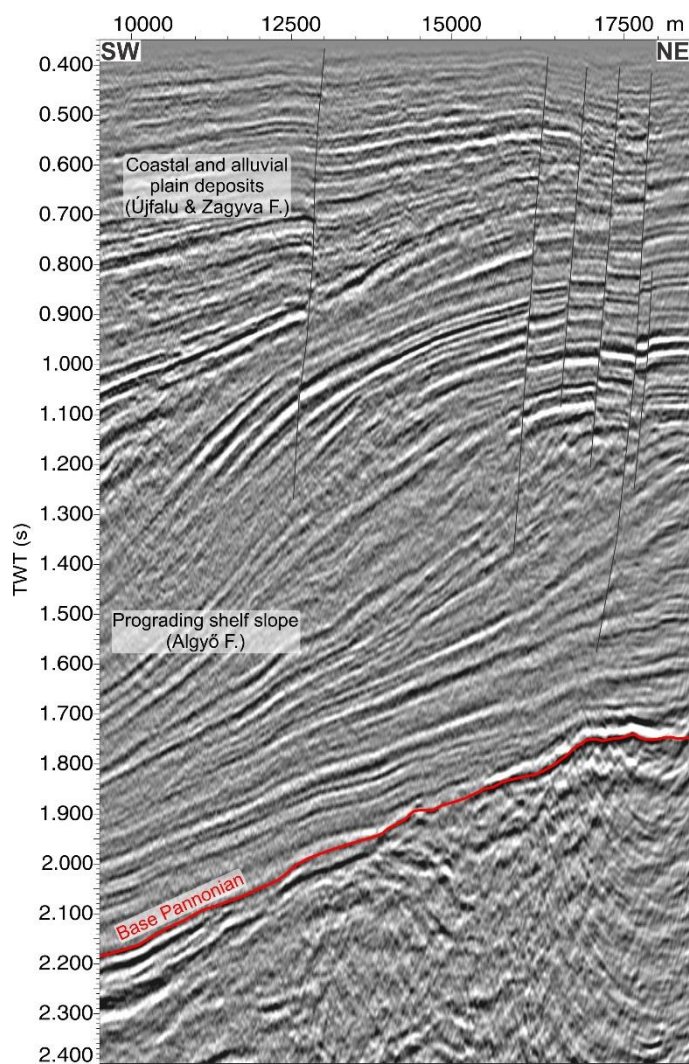
268 Tectonic faults related to the reactivation of pre-existing faults

269 These faults inherit their characteristics from the “parent” fault systems in the basement and  
270 can be considered as “classical” neotectonic faults. In these cases the “parent” fault (i.e., the  
271 primary displacement zone, PDZ) can be often directly identified on the seismic data, and/or  
272 the characteristics of the fault zone developed in the young sedimentary pile are the same as  
273 those of the well-documented tectonic fault reactivations (e.g. flower structures, en-echelon  
274 fault planes connecting to a single root, etc.; *Fig. 4*).

275 Atectonic faults related to compaction or slumping

276 *Faults related to compaction or slumping* are considered as atectonic features (*Fig. 4*) in the  
277 Late Miocene–Pliocene sedimentary pile. Slumping frequently occurred in the unconsolidated  
278 post-rift sedimentary pile of the Pannonian Basin, especially in areas characterized by uneven

279 basement morphology and large thickness variations. *Slump-related faults* are typically  
280 encapsulated into the young sedimentary sequence: they generally start in the upper portion of  
281 the post-rift sequence affecting the Zagyva, Újfalva and Algyő formations, and terminate (or  
282 detach) before reaching the base-Pannonian unconformity (*Fig. 5*). Although such faults do not  
283 have pre-Pannonian roots, they are many times associated with (triggered by?) nearby “real”  
284 neotectonic faults (see faults (in violet) at the Biharkeresztes-Komádi high in the eastern Great  
285 Hungarian Plain, <http://dx.doi.org/10.17632/dnjt9cmj87.1>).



286  
287 *Fig. 5. Example of slump-related faulting above the Komádi basement high (eastern Great*  
288 *Hungarian Plain). Note that all faults terminate within the prograding shelf slope (Algyő F.).*

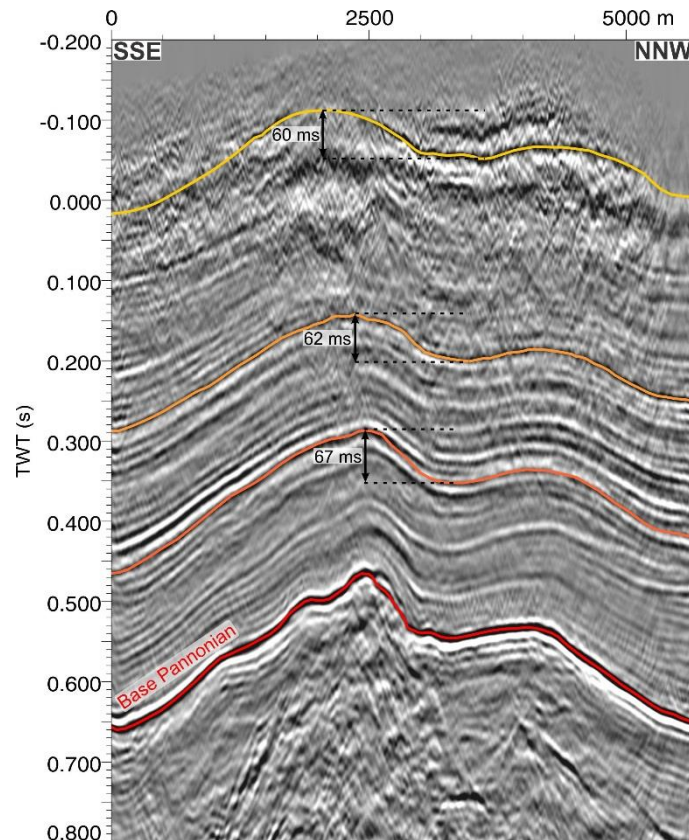
289 *For location see Figure 17b*



290 *Compaction faults* are gravity-driven features formed due to the differential compaction of  
291 young sediments with laterally strongly varying thickness. Compaction faults develop  
292 continuously during sedimentation with increasing overburden (*Fig. 4*) and has similar  
293 characteristics as classical syn-sedimentary normal faults. Compaction faults, considered  
294 previously as “classical” neotectonic faults (e.g., Horváth et al., 2006a, 2009; Nádor et al.,  
295 2007), have been recently described from the eastern part of the Great Hungarian Plain (Balázs  
296 et al., 2016, 2018). Distinction between pure compaction (atectonic) and post-depositional  
297 tectonic faults in the Pannonian Basin is quite challenging occasionally as discussed later (see  
298 Section 6.4.). The faults mapped at the southwestern flank of the Algyő high  
299 (<http://dx.doi.org/10.17632/dnjt9cmj87.1>) are considered as the most typical examples of  
300 compaction faults forming standalone, relatively short features developed above the steep  
301 southwestern flank of the high (see also Balázs et al., 2016).

#### 302 *4.2. Neotectonic folds*

303 The axis of folds within the post-rift sequence displayed on the new map represent synclines  
304 and anticlines formed by tectonic processes. Considering a generally flat sedimentary surface  
305 at all times during the sedimentation, anticlines and synclines developed above the uneven  
306 basement topography by the process of differential compaction were identified by their upward  
307 decreasing (and diminishing) fold amplitudes and were excluded from the mapping (see *Fig.*  
308 *4*). This feature is in contrast with that of (post-sedimentary) tectonic folds, where the fold  
309 amplitude is nearly constant upward within the sequence (i.e. formation occurred after the  
310 deposition of the post-rift sequence, *Fig. 6*).



311

312 *Fig. 6. Example of a tectonic fold developed above the Igal high. Note the upward nearly*  
 313 *constant amplitude of folding of the post-rift strata. Orange and yellow lines indicate*  
 314 *Pannonian marker horizons. For location see Figure 17a*

315 Three groups of neotectonic folds were distinguished considering their origin and geometrical  
 316 properties (*Fig. 4*):

- 317 • Compression related folds
- 318 • Differential vertical motion- and fault-related folds
- 319 • Monoclinial folds

320 Compression-related folds

321 Compression-related folds are those large-scale “classical” folds of structural geology, which  
 322 were formed by far-field compressional lithospheric stresses. As a result, the orientation of  
 323 these (sets of) folds are parallel to each other and perpendicular to the maximum horizontal

324 stress direction. Such folds occur in western and southwestern Hungary (see Sections 6.2. and  
325 6.3.; <http://dx.doi.org/10.17632/dnjt9cmj87.1>).

### 326 Differential vertical motion- and fault-related folds

327 These folds do not reflect directly the effect of the regional, far-field tectonic stresses, but rather  
328 their formation was constrained by nearby neotectonic faulting (i.e. rollover anticlines) or the  
329 orientation of the underlying tectonic fabric, such as basement blocks and pre-existing faults.  
330 Two types of folds were distinguished within this group.

331 *Differential vertical motion-related folds* are associated with large scale regional flexures or  
332 connected to the differential vertical movements of crustal segments, and generally show a close  
333 correlation with basement topography (*Fig. 4*). This relationship can be quite different in case  
334 of some compression-related folds as illustrated by the Lovászi anticline, which was formed  
335 above an inverted graben structure in the Zala basin. Forced folds developed above the footwall  
336 of major reactivated normal faults characterized by abrupt upward transition from faulting to  
337 folding represent typical examples.

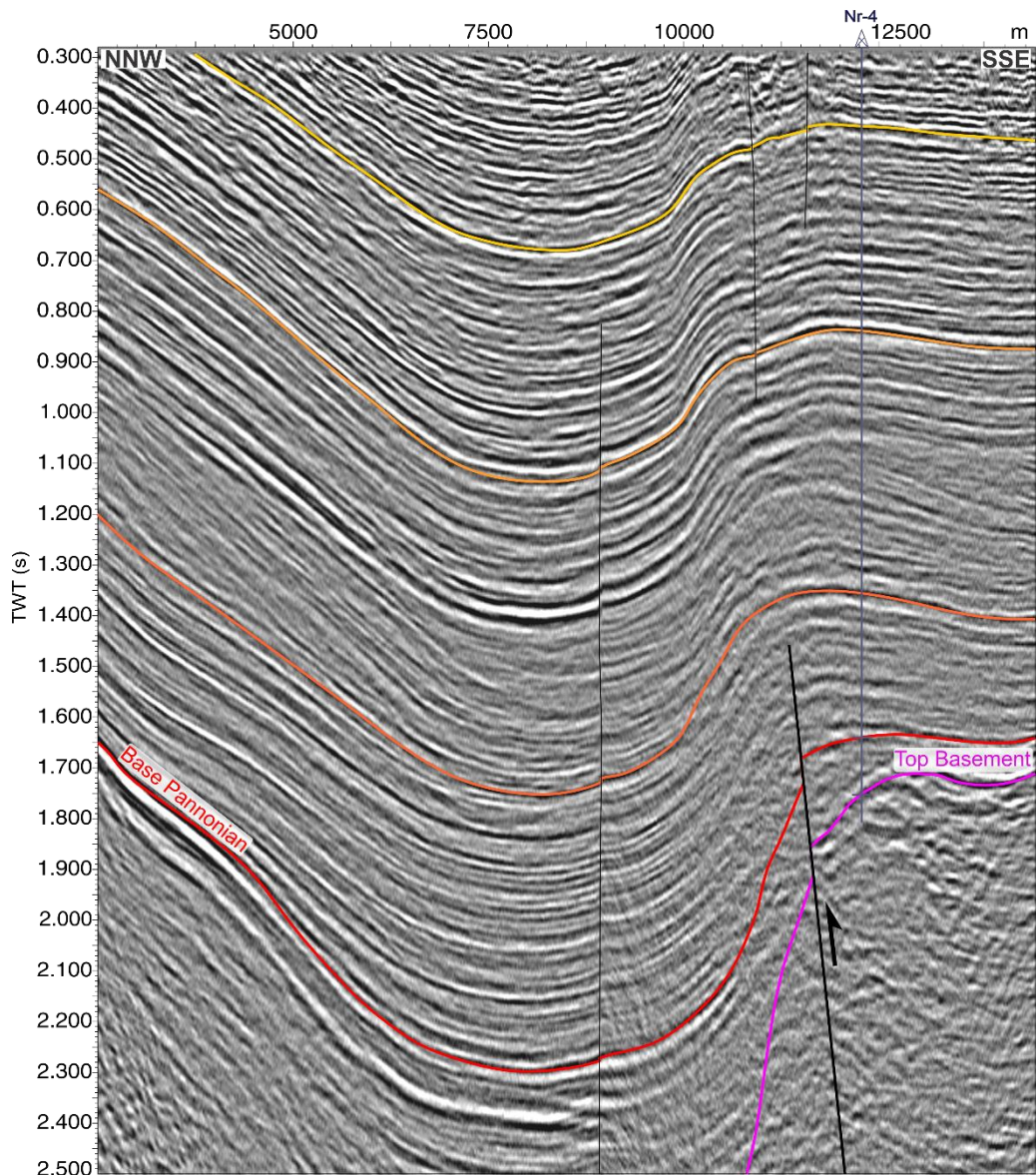
338 It should also be noted that the characteristics of differential vertical motion-related folds of  
339 tectonic origin and significantly eroded compaction-related drape-over folds are very similar,  
340 since erosion removes the upper part of the anticline or syncline, which could be best used to  
341 identify the upward decreasing amplitude used for the differentiation. Similarly, low-amplitude  
342 tectonic-related folds and compaction folds are rather difficult to differentiate without detailed  
343 tectono-sedimentological investigations. In the present study folds without any significant  
344 upward decrease in the amplitude of folding were classified as differential vertical motion-  
345 related structures.

346 *Fault-related folds* are represented by drag folds, roll-over anticlines, en-echelon folds, and  
347 folds related to flower structures (*Fig. 4*). The fault(s) constraining their formation and  
348 geometrical properties were always identifiable. Such folds are widespread in the whole

349 country, and they are typically oriented parallel to sub-parallel, or with en-echelon geometry to  
350 faults, along which the major deformation occurred. Both the wavelength and amplitude of such  
351 folding is generally (significantly) smaller than those of compression- or differential vertical  
352 motion-related folds, although they might form remarkable local structures (e.g., Fodor et al.,  
353 2005a-b; Ruzkiczay-Rüdiger et al., 2007).

#### 354 Monoclinial folds

355 Monoclinial folds usually develop above reactivating reverse faults, however, as numerical and  
356 seismic examples show (Hardy, 2011; Nollet et al., 2012) they can also be formed by subtle,  
357 normal sense reactivation of steep normal faults. The neotectonic displacement above the  
358 controlling faults were small (*Figs. 4, 7*), therefore the faults did not cut up the post-rift  
359 sequence high enough to be classified as “classical” neotectonic faults defined earlier. This  
360 group of folds comprising only a few typical structures in SW Transdanubia (*Fig. 7*,  
361 <http://dx.doi.org/10.17632/dnjt9cmj87.1>), which were identified based on their characteristic  
362 geometric appearance on the seismic profiles.



363

364 *Fig. 7. Example of a monoclinical fold (right) related to a reactivated blind reverse fault. The*  
 365 *asymmetric fold joins to a major syncline of compressional origin (left) towards the North*  
 366 *(Zala basin, western Hungary). For location see Fig. 13.*

367 *4.3. Pre-Pannonian root zones*

368 An essential novelty of the new map is that not only the near surface manifestations of  
 369 neotectonic faults but also their roots in the underlying pre-Pannonian substratum were mapped  
 370 and displayed. The roots display the localities of the faults formed mostly during the preceding  
 371 Early–Middle Miocene basin evolution (Fodor et al., 2005a,b; Bada et al., 2007), which either

372 were (partly) reactivated during the neotectonic phase or had any (even atectonic) role in the  
373 deformation of the youngest sedimentary cover. In other words, not all mapped pre-Pannonian  
374 faults zones were reactivated tectonically during the neotectonic phase producing a near surface  
375 deformation, still, their complete representation on the new map was essential in order to  
376 provide a coherent, regional structural background.

377 During interpretation of the roots hosted in the often poorly imaged Miocene or pre-Cenozoic  
378 basement literature data and Bouguer anomaly maps were also essential sources of information  
379 beside seismic data. The primary formation age of the mapped pre-Pannonian faults is varying,  
380 however most of them are connected to the Early/Middle Miocene tectonics of the basin. It also  
381 needs to be emphasized that the location of the root zones could not be referenced to a common  
382 stratigraphic horizon (e.g., base Pannonian) because the roots where the individual fault planes  
383 of a complex fault zone connect into a common “line” are located at different depth and within  
384 different stratigraphic units even along the same fault zone (Paleozoic–Mesozoic basement or  
385 within the overlying Paleogene–Middle Miocene basin fill).

## 386 ***5. Mapping principles***

387 In the followings the principles and the most important aspects of the structural interpretation  
388 and subsequent map construction are summarized.

### 389 *5.1. Structural interpretation*

390 The primary source of information about the mapped faults and folds displayed on the map  
391 were the seismic datasets. Mapping of these structures using a countrywide uniform reference  
392 horizon was hampered by (i) the varying quality of the available seismic datasets (i.e., no or  
393 poor quality imaging in the uppermost, 0–0.4s TWT range), and (ii) by the changing basement  
394 topography. The mapped fault traces typically refer to ~400-600ms TWT in basin areas, and to  
395 200-300ms near the basin margins, respectively, which represent roughly the highest mapable  
396 occurrence of faults in the given areas. Considering the varying reference depth of the mapping

397 and the dip of the fault planes, several hundred meters general fault trace uncertainty can be  
398 considered when projected to the surface. Fold axis positions were determined using the  
399 shallowest, still well-imaged and laterally traceable post-rift reflection-package.

400 Modern 3D seismic data volumes served as starting points for the regional mapping. Coherency  
401 volumes were calculated for all 3D seismic data volumes, and coherency time slices were  
402 subsequently used as the primary tool for identification and correlation of faults (see also *Fig.*  
403 *19*). The primary fault segment interpretation was subsequently cross-checked in the seismic  
404 profiles in order to verify the actual position and extension of the identified fault segments and  
405 to filter out artificial linear features. The recognized dominant structural pattern and style were  
406 considered and consequently applied during the interpretation of adjacent 2D datasets resulting  
407 in a coherent structural interpretation covering larger areas. For the correlation of structural  
408 elements between 2D seismic lines, trends seen on geophysical maps as well as on regional  
409 geological maps were fully taken into account. Published neotectonic maps were also  
410 considered, revised if needed, and integrated during interpretation, especially in areas with poor  
411 seismic coverage.

412 During mapping two quality classes were defined both for the faults and for the root zones:

- 413 ➤ Constrained (i.e., proven) faults are sufficiently defined by available subsurface and  
414 surface data. Faults of this qualification, regardless of their origin, are clearly  
415 identifiable in the seismic record and deform the highermost post-rift strata, or they have  
416 been well documented by surface geological observations and/or well data.
- 417 ➤ Poorly constrained (/suspected) classification was generally applied when the fault  
418 identification itself and/or its correlation was hampered by poor seismic quality and/or  
419 insufficient coverage. This class was also used for faults with ambiguous timing of  
420 faulting occurring mostly in uplifted areas covered by older (>6–8 Ma), eroded basin  
421 margin strata (i.e., mountain ranges and their surroundings). The neotectonic activity of

422 several important fault zones was suspected based only on scarce surface geological  
423 data published in the literature (Darnó zone in northeastern Hungary for example; see  
424 Fodor et al., 2005c). If neotectonic activity could not be not confirmed by our data at  
425 other localities along the fault, the “suspected” category was applied considering the  
426 entire fault.

427 Identification and classification of neotectonic faults were also aided by the map of historical  
428 and recent (from 1995 on) earthquakes (Tóth et al., 2020). These data were especially useful in  
429 mountainous areas characterized by a reduced or completely missing post-rift cover or poor  
430 seismic imaging.

### 431 *5.2. Map construction*

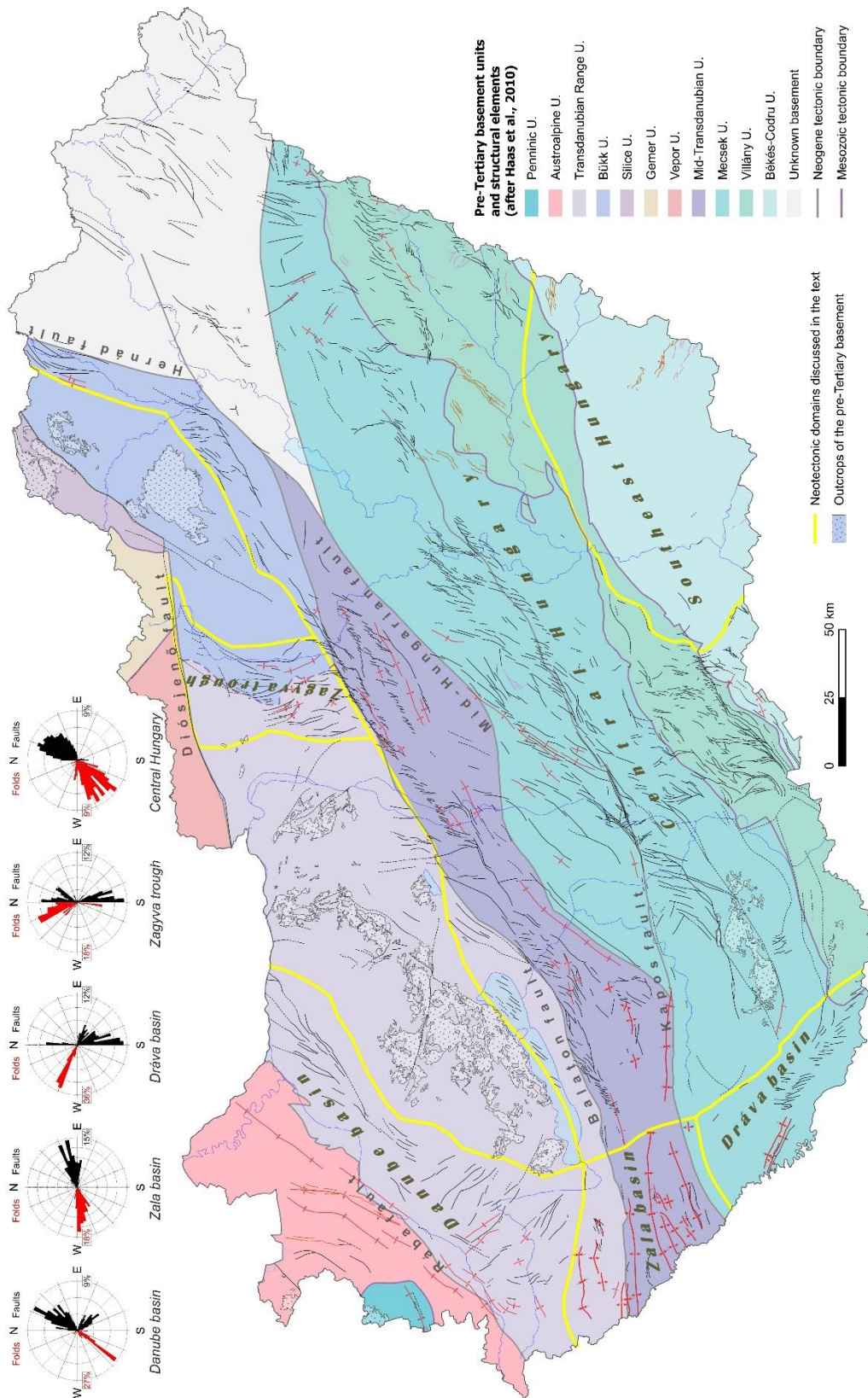
432 During final map construction the completed primary structural interpretations carried out on  
433 the integrated 2D and 3D seismic datasets has been generalized to the applied, 1:500 000 map  
434 scale. During this process, only short, irrelevant fault segments were removed, the overall  
435 structural pattern was preserved and not simplified into single tectonic lines.

436 Mountain ranges and their close surroundings are often characterized by the complete lack of  
437 Late Miocene–Pliocene strata, as well as very poor or no seismic coverage. In these areas  
438 neotectonic structures shown on the map essentially derive from published data (for details see  
439 Section 3). This also holds true for the Lake Balaton where published fault and structural maps  
440 were found to form a coherent and adequate neotectonic model in this area, making  
441 reinterpretation unnecessary. The published models (often using different methods and  
442 datasets) were always cross-checked with each other and with available (often sparse) seismic  
443 data, and critical re-evaluation was performed, if needed. Utilization of neotectonic results  
444 lacking any surface or subsurface geological/geophysical verification (e.g., models relying  
445 exclusively on remote sensing data; Czakó and Zelenka, 1981; Brezsnýánszky and Síkhegyi,  
446 1987) was generally avoided during map construction.



447 **6. Results and Discussion**

448 Considering the important differences in the prevailing orientation and/or style of identified  
449 neotectonic deformations several major neotectonic domains — Danube-, Zala- and Dráva  
450 basins, Central Hungary, Southeast Hungary, Zagyva trough (*Fig. 8*) — could be distinguished  
451 in the country, even if their boundaries are somewhat arbitrary. The relationship between the  
452 defined domains and major tectonic units of the pre-Cenozoic basement (*Fig. 8*) provides a  
453 regional structural context for the following sections.



454

455 *Fig. 8. Definition of neotectonic domains (yellow lines) based on the observed deformation*

456 *pattern (for the legend of the mapped structures see Fig. 9). Rose charts (upper left) show the*

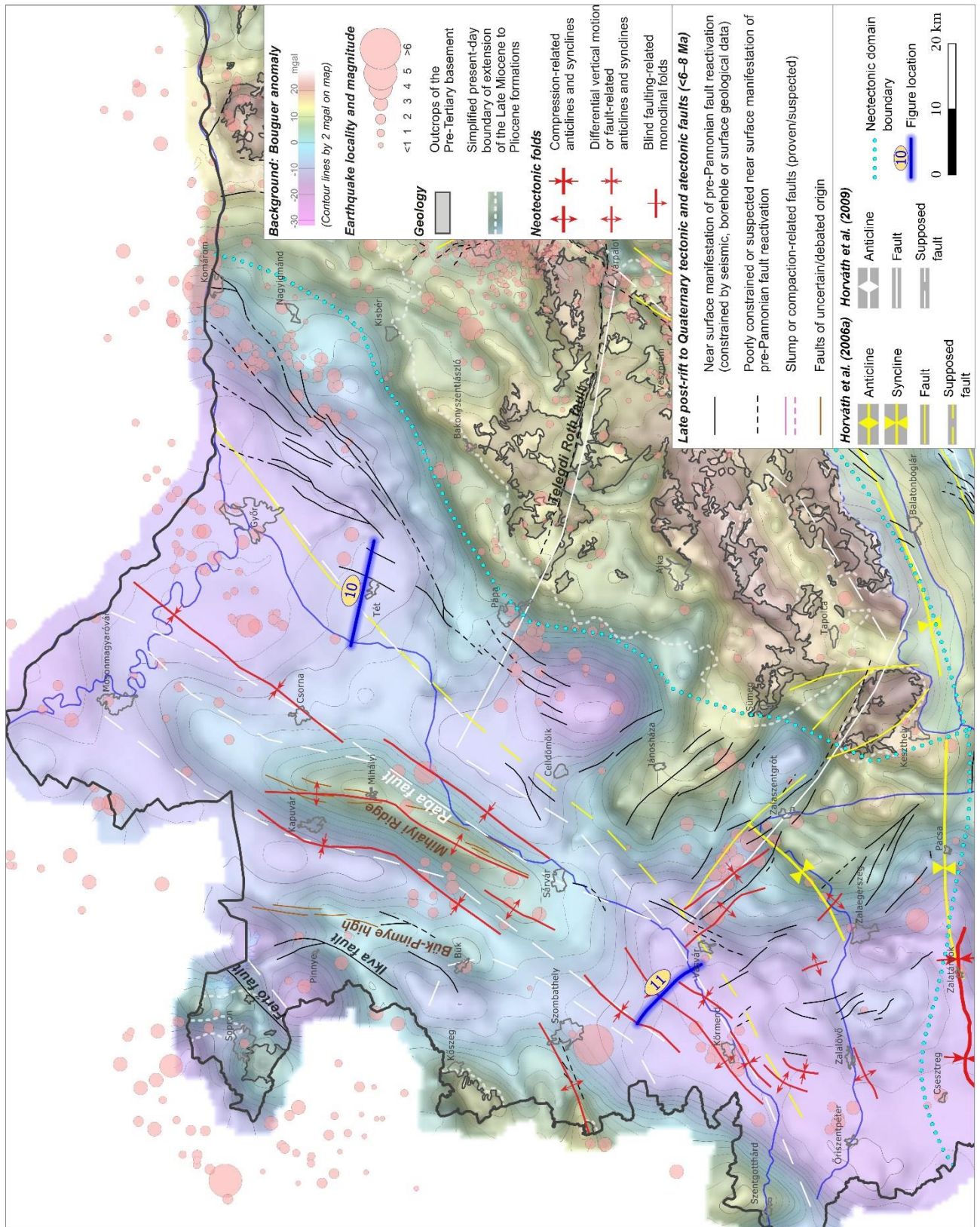
457 *orientation distributions of various neotectonic structures within the domains. Background*  
458 *image shows the major tectonic units of the pre-Cenozoic basement (after Haas et al., 2010)*

### 459 *6.1. Danube basin*

460 The Danube basin is located in the northwestern part of the country (*Figs. 1, 8*) having sufficient  
461 2D and a few 3D seismic coverage (*Fig. 3*). In general moderate neotectonic activity is observed  
462 in this domain manifested mostly in the appearance of (N)NE–(S)SW and (W)NW–(E)SE  
463 striking faults and similarly oriented folds. Using the methodology shown on *Fig 4*, the  
464 identified folds were all classified as differential vertical motion-, or fault-related  
465 (<http://dx.doi.org/10.17632/dnjt9cmj87.1>). This neotectonic deformation pattern shows a close  
466 relationship with the overall (N)NE–(S)SW structural trends of the pre-Tertiary basement  
467 consisting of various Austroalpine nappes formed during the Cretaceous (Eoalpine)  
468 tectogenesis and overprinted by Miocene extension (Tari, unpubl., 1996; Tari and Horváth,  
469 2010).

470 The main (N)NE–(S)SW structural trend of the basement formed during multiple pre- and  
471 synrift deformations is cut by numerous (W)NW–(E)SE striking faults of Neogene age (Haas  
472 et al., 2010). Neotectonic structures of this orientation occur mostly in the southeastern part of  
473 the domain, and belong to the Transdanubian Range unit representing the highest tectonic  
474 element of the Eoalpine nappe stack. This set of neotectonic faults is practically missing in the  
475 western part of the domain underlain by deeper Austroalpine and the structurally lowest  
476 Penninic units (Haas et al., 2010) below the main Miocene extensional detachment fault (i.e.,  
477 the Rába fault: Tari, unpubl., 1996; see also *Figs. 8, 9*). This indicates reactivations of deeper  
478 faults and a strong control of basement tectonics on the neotectonic orientations.

479 There are three subjects, where our work brought new insights and progress into the neotectonic  
480 understanding of the region (see also *Fig. 9*):



481

482

*Fig. 9. Detailed view of the mapped structures in the Danube basin compared to earlier*

483

*regional studies (Horváth et al., 2006a; Horváth et al., 2009). Seismicity is shown after Tóth*

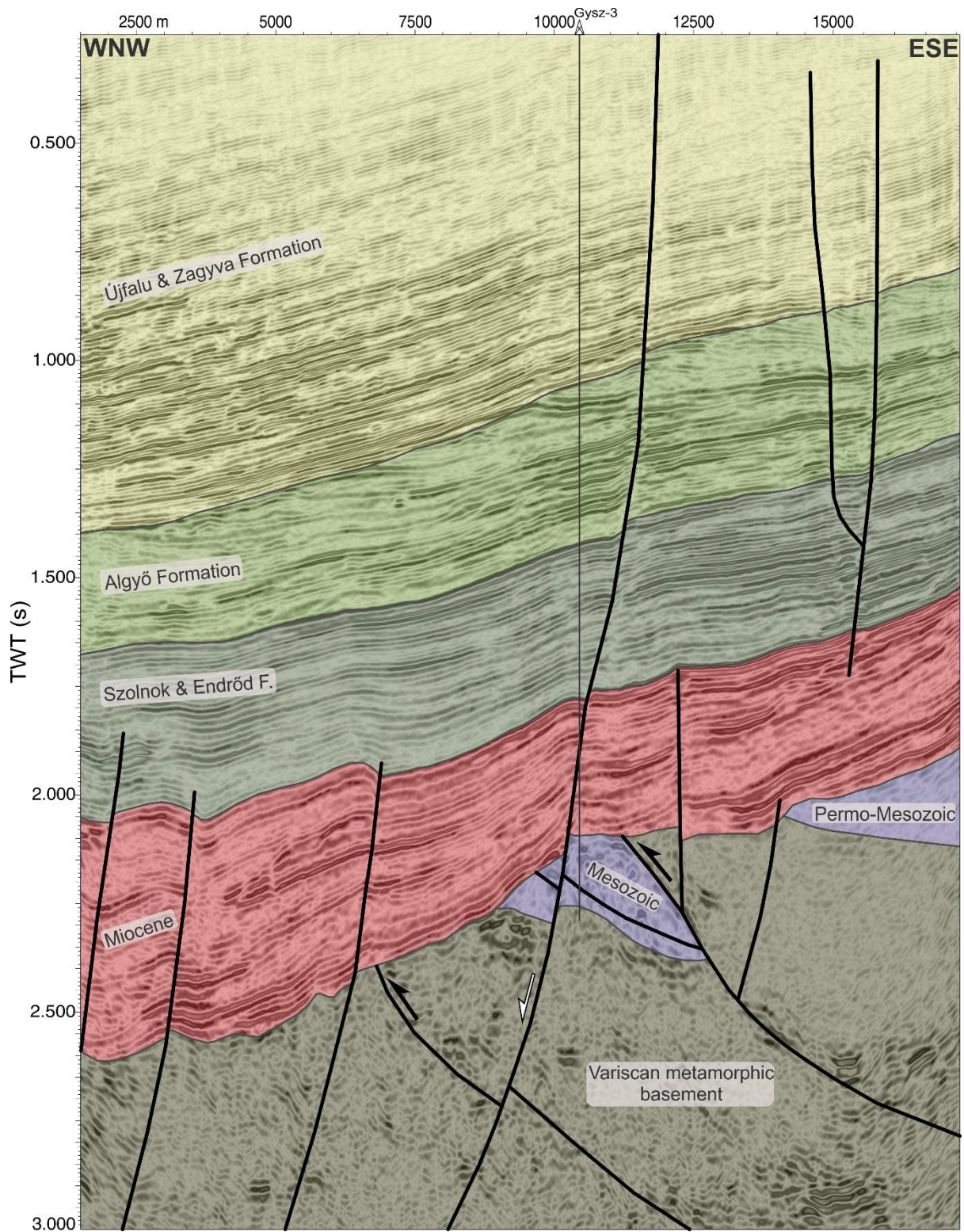
484

*et al. (2020).*

485 (i) correlation of a wide, NE–SW striking neotectonic fault zone in the southeastern flank of  
486 the Danube basin (between the towns of Komárom and Pápa), (ii) identification of a set of NW–  
487 SE striking neotectonic faults in the southeastern part of the domain, (iii) identification of  
488 differential vertical motion-related folds occurring mostly in the western and southern part of  
489 the domain. In addition, several other, less prominent structures were correlated in the western  
490 part of the domain based on seismic interpretation and integration of published surface  
491 geological and geomorphological data (Székely et al., 2009; Zámolyi et al., 2010, Kovács et al.,  
492 2015), which show remarkable correlation with known Miocene extensional faults (Fertő-,  
493 Ikva-, Rohonc faults; see *Fig. 9* and Tari and Horváth, 2010).

494 The wide fault zone between the towns of Komárom and Pápa comprises several anastomosing,  
495 NNE–SSW and NE–SW oriented fault branches forming an acute angle with each other. A  
496 shorter fault branch between Pápa and Celldömölk with similar overall orientation forms  
497 probably its southwestern continuation. The arrangement of the individual NNE–SSW striking  
498 faults/fault branches and the mapped root zones largely resembles that of synthetic Riedel  
499 shears suggesting sinistral shearing along the fault zone. Although poorly constrained we  
500 believe that this fault zone continues up to the town of Komárom towards the northeast. This  
501 correlation is also supported by historical (i.e., the Komárom earthquake in 1763 with an  
502 estimated magnitude of 6.2) and recent seismicity (Tóth et al., 2020; *Fig. 9*).

503 The discussed fault zone transects the western flank of the Transdanubian Range unit  
504 comprising here non-metamorphic Permo-Mesozoic and underlying Lower Paleozoic low-  
505 grade metamorphic rocks (c.f., Haas et al., 2010). Integrated analysis of seismic sections and  
506 available well data suggests that neotectonic activity is related to the reactivation of a  
507 westnorthwest-dipping Miocene synrift normal fault cutting and displacing also an Eoalpine  
508 (Cretaceous) thrust in the pre-Tertiary basement (*Fig. 10*).



509

510 *Fig. 10. WNW–ESE directed seismic profile indicating neotectonic faulting coupled with the*

511 *reactivation of pre-existing, westnorthwest-dipping synrift fault within the pre-Tertiary*

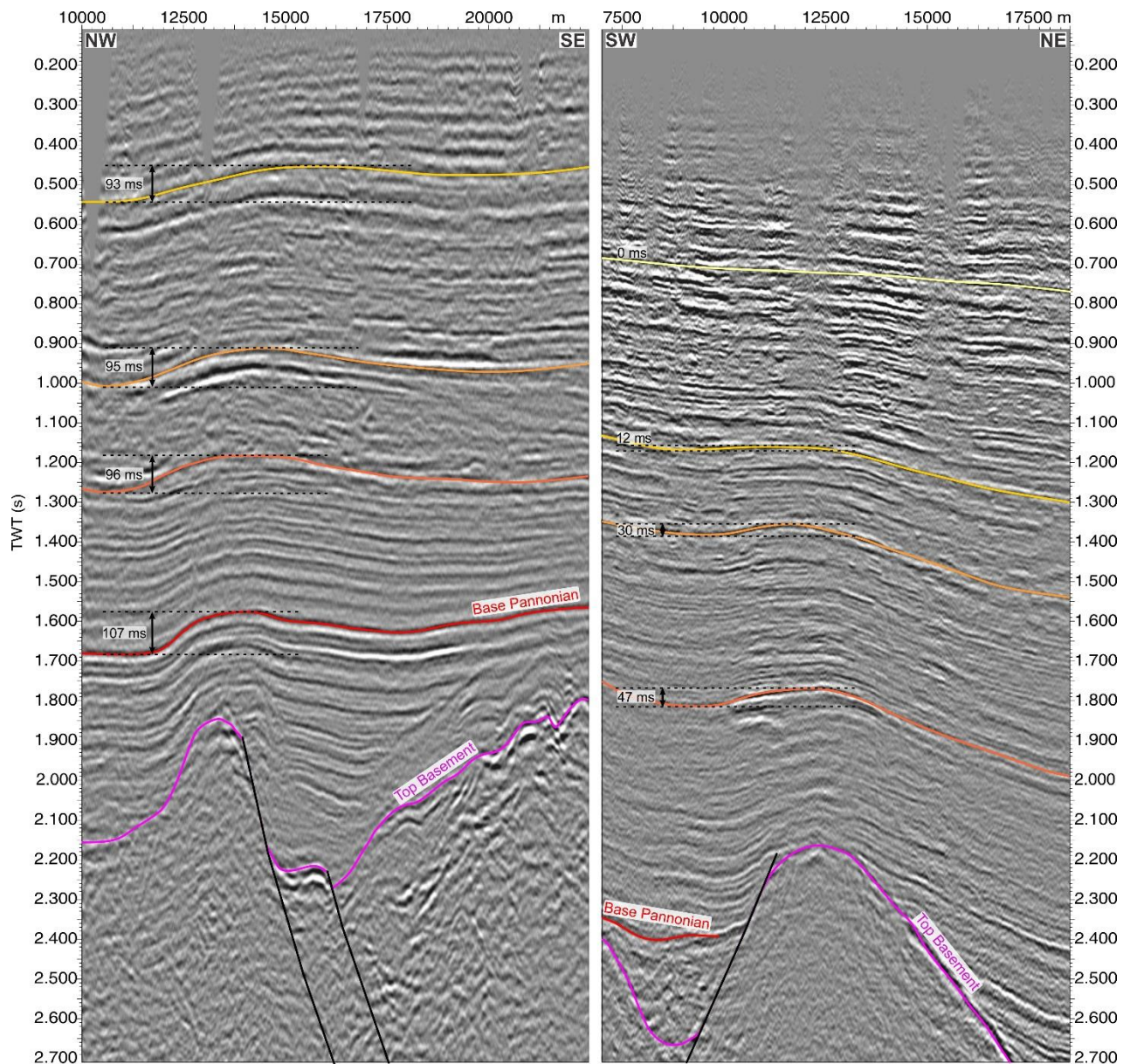
512 *basement of the Transdanubian Range unit. For location see Figure 9*

513 Further to the southwest neotectonic faulting was also interpreted to be related to the  
514 reactivation of a synrift normal fault that joins directly to a low-angle Cretaceous thrust surface  
515 (Tari and Horváth, 2010), postulating an intimate structural relationship between extensional  
516 synrift and contractional pre-rift structures.

517 A novel outcome of the new mapping is the correlation of several NW–SE striking neotectonic  
518 faults and fault-related folds in the southeastern part of the domain above the buried Mesozoic  
519 formations of the Transdanubian Range unit. Similar neotectonic faults previously were only  
520 indicated at the margins of the Keszthely Mts. and along the Telegdi-Roth fault (e.g Horváth et  
521 al., 2006a; Horváth et al., 2009; *Fig. 9*). Regarding their origin, large part of these reactivating  
522 NW–SE striking faults was considered to be related either to Cretaceous compression (e.g., Tari  
523 and Horváth, 2010), or preceding pre-orogenic (Late Triassic to Jurassic) tension (Héja et al.,  
524 2018), that were in part reactivated as normal or dextral faults during Miocene basin evolution.  
525 Neotectonic activity probably also occurred along these faults in the uplifted part of the  
526 Transdanubian Range unit, however, this cannot be verified due to the limited  
527 presence/thickness of young sediments and to the lack of appropriate seismic coverage.

528 Widespread occurrence of tectonic (differential vertical motion-related) folding in this domain  
529 were not shown previously (c.f., *Fig. 9*). These folds generally follow the main (N)NE–(S)SW  
530 structural trend of the domain and show a close correlation with basement morphology  
531 (<http://dx.doi.org/10.17632/dnjt9cmj87.1>) resembling the characteristics of drape-over  
532 anticlines of compaction origin at a first sight. Detailed analysis reveals however, that they are  
533 characterized by a practically constant amplitude of folding vertically within the entire imaged  
534 post-rift sequence being incompatible with a purely compactional origin (c.f., *Figs. 4, 11*). The  
535 striking spatial correlation between fold locations of this study and the very gentle surface  
536 morphological trends observed in the youngest fluvial sediments of the Rába river (*Fig. 12*)  
537 suggest that folding affects even the youngest sediments of the present day surface. This is also

538 an indication against their compaction origin. Taking into account the young uplift of the  
539 neighboring mountain ranges (e.g., Tari, unpubl.; Horváth, 1995; Sacchi et al., 1999) we  
540 consider these folds to be related to the tectonically driven differential vertical movements of  
541 adjacent basement segments.

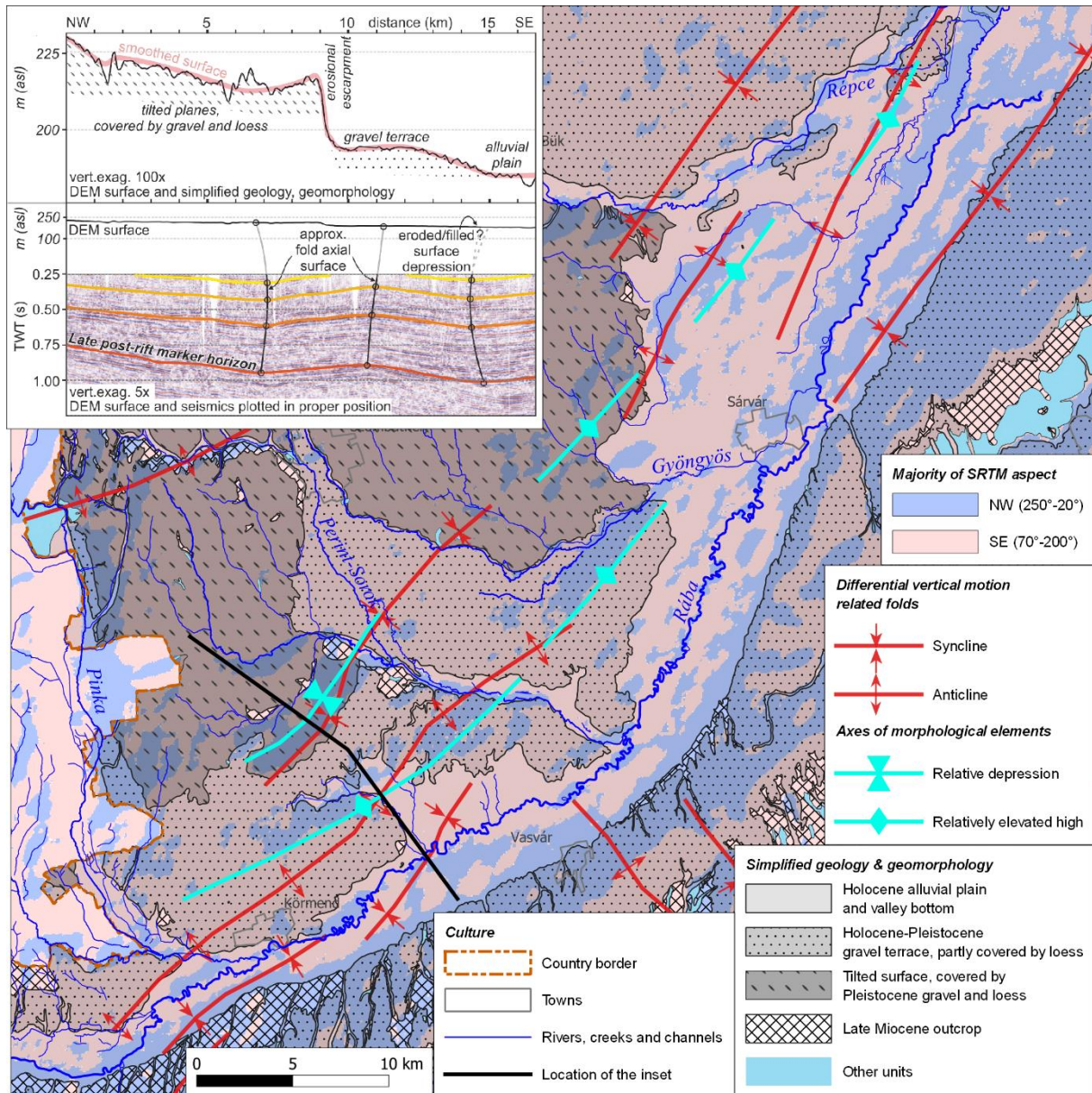


542  
543 *Fig. 11. Fold characteristics from SW Danube basin (left) compared to the drape-over*  
544 *anticline above the Algyő high (SE Great Hungarian Plain; right). Note the strikingly*  
545 *different vertical pattern of fold amplitudes (constant vs. upward diminishing) supporting the*



546 presence of tectonic folding in the Danube Basin. Orange and yellow lines indicate arbitrary,  
 547 uncorrelated Pannonian marker horizons. For location see Figs. 9 and 17a.

548



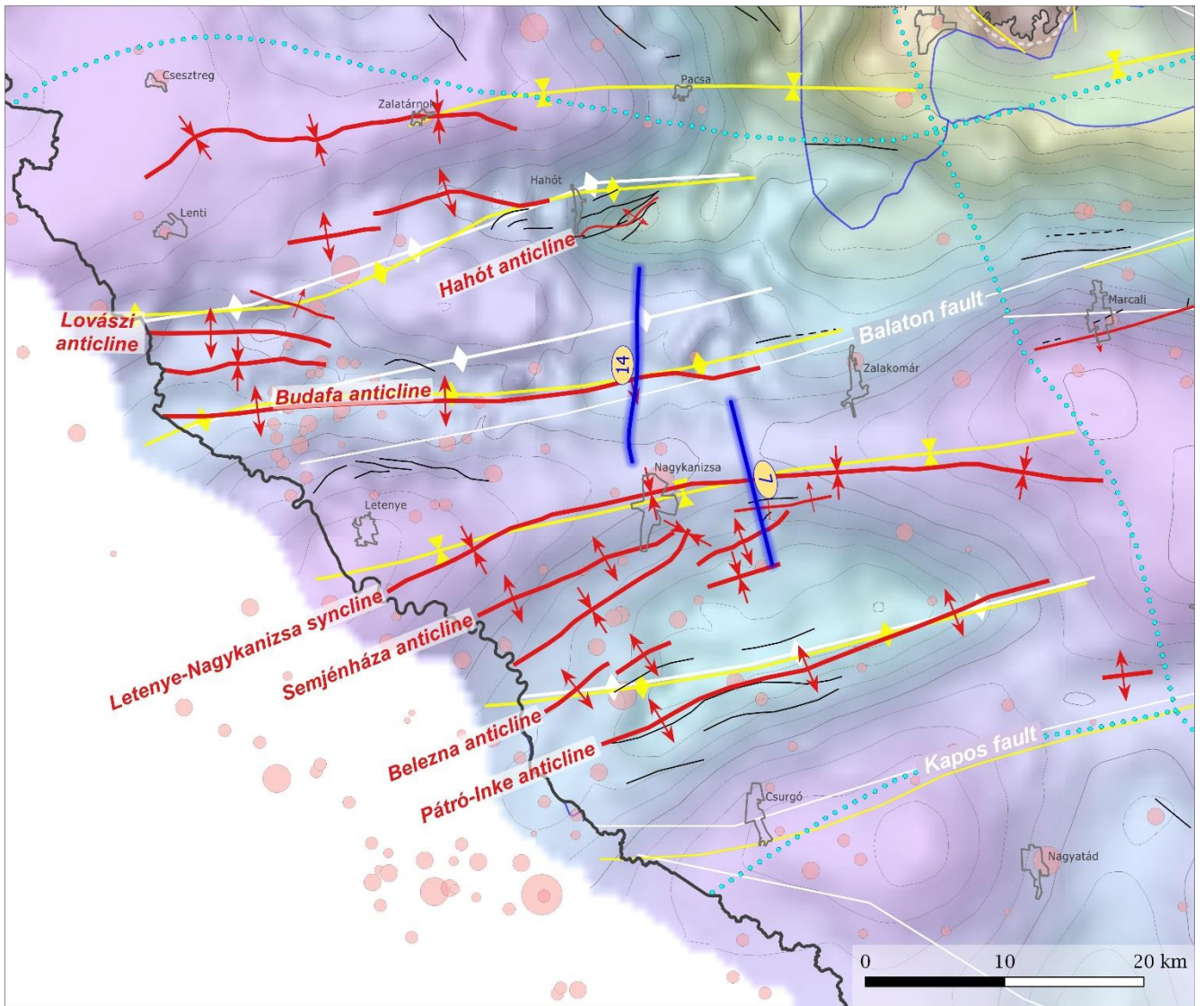
549

550 Fig. 12. Spatial correlation between fold locations of this study and surface morphological  
 551 elements revealed by independent analysis of digital elevation models (SRTM and DDM-10;  
 552 Kovács et al., 2014). The very gentle morphological trends within the fluvial sediments of the  
 553 Rába river shown by the terrain aspect attribute of the DEM correlate well with underlying  
 554 folds interpreted on the seismic dataset.

555 6.2. Zala basin

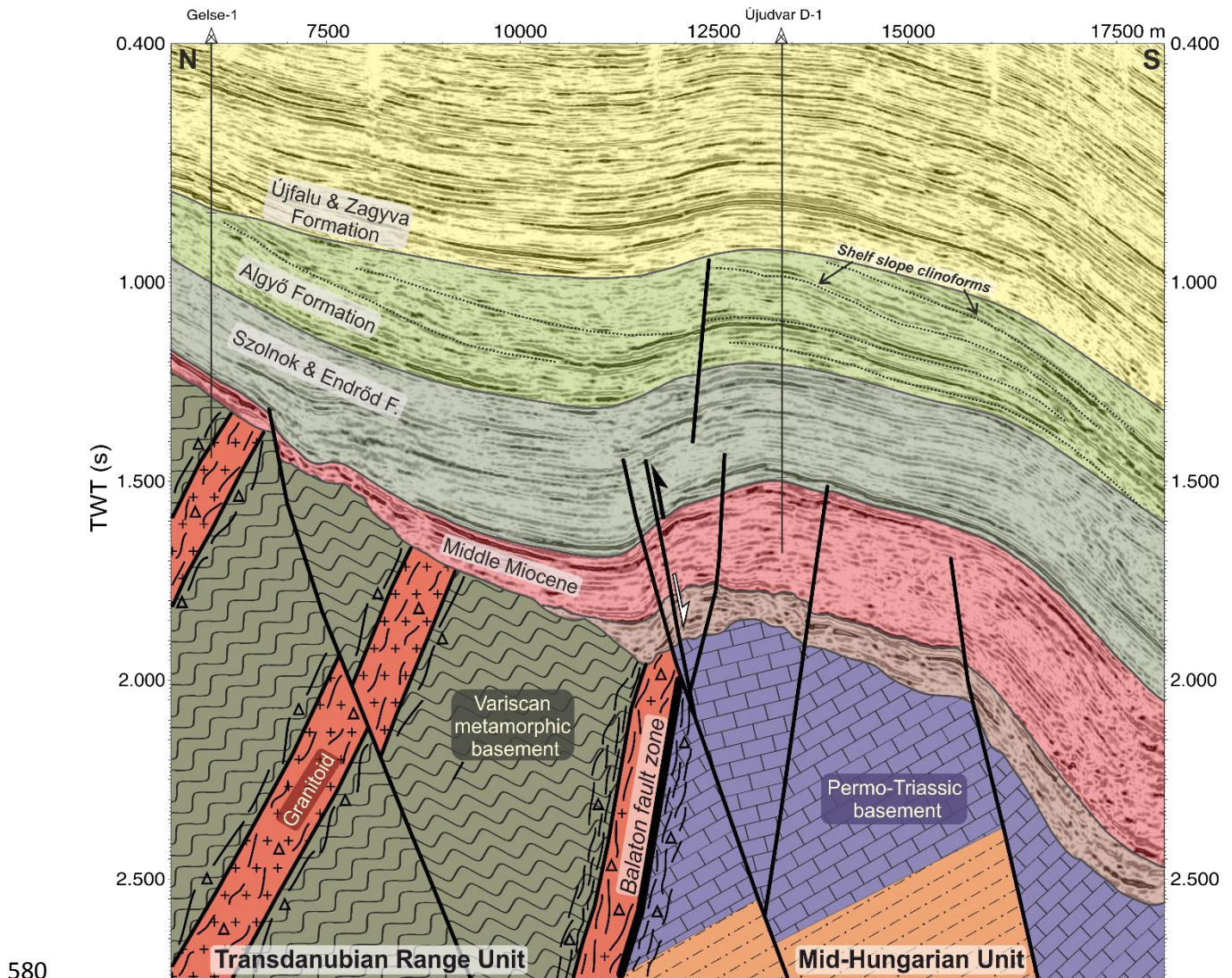
556 The Zala basin (*Figs. 1, 8*) represents the classic area of Hungarian structural geology, where  
557 E–W trending, compression-related folds were described from the early twentieth century on  
558 (Pávai Vajna, 1925; Dank, 1962; Horváth and Rumpler, 1984). These folds clearly dominate  
559 the overall neotectonic deformation style of the domain (c.f., also Fodor et al., 2005a-b; Bada  
560 et al., 2006, 2007, 2010; <http://dx.doi.org/10.17632/dnjt9cmj87.1>). The E–W and ENE–WSW  
561 oriented structural trends generally characterize the domain despite the fact, that the area  
562 comprises several large tectonic units separated by first order tectonic fault zones (i.e., Balaton  
563 and Kapos fault zones; *Figs. 8, 13*).

564 Compression-related neotectonic folding was essentially coupled with north-vergent blind  
565 reverse faulting along pre-existing synrift normal faults in the Zala basin (Horváth and Rumpler,  
566 1984; Horváth, 1995; Fodor et al., 2005a-b, 2013; Bada et al., 2006). The folding therefore was  
567 directly related to the regional neotectonic stress field characterized by a ca. N–S oriented  
568 horizontal maximum stress axis ( $\sigma_1$ ). The most prominent example is the long-known, E–W  
569 trending Budafa anticline (*Fig. 14*), but several smaller folds of this type (e.g., the Belezna and  
570 Semjénháza anticlines and an associated syncline between them) were also correlated. These  
571 smaller folds were not or often inaccurately shown in former neotectonic syntheses (e.g., Fodor  
572 et al., 2005a-b, 2013; Horváth et al., 2006a, 2009; Bada et al., 2007; 2010; see *Fig. 13*). The  
573 location of the blind reverse faults coupled with prominent contractional anticlines (Fodor et  
574 al., 2013) are in good agreement with the identified monoclinial structures developed above  
575 these faults.



576

577 *Fig. 13. Detailed view of the Zala basin folds compared to earlier regional studies (yellow:*  
 578 *Horváth et al., 2006a; white: Horváth et al., 2009; for detailed legend see Fig. 9). Location of*  
 579 *Figs. 7 and 14 is shown by blue line. Seismicity is shown after Tóth et al. (2020).*



580

581 *Fig. 14. Compressional folding related to graben inversion: the Budafa anticline. For*  
 582 *location see Figure 13*

583 Beside its fold-dominated nature another striking feature of this domain is the subordinate role  
 584 of neotectonic faults. They are typically oriented (sub)parallel to fold hinges and the underlying  
 585 pre-Pannonian faults (<http://dx.doi.org/10.17632/dnjt9cmj87.1>), and often represent the  
 586 continuation of blind reverse faults to shallow stratigraphic levels. Their symmetrical  
 587 arrangement on both sides of the Budafa anticline (*Fig. 13*) indicates the formation (or  
 588 contemporaneous reactivation) of an antithetic, north-dipping fault producing a pop-up like  
 589 structure during inversion in the middle sector of the anticline. In other cases faults either form  
 590 flower structures (Hahót anticline; c.f., also Bada et al., 2006: Fig. 4) or are organized into a set

591 of steep, (sub)parallel faults (Pátró-Inke anticline) in seismic sections. These observations  
592 altogether indicate a compressional stress regime being perpendicular to the pre-existing  
593 structural fabric during the neotectonic deformation phase in this area.

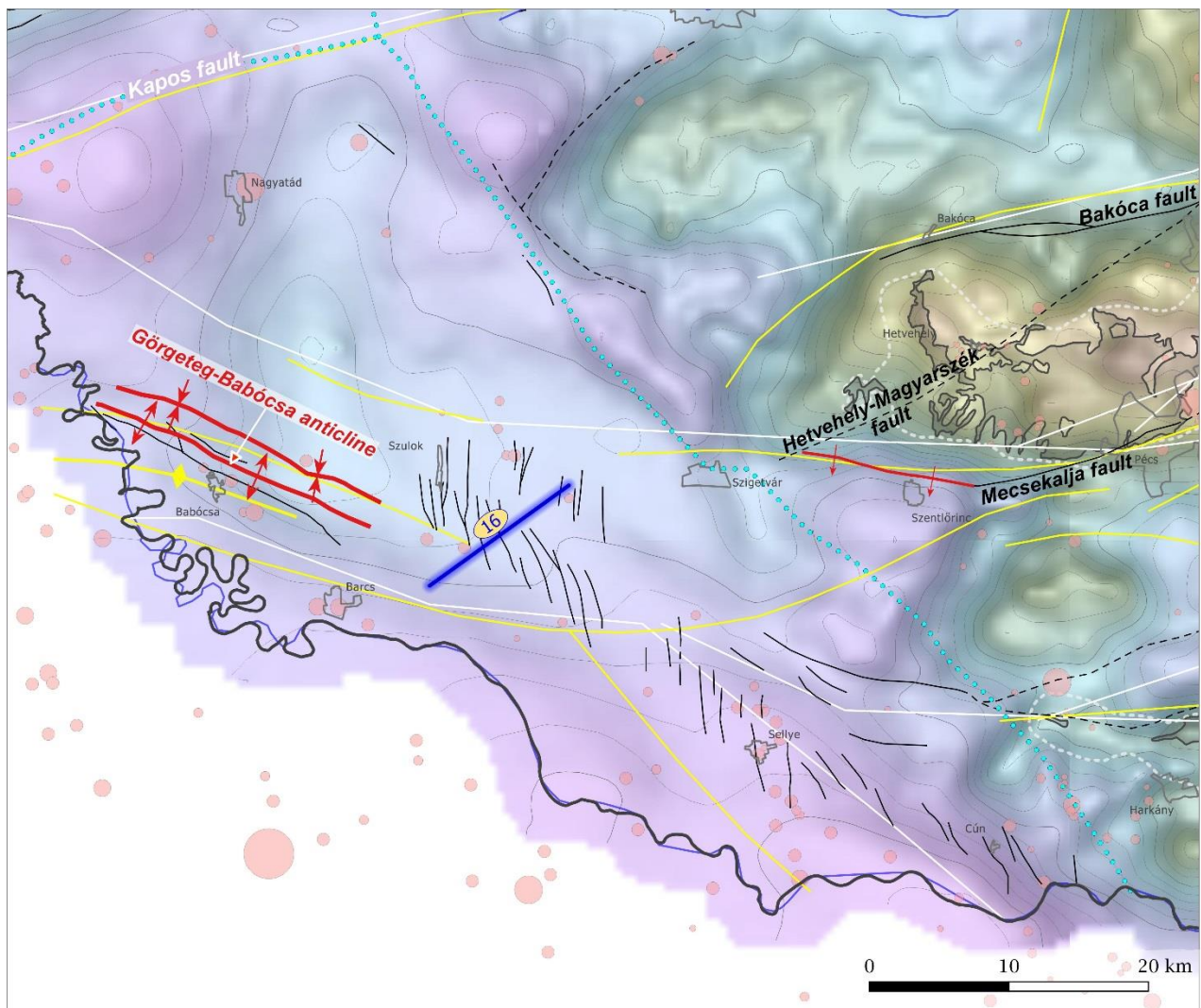
594 It is important to emphasize, that practically no near surface manifestation of neotectonic  
595 faulting occurs along the western segments of the Balaton and Kapos faults being in contrast  
596 with their eastern continuations characterized by peculiar neotectonic flower structures in the  
597 shallow post-rift strata (see also Section 6.4.). This feature indicates the lack of detectable  
598 strike-slip reactivation of these faults within the domain (questioned also by e.g., Bada et al.,  
599 2010) being in contrast with former regional neotectonic models (c.f., *Fig. 13*). However, based  
600 on recent and historical seismicity (Tóth et al., 2020) the western segments of these major fault  
601 zones can be considered as seismoactive (*Fig. 13*).

### 602 *6.3. Dráva basin*

603 The Dráva basin is located in the southwestern part of the country extending in a NW–SE  
604 direction parallel to the river Dráva (*Figs. 1, 15*). Good seismic coverage with numerous  
605 modern 3D seismic volumes is available (*Fig. 3*) except for the area of the Mecsek and Villány  
606 Mts.

607 The Dráva basin represents a unique domain in the sense that the prominent (W)NW–(E)SE  
608 neotectonic structural trend is not characteristic elsewhere in the country. This structural trend  
609 has been long recognized in the basement structure (Csalagovits et al., 1967; Fülöp and Dank,  
610 1987; Haas et al., 2010). Altogether a moderate neotectonic activity occurs in this domain  
611 manifested in the formation of pronounced, NW–SE striking right lateral shear zones as well  
612 as compression-related folds. The new mapping has complemented the existing tectonic  
613 knowledge of the area and provided a detailed model of the Szulok-Sellye-Cún dextral strike-  
614 slip fault zone. The map also proposes an alternative structural model compared to other

615 (neo)tectonic maps regarding the boundary of the Dráva and Mecsek-Villány tectonic units  
616 (<http://dx.doi.org/10.17632/dnjt9cmj87.1>; Fig. 15).

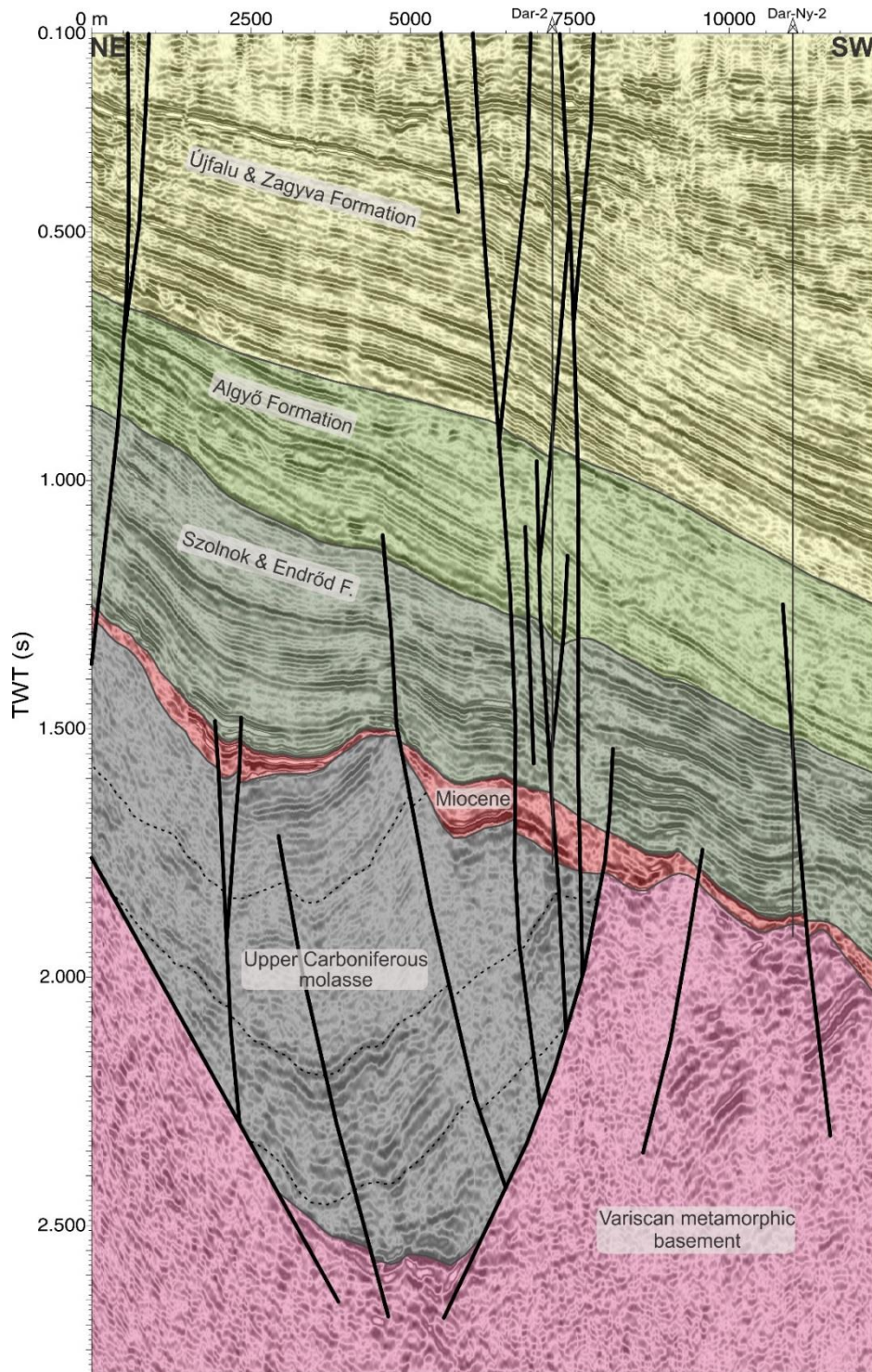


617  
618 *Fig. 15. Detailed view of the mapped structures in the Dráva basin compared to earlier*  
619 *regional studies (yellow: Horváth et al., 2006a; white: Horváth et al., 2009; for detailed*  
620 *legend see Fig. 9). Location of Figure 16 is shown by blue line. Seismicity is shown after Tóth*  
621 *et al. (2020).*

622 The dominant neotectonic feature of the domain is a nearly 60 kilometer long, WNW–ESE  
623 striking fault zone running between the localities of Szulok and Cún. The fault zone is built up  
624 by a large number of individual fault segments up to a length of ca. 6 kilometers oriented  
625 between NW–SE and N–S. Both their map view arrangement (i.e., typical en-echelon

626 geometry) and their seismic image (i.e., characteristic flower structure) clearly suggest a strike-  
627 slip fault zone of dextral shear. This fault zone provides an excellent example for the  
628 neotectonic reactivation of ancient basement structures (*Fig. 16*): it was partly developed along  
629 the southwestern border fault of a Carboniferous (see Haas et al., 2010) molasse graben, but  
630 neotectonic fault reactivation also occurs at the northern graben margin to a limited extent  
631 (<http://dx.doi.org/10.17632/dnjt9cmj87.1>).

632



633

634 *Fig. 16. NE–SW oriented seismic profile showing neotectonic reactivation of the border faults*  
 635 *of a Late Carboniferous molasse graben. Note also the folding of the graben fill (marker*  
 636 *horizons by dotted lines) due to Late Variscan and/or Eoalpine (Cretaceous) compressional*  
 637 *event(s). For location see Figure 15*



638 The graben gradually becomes narrower towards the southeast and finally disappears (near  
639 Sellye), however, a southwestward facing basement fault with associated neotectonic  
640 reactivation can be traced further in the seismic dataset up to the locality Cún. Recent seismicity  
641 documented along the entire length of the fault zone, and especially near the locality Sellye  
642 (Tóth et al., 2020; *Fig. 15*) is in good accordance with the observed neotectonic activity.

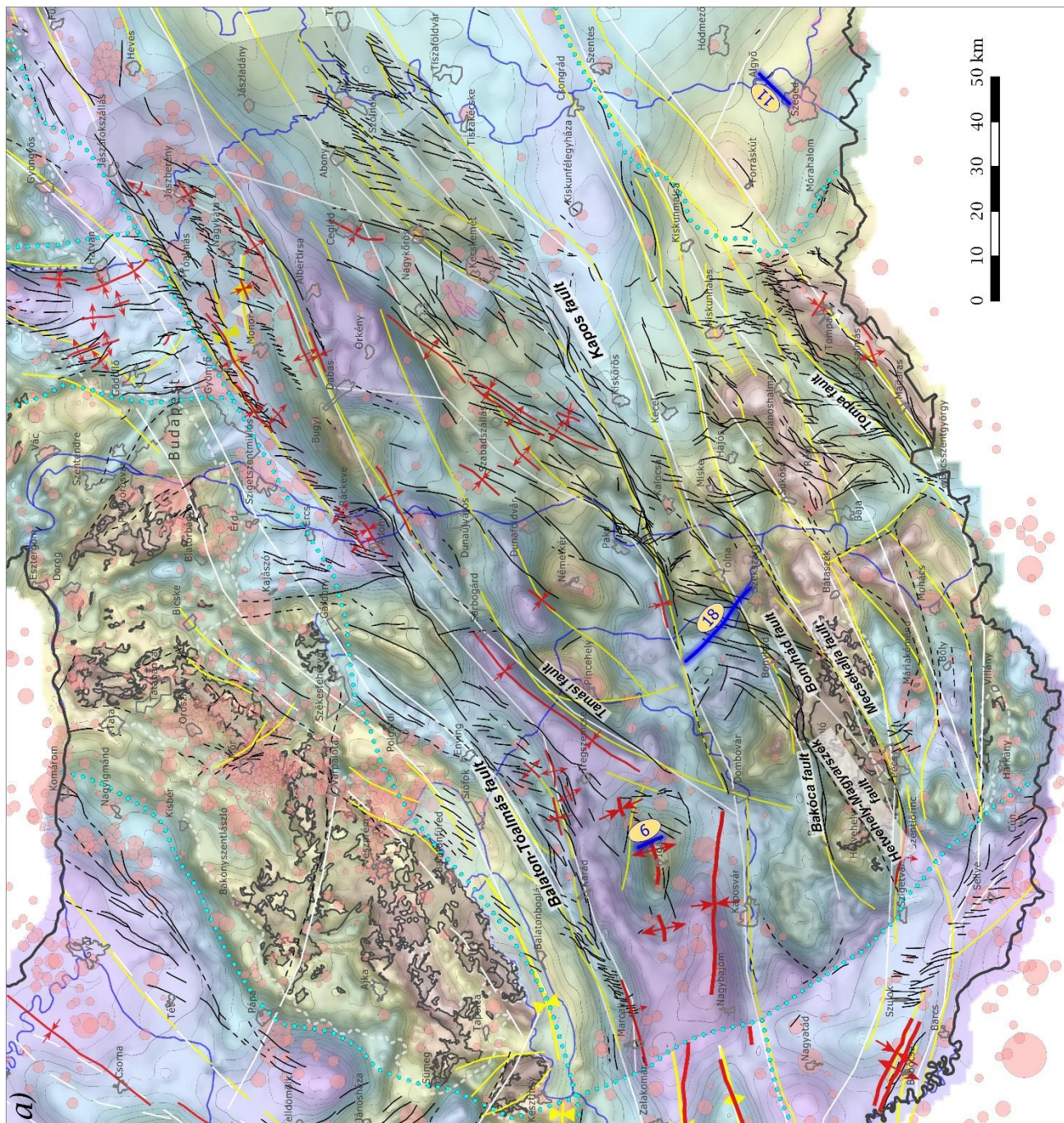
643 The Görgeteg-Babócsa anticline is probably the best-known neotectonic structure of the  
644 domain, which (together with the associated, parallel syncline to the north) was mapped, in  
645 great details (c.f., *Fig. 15*). A prominent, mostly northeast-dipping neotectonic fault is situated  
646 south of the anticline axis, whereas a shorter parallel fault segment north of the anticline axis  
647 represents a minor southwest-dipping antithetic fault. The formation of this anticline was  
648 generally connected to the reverse reactivation of a former, southwest-dipping fault appearing  
649 at the northwestern part of the anticline by compressional forces (Saftić et al., 2003; Wórum  
650 and Hámori, unpubl.; Horváth et al., 2015) using the structural analogy of the Zala basin (see  
651 Section 6.2.).

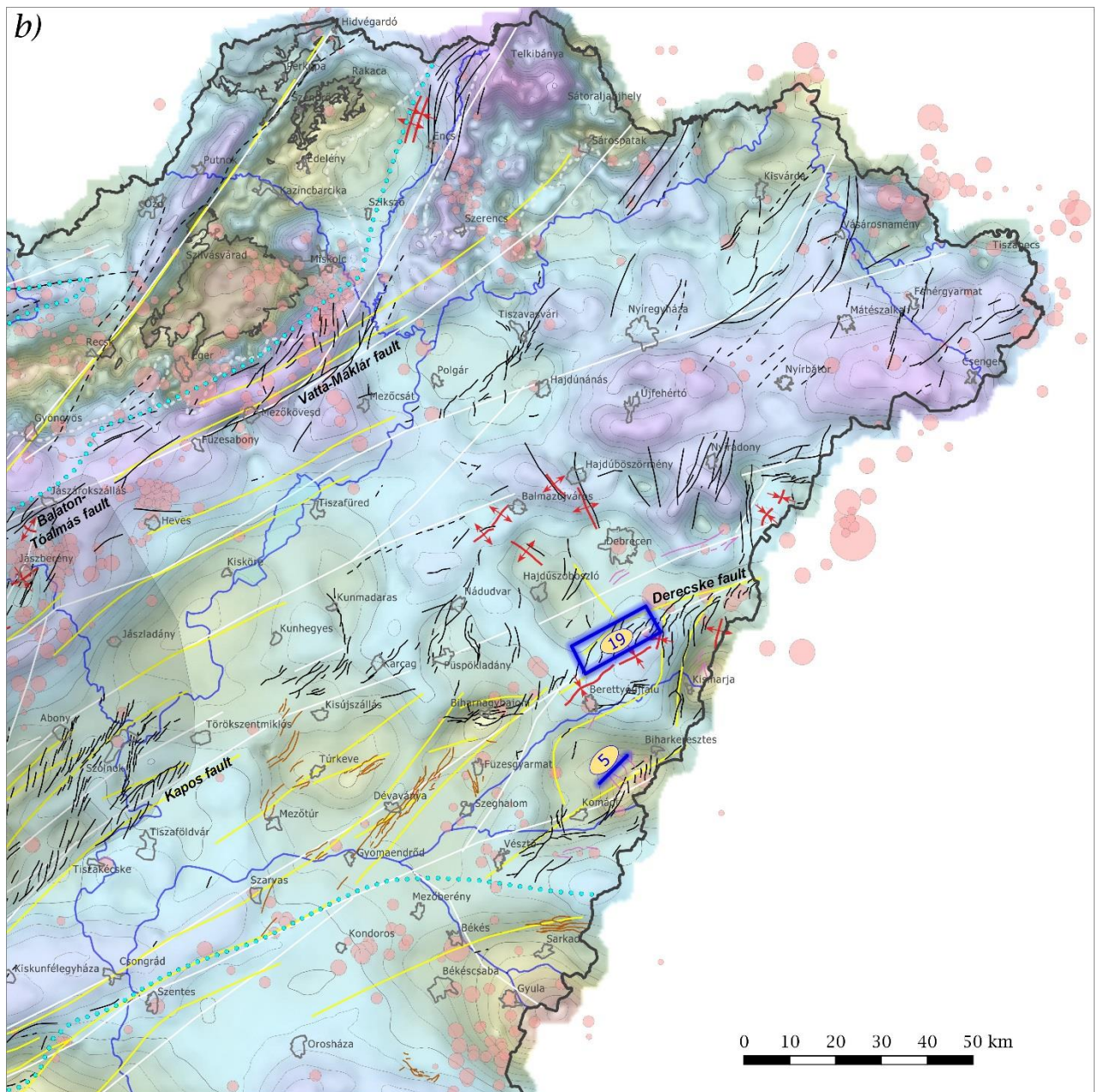
652 For the eastern boundary of the Dráva domain an alternative structural model is proposed  
653 (reflected by the pre-Pannonian fault pattern, <http://dx.doi.org/10.17632/dnjt9cmj87.1>), where  
654 we favor a prominent, NW–SE striking fault separating the Dráva and the Central Hungary  
655 domains between the Kapos fault zone and Hungarian-Croatian border. This interpretation is  
656 based on Bouguer anomaly patterns and only on limited number of seismic surveys. However,  
657 it was necessitated, because available data do not support the direct structural continuation of  
658 the Mecsek-alja and other parallel fault zones of the Central Hungary domain (see also Section  
659 6.4.) into the Dráva domain as it was indicated in former models (c.f., *Fig. 15*). In our view this  
660 fault represents the northern limit of the “Dinaric” type structural orientations being also  
661 dominant in Croatia, although this area is considered as part of the Tisza megaunit (Schmid et  
662 al., 2008; Haas et al., 2010).

663 *6.4. Central Hungary*

664 This domain comprises the central portion of the country including southeastern Transdanubia  
665 and large part of the Great Hungarian Plain (*Figs. 1, 8*). Apart from the area of the Mecsek and  
666 Villány Mts. and their surroundings good seismic coverage (including many 3D seismic  
667 volumes in the east) exists in this area (*Fig. 3*).

668 The overall neotectonic deformation pattern is dominated by ENE–WSW and NE–SW trending  
669 faults/fault zones and associated fault-related, rarely en-echelon folds, whereas structures of  
670 other orientations occur less frequently. Despite the generally dominant ENE–WSW and NE–  
671 SW structural trends notable differences exist in the neotectonic deformation pattern within this  
672 large domain allowing the separation of several distinct subareas. These include (i) the re-  
673 defined Mid-Hungarian mobile belt south of the Balaton-Tóalmás fault zone (ii) the southern  
674 Danube-Tisza interfluvium and (iii) the Eastern Great Hungarian Plain. The whole Central  
675 Hungary domain displays a significantly more complex neotectonic deformation pattern than  
676 shown by former neotectonic syntheses (*Fig. 17a-b*).





678

679

680

681

682

683

684

*Fig. 17. Detailed view of the mapped structures in the western (a) and eastern (b) Central Hungary domain, and their comparison to earlier regional studies (yellow: Horváth et al., 2006a; white: Horváth et al., 2009; for detailed legend see Fig. 9). Shaded gray polygon indicates the area of the Mid-Hungarian mobile belt redefined in this study. Locations of Figs. 5, 6, 11, 18 and 19 are shown by blue lines. Seismicity is shown after Tóth et al. (2020).*

685        Mid-Hungarian mobile belt (redefined after Detzky Lőrincz et al., 2002)

686        The northern part of the Central Hungary domain consists of an approx. 60-80 km wide belt of

687        distributed strike-slip deformation that can be followed more than 200 kilometers along strike

688        (*Fig. 17a*). The eastern part of this wide zone located between the ENE–WSW striking Balaton-

689        Tóalmás fault in the north and the eastern Kapos fault in the south was previously recognized

690        and called as *Mid-Hungarian mobile belt* (Detzky Lőrincz et al., 2002; Juhász et al., 2013). In

691        the pre-Tertiary basement it incorporates the entire Mid-Transdanubian unit (i.e., the classical

692        area of the Mid-Hungarian Fault Zone; Csontos and Nagymarosy, 1998) and the northern

693        portion (i.e., the Mecsek unit) of the Tisza-Dacia megaunit (see *Fig. 8*). Considering the new

694        mapping as well as most recent neotectonic models (Horváth et al., 2019) we extend this

695        deformation belt towards the southwest up to the town of Szigetvár. The southwestern extension

696        contains the Bonyhád fault zone joining to the Northern Imbricate Zone of the Mecsek Mts.,

697        the Bakóca and Hetvehely-Magyarszék faults, and the Mecsekalja fault zone (*Fig. 17a*). These

698        tectonic elements seem to accommodate most of the young deformations (e.g., Tari, 1992;

699        Horváth et al., unpubl., 2019; Csontos et al., 2002; Wórum and Hámori, unpubl.; Konrád and

700        Sebe, 2010; Kovács et al., 2018) southwest of the river Danube, whereas only minor, westward

701        diminishing neotectonic faulting appears along the western Kapos fault (Horváth et al., 2019).

702        The same holds true for the Balaton-Tóalmás fault zone west of the town Marcali, where folding

703        dominates the neotectonic deformation instead of near surface faulting (see Section 6.2.).

704        Towards the East intensive near surface neotectonic faulting along the Mid-Hungarian mobile

705        belt seems to diminish near the towns Jászberény and Szolnok

706        (<http://dx.doi.org/10.17632/dnjt9cmj87.1>). Hence, our study does not verify the presence of

707        regional-scale neotectonic strike-slip shear zones crosscutting the entire territory of Hungary

708        (c.f., Horváth et al., 2009). Although near-surface neotectonic faulting is not continuous, our

709        detailed mapping suggests that the northernmost root zone of the Balaton-Tóalmás fault zone

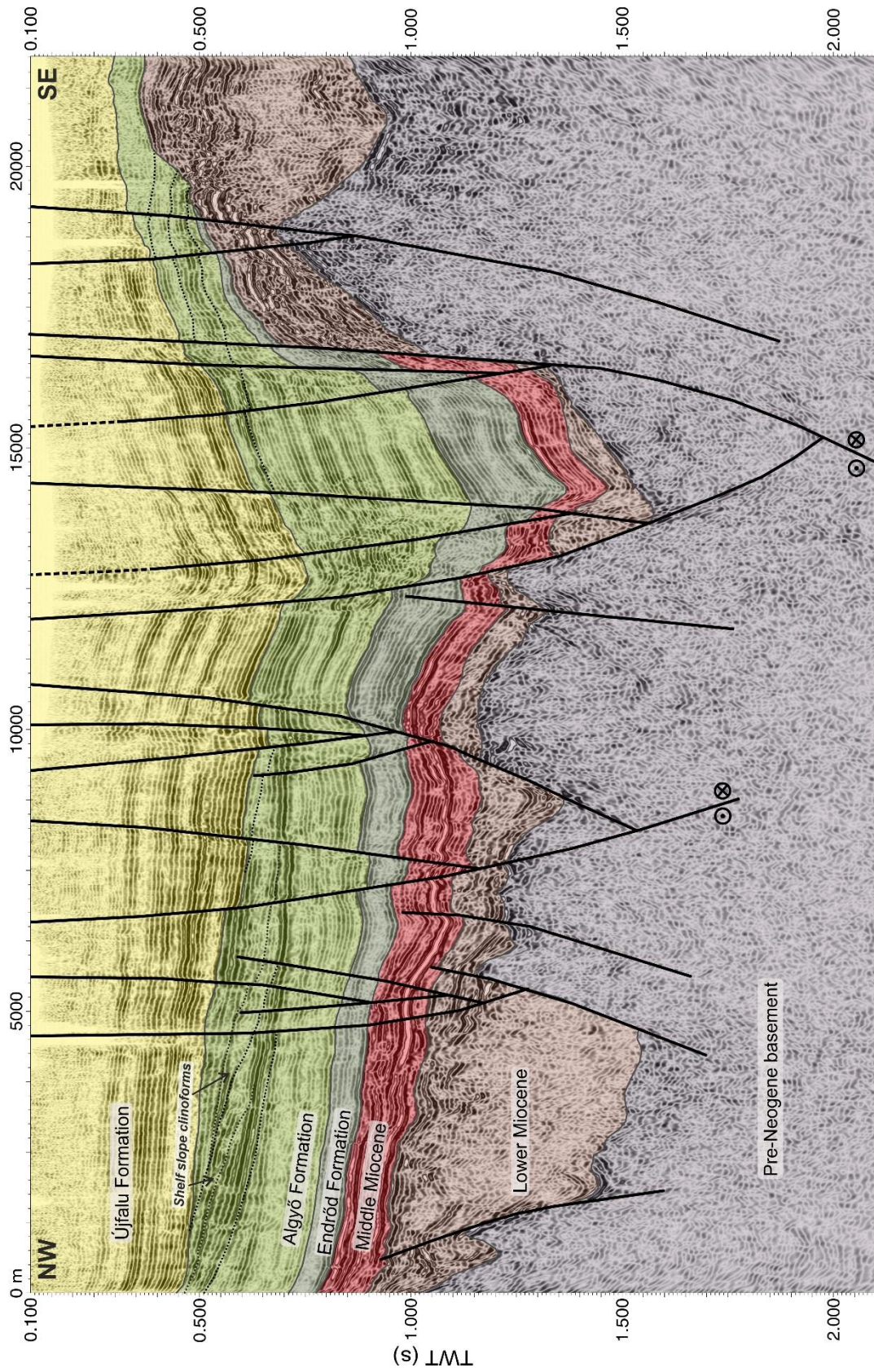
710 (i.e., the Tápió-Tóalmás fault; Ruszkiczay-Rüdiger et al., 2007) towards the east is connected  
711 to the ENE–WSW striking boundary fault system of the Vatta-Maklár trough showing  
712 prominent neotectonic reactivation. East of the Vatta-Maklár trough the continuation is  
713 uncertain due to lack of seismic data, its correlation with the neotectonically active Hernád fault  
714 towards the northeast is highly model-driven and was primarily based on gravity data.

715 Although poorly constrained below the thick Miocene volcanites we share the view of Fülöp  
716 and Dank (1987) that the prominent, well-expressed fault zone between Dabas and Albertirsa  
717 continues towards the northeast into the Nyírség area (through the localities of Polgár and  
718 Tiszavasvári; see also <http://dx.doi.org/10.17632/dnjt9cmj87.1>). This interpretation is in line  
719 with tectonic restorations connecting the Bogdan-Voda Dragos-Voda fault system of the  
720 Eastern Carpathians (*Fig. 1*) to the Mid-Hungarian Fault Zone (Györfi et al., 1999; Tischler et  
721 al., 2007). The Nyírség area (underlain mostly by Miocene volcanics) was a former neotectonic  
722 “white patch” of the country. Our new mapping revealed here a predominate ENE–WSW and  
723 (N)NE–(S)SW oriented neotectonic fault pattern, similarly to the western parts of the Central  
724 Hungary domain.

725 Our study has managed to reveal not only the internal fine structure, but also the regional  
726 structural relationships of the Mid-Hungarian mobile belt in such details that were not seen  
727 before. As well-reflected also on the background Bouguer anomaly image of the new map the  
728 Mid-Hungarian mobile belt is made up of a system of NE–SW and ENE–WSW oriented,  
729 elongated morphological elements (e.g., small basins at Adony, Örkény and Bonyhád for  
730 example, and a set of en-echelon oriented narrow highs between the municipality of Pincehely  
731 and Lajosmizse, <http://dx.doi.org/10.17632/dnjt9cmj87.1>). These morphological units are  
732 bounded by faults (e.g., the Paks-Szabadszállás, Kalocsa-Szabadszállás-Lajosmizse,  
733 Kecskemét-Nagykőrös-Abony and the fault system in the Tiszakécske-Szolnok area), which all  
734 connect to the Kapos fault (and less clearly to the Mid-Hungarian fault zone in the north). These

735 elements are all characterized by pronounced neotectonic activity represented by a complex  
736 system of individual en-echelon faults in the young sedimentary section. The internal structure  
737 of these fault zones generally show typical flower structures on the seismic profiles recording  
738 strike-slip tectonics along them (*Fig. 18*) being in agreement with previous results obtained for  
739 the various elements of the Mid-Hungarian mobile belt (Pogácsás et al., 1989; Detzky Lőrincz  
740 1997; Tóth and Horváth, 1997; Csontos and Nagymarosy, 1998; Detzky Lőrincz et al., 2002;  
741 Tóth, unpubl.; Csontos et al., 2005; Fodor et al., 2005a-b; Ruszkiczay-Rüdiger et al., 2007;  
742 Bada et al., 2010; Palotai and Csontos, 2010; Várkonyi, unpubl.; Várkonyi et al., 2013; Juhász  
743 et al., 2013; Visnovitz et al., 2015; Horváth et al., 2019).

744 The fine internal structure of these fault zones, together with the overall alignment and  
745 geometry of the morphological elements mentioned above suggests a general left-lateral shear  
746 between the Kapos and Balaton-Tóalmás faults both during the Middle Miocene and the  
747 neotectonic deformation phase. This large scale shearing and deformation is manifested both  
748 on a local (individual (N)NE–(S)SW oriented, en-echelon Riedel or oblique-slip faults) and on  
749 the meso-scale (en-echelon/shear duplex geometry of the larger morphological elements — pull  
750 apart basins and horsts — within this mega-shear). Based purely on neotectonic fault pattern  
751 analysis, the largest fault offsets are occurring along the boundary of this shear zone (NE of the  
752 municipality of Gyömrő along the Tóalmás fault and north of Kalocsa along the Kapos fault),  
753 where the individual neotectonic Riedel faults were crosscut/replaced by subsequently  
754 developed Y-faults creating 20–25km long continuous fault segments above the PDZs.



755

756 *Fig. 18. Neotectonic strike-slip faulting in the Bonyhád basin associated with typical flower*

757 *structures. For location see Figure 17a*



758 Neotectonic fault reactivation occurring along the complex, interconnected network of ENE–  
759 WSW and NE–SW striking faults are bounding transtensional/transpressional fault domains  
760 and strike-slip duplexes (see also Fodor, unpubl.). Neotectonic transtensional/transpressional  
761 fault reactivation seems to be basically the function of structural orientation indicating a  
762 consistent, ~NNE–SSW oriented maximum horizontal stress direction during the neotectonic  
763 phase: transtension is namely connected to ~NE–SW striking fault segments (see e.g., Horváth  
764 et al., 2019), whereas transpression appears along ~E–W (Mecsekfalja fault zone near  
765 Szentlőrinc, Northern Imbricate Zone of the Mecsek Mts (Tari, 1992)), or WNW–ESE (Palotai  
766 and Csontos, 2010) oriented fault segments. As suggested by the identified overall neotectonic  
767 fault pattern (<http://dx.doi.org/10.17632/dnjt9cmj87.1>), transpressional reactivation rather  
768 occurred only at certain segments of the ENE–WSW striking Tóalmás fault zone than along the  
769 entire fault (Ruszkiczay-Rüdiger et al., 2007; Palotai and Csontos, 2010).

770 The predominant ENE–WSW and NE–SW structural trends of the belt are explicitly reflected  
771 both in gravity data (<http://dx.doi.org/10.17632/dnjt9cmj87.1>) and the basement structure  
772 (Fülöp and Dank, 1987; Haas et al., 2010). Their origin was related essentially to the Early  
773 Miocene juxtaposition of the Alcapa and Tisza-Dacia megaunits (see also Section 2. and *Fig.*  
774 *1*) by large-scale horizontal movements along the Mid-Hungarian Fault Zone. However, the  
775 observed neotectonic fault pattern indicates that the easily reactivating weakness zones of the  
776 crust only partly coincide with the presently known tectonic boundaries of major pre-Tertiary  
777 units (*Fig. 8*), and even if this relationship exists in certain segments it can rapidly change along  
778 strike.

#### 779 Southern Danube-Tisza interfluvium

780 Neotectonic deformation in this area has resulted in a more complex fault pattern than in the  
781 adjacent Mid-Hungarian mobile belt, since previously not considered NNW–SSE and N–S  
782 oriented fault systems also appear (<http://dx.doi.org/10.17632/dnjt9cmj87.1>) beside the

783 prevailing ENE–WSW and (N)NE–(S)SW structural trends. NNW–SSE and N–S striking  
784 neotectonic faults occur mostly at the margins of shallow seated basement blocks (Miske,  
785 Sükösd-Rém and Jánoshalma basement highs) in the northern part of the area that form the  
786 direct eastern continuation of the outcropping Mecsek and shallow subsurface Villány (i.e., the  
787 Máriakéménd zone) nappes of the Tisza-Dacia megaunit. The underlying faults were probably  
788 formed during Miocene extension similarly to the major, NW–SE striking synrift faults in the  
789 adjacent Southeast Hungary domain (see Section 6.5.). The small, elongated basin bounded by  
790 such NNW–SSE to N–S striking faults at the town of Baja  
791 (<http://dx.doi.org/10.17632/dnjt9cmj87.1>) gives a typical example. Identified NNW–SSE  
792 striking roots display a significantly more complex geometry in the pre-Cenozoic basement  
793 than shown previously (Haas et al., 2010).

794 The most prominent neotectonic element of this area is the ENE–WSW striking  
795 Bácszentgyörgy-Tompa fault zone (Pogácsás et al., 1989; referred as Tompa fault on *Fig. 17a*)  
796 separating the elongated Tompa-Madaras basement high and the Bácsalmás basin.  
797 Characteristic Riedel fault pattern indicates sinistral kinematics along this major fault  
798 (<http://dx.doi.org/10.17632/dnjt9cmj87.1>). Its root zone is represented by a steeply, NNW-  
799 dipping Miocene border fault running roughly parallel to the inferred nearby Cretaceous nappe  
800 contact of the Villány and Békés-Codru units (Haas et al., 2010; *Fig. 8*) suggesting a possible,  
801 but in details not studied connection between the two.

802 The sigmoid shape of the Bácsalmás depression, as well as the geometry of the bounding ENE–  
803 WSW and (N)NE–(S)SW striking fault system argues for its pull-apart origin during Miocene  
804 tension/transtension in a left-lateral strike-slip shear zone. Moreover, this basin is divided into  
805 two smaller, elongated subbasins by a NNE–SSW oriented narrow ridge as shown both by the  
806 Bouguer residual anomaly map and the seismic sections. Most of the bounding faults, including  
807 the fault underlying the mentioned narrow ridge, were — at least partly — reactivated during

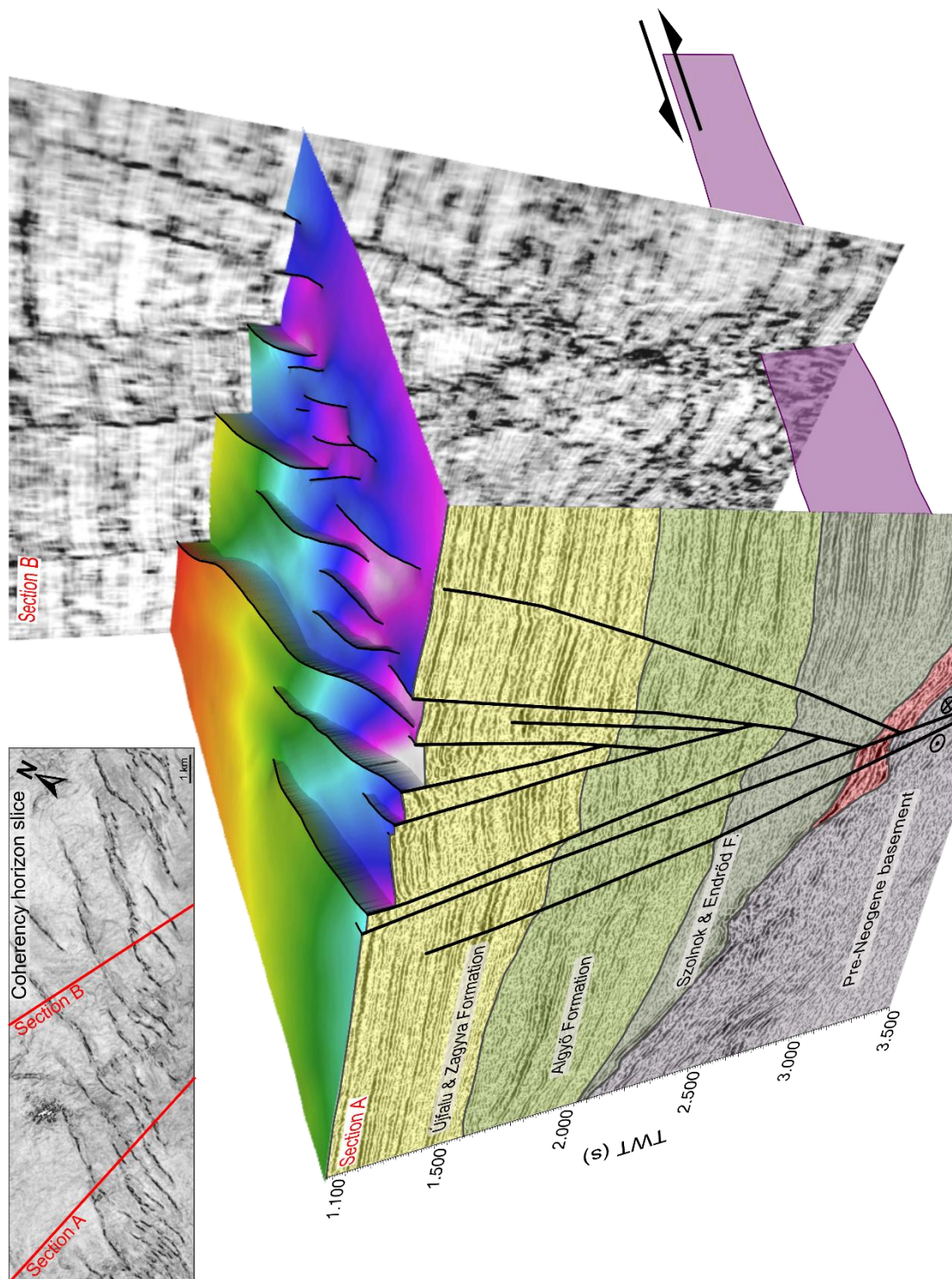
808 the neotectonic phase. The map view arrangement of the individual (N)NE–(S)SW striking fault  
809 branches joining to the major ENE–WSW striking fault zone suggest sinistral kinematics,  
810 similarly to the observed Riedel fault pattern further to the east. Although at a much smaller  
811 scale, but the overall alignment of the deformation pattern in this area is similar to the shearing  
812 within the Mid-Hungarian mobile belt discussed above, where the sinistral deformation occurs  
813 along a wide zone and is reflected both in the local and in the meso-scale tectonic features.

#### 814 Eastern Great Hungarian Plain

815 The neotectonic deformation pattern in the eastern part of the Great Hungarian Plain is similar,  
816 yet very different from that of the other parts of the Central Hungary domain. In general ENE–  
817 WSW and NE–SW striking faults dominate here as well, but NNW–SSE, N–S and locally E–  
818 W oriented fault systems and associated fault-related folds also occur  
819 (<http://dx.doi.org/10.17632/dnjt9cmj87.1>). These structural trends seem to appear in smaller,  
820 spatially separated areas creating for a first glance a “diffuse”, patchy network of variably  
821 oriented faults/fault systems without any well-defined regional trend. Although deep-seated  
822 structural connection seems to exist (see pre-Pannonian fault pattern), the neotectonic near-  
823 surface deformation in this area cannot be considered as the eastern continuation of the  
824 deformation zone in the Mid-Hungarian mobile belt, which appears to diminish near  
825 Törökszentmiklós.

826 NNW–SSE, N–S and subordinate E–W striking neotectonic faults occur mainly in the northern  
827 part of the area. The roots of these faults north of the city Debrecen bound small (half)grabens  
828 and horsts in the pre-Pannonian basement that were most probably formed during E(SE)–  
829 W(NW) directed Middle Miocene tension (e.g. Fodor et al., 1999). Such structures were also  
830 identified further to the southwest (near the towns of Hajdúszoboszló, Püspökladány and  
831 Kunhegyes).

832 South of this area the ENE–WSW oriented, well-documented Derecske fault zone forms the  
 833 most prominent neotectonic element (*Fig. 19*) between the Hungarian/Romanian national  
 834 border and the Biharnagybajom basement high (<http://dx.doi.org/10.17632/dnjt9cmj87.1>).



835  
 836 *Fig. 19. Neotectonic sinistral strike-slip faulting in the Derecske through as indicated by the*  
 837 *characteristic Riedel fault array observed on the coherency horizon slice (upper left) mapped*

838 *within the alluvial plain deposits. Cross sections A and B (locations shown by red lines on the*  
839 *coherency horizon slice) show typical negative flower structure. For location see Figure 17b*

840 The Érmellék earthquake with estimated magnitude of 6.2 in 1834 was directly related to its  
841 eastern continuation in Romania associated with faults reaching even the surface. The fault zone  
842 runs along the northern margin of the Derecske trough and is characterized by a typical Riedel  
843 fault array indicating sinistral shearing (*Fig. 19*) as also indicated by several tectono-  
844 sedimentological and modelling studies (Lemberkovics et al., 2005, Windhoffer and Bada,  
845 2005; Windhoffer et al., 2005). Interestingly, Riedel fault array changes to anastomosing,  
846 subparallel network of faults with rare Riedel elements above the Biharnagybajom high, which  
847 (as confirmed by seismic data) forms the direct western continuation of the Derecske fault zone.  
848 Correlation of its pre-Pannonian roots towards the southwest and west indicates a structural  
849 connection with the NE–SW oriented Dévaványa-Gyomaendrőd and possibly also with the  
850 Túrkeve and Mezőtúr basement highs. Near surface faulting appears all above(/near) these  
851 basement highs, showing dominantly an anastomosing fault pattern.

852 Balázs et al. (2016, 2018) recently proposed the compaction origin of the faults above the  
853 Dévaványa and Túrkeve highs based on various criteria. Without doubt typical Riedel fault  
854 pattern and significant lateral offset are missing above the mentioned highs, instead, a network  
855 of anastomosing, subparallel faults appear forming characteristic flower structures in a cross  
856 section (Balázs et al., 2018). Similar neotectonic fault pattern, however, exists elsewhere in the  
857 broader area (near the town of Paks (Horváth et al., 2019), Biharnagybajom, SW of Komádi),  
858 where the tectonic origin is unquestionable. Among these the Biharnagybajom high represents  
859 the direct western continuation of the Derecske fault zone without any interruption in  
860 neotectonic activity. Therefore, the change in the fault segment geometry from typical en  
861 echelon array to anastomosing, subparallel pattern above this high is rather attributed to the

862 strongly changing basement morphology (and/or root zone geometry) than to the change in  
863 faulting mechanism (i.e., from tectonic to compaction faulting).

864 Seismic sections across fault systems of tectonic origin developed above basement highs  
865 generally show characteristic flower structures and direct rooting into underlying pre-  
866 Pannonian fault(s). Literature data indicate, however, that compaction faults typically form  
867 standalone (Misra, 2018; like those developed at the margins of the Algyó high,  
868 <http://dx.doi.org/10.17632/dnjt9cmj87.1>), graben-like (Maillard et. al., 2003), or locally, a set  
869 of uniformly dipping or conjugate, usually rootless structures (Williams, 1987, Xu et. al., 2015).  
870 Flower structures of compactional origin with roots in the basement are explicitly rare (e.g., Xu  
871 et. al., 2015).

872 Taking the above mentioned characteristics and different structural interpretations into account,  
873 we classified the localized young faults above these basement highs with anastomosing,  
874 subparallel fault geometry as faults with uncertain/debated origin, but with a bias toward  
875 tectonics. Observed seismicity (Tóth et al., 2020) seems to support the tectonic origin of the  
876 fault systems developed above the Biharnagybajom, Dévaványa-Gyomaendrőd, Endrőd-  
877 Szarvas, Szeghalom, Komádi and Kismarja basement highs (*Fig 17b*). If one accepts their  
878 tectonic origin the neotectonic fault pattern and the overall alignment of the deformation zones  
879 in Eastern Hungary resemble the elements of a wide, left-lateral shear zone being in agreement  
880 with the deformation style identified further to the west. The main participants of this large-  
881 scale sigmoid shape, often fragmented shear zone includes the Derecske fault, the fault system  
882 above the Dévaványa-Gyomaendrőd highs as well as the fault zones developed along the  
883 Komádi-Biharkeresztes and Kismarja highs.

884 *6.5. Southeast Hungary*

885 This domain (*Fig. 8*) hosts the deepest depocenters (Szeged and Békés basins, Makó trough;  
886 *Fig. 1*) in the whole Pannonian Basin. It is largely covered by modern 3D seismic volumes  
887 providing excellent opportunity for the identification of neotectonic deformations (*Fig. 3*).  
888 Despite of this practically no neotectonic activity was identified, representing the most striking  
889 and surprising characteristic of this domain. Identified rare young faults (both with tectonic and  
890 atectonic origin) strike NW–SE at the margins of the Békés and Szeged basins  
891 (<http://dx.doi.org/10.17632/dnjt9cmj87.1>) underlain by major Neogene faults (Haas et al.,  
892 2010) formed during Miocene basin formation (see e.g., Tari et al., 1999). The general lack of  
893 NE–SW striking neotectonic faults is an important difference compared to the adjacent Central  
894 Hungary domain (see Section 6.4.).

895 The “missing” neotectonic activity is a still poorly understood feature of this domain, especially  
896 in comparison to the adjacent Central Hungary domain. On one hand, the neotectonic  
897 reactivation of the predominant NW–SE striking faults might have been hampered by the  
898 unfavorable orientation of the neotectonic stress field characterized by a ca. NE–SW directed  
899 maximum horizontal stress axis in this area (Bada, 1999; Bada et al., 1999, 2007; Horváth et  
900 al., 2006a).

901 On the other, recent claybox modelling study of Hatem et al. (2017) draws the attention to the  
902 importance of the depth of basal shear, and the presence of preexisting faults in strike-slip fault  
903 development, fault complexity and the kinematic efficiency of a fault zone. Considering their  
904 modelling results and scaling factors an estimated 750–1800m of lateral displacement is  
905 required along a deep-seated, localized PDZ (3–6km, similar to the Neogene thickness in SE  
906 Hungary) in the basement until distributed shear becomes focused and the first Riedel shears  
907 appear near the surface. The same amount of displacement in case of a shallow-seated PDZ  
908 (1.5–3km) is more than enough to produce interaction and propagation of Riedel shears  
909 resulting in a well-developed Riedel system above the PDZ (for more details see also Section

910 6.7.). In other words, it is speculated, that the thick sedimentary cover and/or the smaller  
911 displacement along the basal PDZ-s in SE Hungary compared to other parts of the country  
912 simply did not “allow” the formation of neotectonic faults within the Late Miocene–Pliocene  
913 sequence. The exact background of this phenomenon should be addressed by further detailed  
914 (modelling) studies.

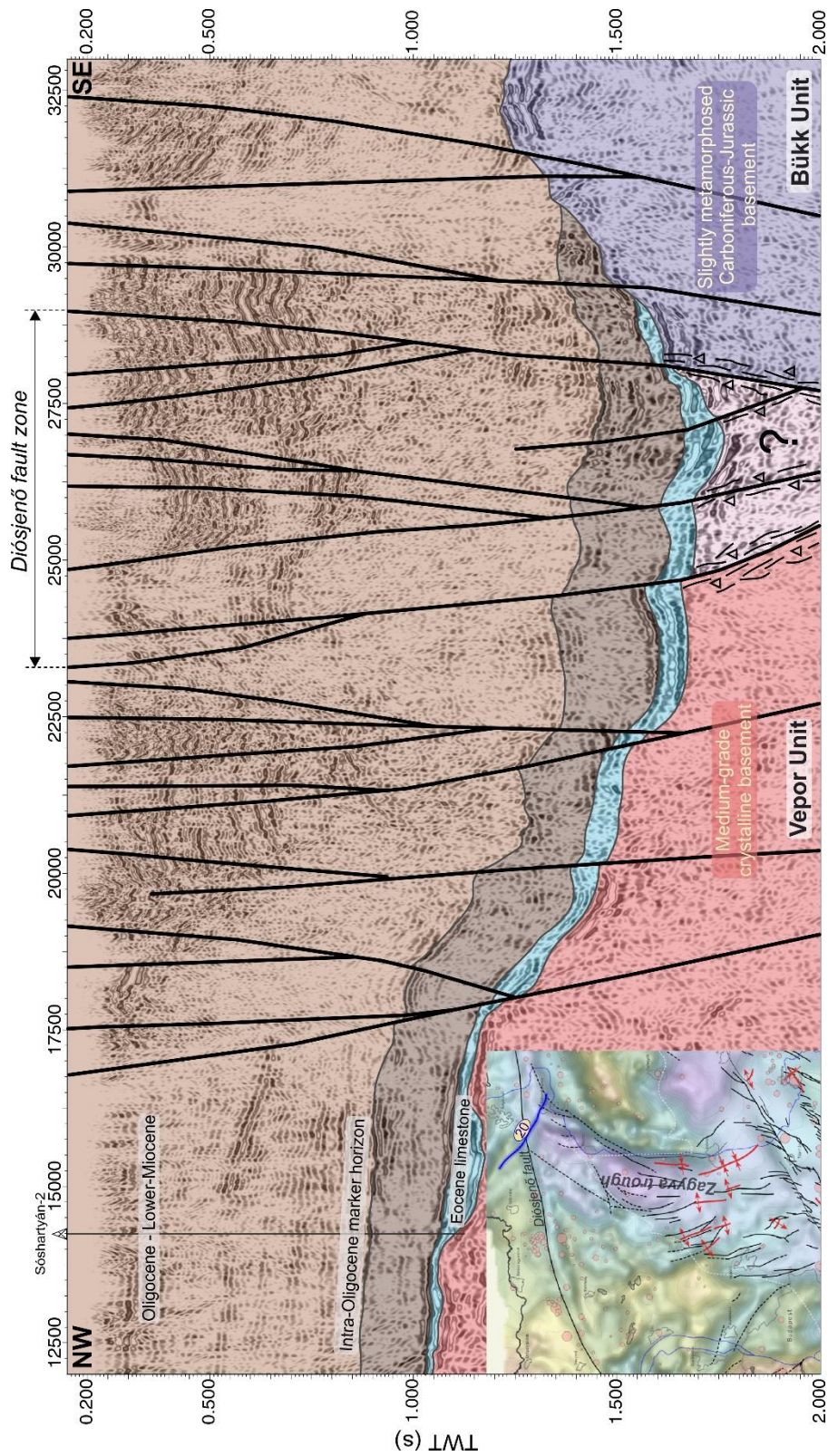
#### 915 6.6. Zagyva trough

916 The neotectonic deformation pattern in the Zagyva trough includes NNW–SSE oriented faults  
917 and fault-related folds in the southern part of the domain, but towards the North the general  
918 orientation gradually changes to NE–SW along the trough axis  
919 (<http://dx.doi.org/10.17632/dnjt9cmj87.1>). The overall neotectonic deformation pattern  
920 displays a pronounced contrast compared to the adjacent areas: in the south the bounding  
921 Balaton-Tóalmás fault (see also Section 6.4.) and the whole Central Hungary domain in general  
922 are characterized by prevailing ENE–WSW oriented structures. To the west a prominent  
923 Neogene NW–SE striking fault system (Haas et al., 2010) appears that developed during the  
924 synrift phase (Fodor et al., 1999; Fodor, unpubl.). Certain elements of this system might have  
925 been neotectonically reactivated (<http://dx.doi.org/10.17632/dnjt9cmj87.1>) considering the  
926 results of detailed single- and multi-channel seismic surveys carried out on the river Danube  
927 (Oláh et al., 2014), as well as outcomes of surface geological studies in the nearby Buda Mts.  
928 (Fodor et al., 1994; Korpás et al., 2002; Palotai et al., 2012).

929 In the north the Zagyva through is bounded by the ENE–WSW striking Hrubanovo-Diósjenő  
930 fault (referred as Diósjenő fault on *Fig. 8*) forming a first-order tectonic boundary that separates  
931 the Transdanubian Range and Bükk units from the Veporic and Gemeric units of the Inner  
932 Western Carpathians (Balla, 1989; Haas et al., 2010). Despite the absence of post-rift strata and  
933 poor seismic coverage (*Fig. 3*) the prominent seismicity (Tóth et al., 2020) suggests the  
934 neotectonic activity of this element being in agreement with the results from the Slovakian part



935 of Danube basin (Kováč et al., 2002). Although Middle Miocene and younger Neogene  
936 sediments are missing, available seismic data indicate intense faulting even within the  
937 shallowest imaged late Paleogene to earliest Miocene strata along this fault zone (*Fig. 20*). The  
938 age of faulting can not be determined more precisely (at least Neogene), however, the evidences  
939 introduced above strongly support the neotectonic classification of this fault.



940

941 *Fig. 20. Seismic profile crossing the Hrubanovo-Díósjenő fault zone displacing Paleogene–*

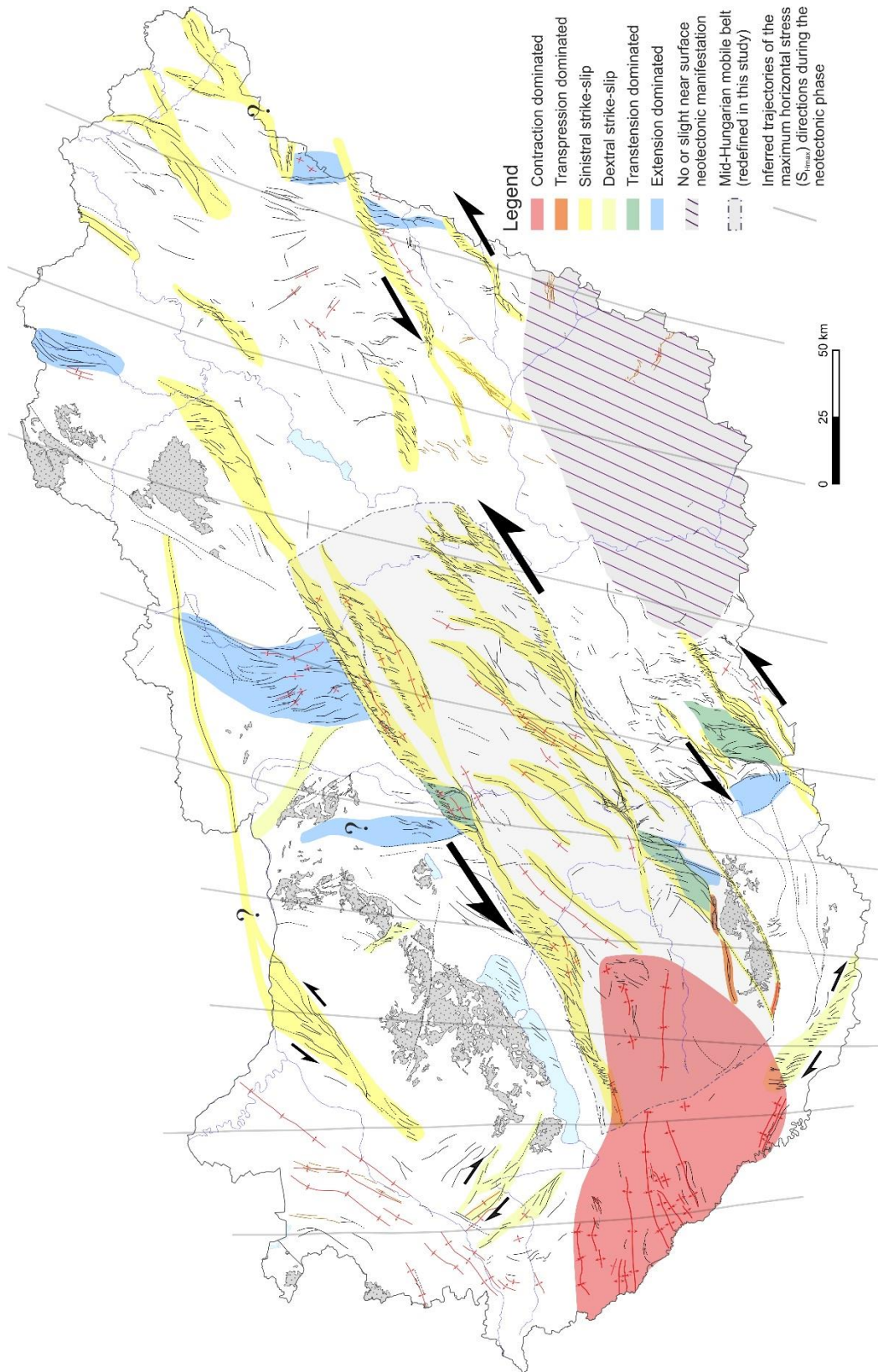
942 *Earliest Miocene strata. For location see inset map at lower left, legend given in Fig. 9.*

943 The “anomalous” neotectonic structural trend of the Zagyva through agrees with that of the  
944 underlying fault system formed basically during the Middle Miocene rifting phase of the  
945 Pannonian basin (e.g., Benkovics, unpubl.; Tari et al., 1992; Tari, unpubl.; Fodor et al., 1999;  
946 Fodor, unpubl.; Soós, unpubl.), and is well reflected in the Bouguer anomaly map  
947 (<http://dx.doi.org/10.17632/dnjt9cmj87.1>). Further to southwest the small Kajászó basin  
948 (Dudko, 1988; Horváth et al., 2004) between the river Danube and the lake Velence represents  
949 a structurally (Balla et al., 1987) largely analogous area north of the Tóalmás-Balaton fault zone  
950 characterized by similar N–S oriented neotectonic fault pattern and associated recent seismicity  
951 (Tóth et al., 2020; *Fig. 17a*).

952 Regarding the regional structural pattern introduced above we propose that the Zagyva through  
953 was formed and acted as an important transfer zone during the Miocene and neotectonic phases  
954 accommodating extension by a complex set of normal faults (Soós, 2017) between the left-  
955 lateral (Fodor et al., 1999; Fodor, unpubl.) Tóalmás-Tápió fault in the south and the similarly  
956 oriented Hrubanovo-Diósjenő fault in the north (*Fig. 21*). Mapping results show significant  
957 neotectonic activity along this complex fault system with sinistral kinematics along the  
958 Tóalmás-Tápió fault (see Section 6.4.), whereas sinistral shear is also supposed along the  
959 Hrubanovo-Diósjenő fault based on its orientation and obtained stress field data for the  
960 neotectonic phase (Bada, 1999; Bada et al., 1999, 2007, Fodor et al., 2005a, Ruzkiczay-  
961 Rüdiger et al., 2007). This model can explain the decreasing (and diminishing) neotectonic  
962 activity along the Tóalmás-Tápió fault east of the Zagyva trough, since deformation was more  
963 accommodated by the transfer zone (i.e., the Zagyva trough itself) and the Hrubanovo-Diósjenő  
964 fault in the north. The basic kinematic characteristics in the Zagyva trough seem to be largely  
965 stable during the Late Neogene that is compatible with determined late Middle Miocene stress  
966 field evolution characterized basically by ca. E–W oriented, minimum horizontal stress axis  
967 ( $\sigma_3$ ) (Fodor et al., 1999, 2005a; Ruzkiczay-Rüdiger et al., 2007; Fodor, unpubl.).

968 6.7. *General kinematics*

969 Summarizing all observations on neotectonic fault kinematics a fairly consistent pattern is seen  
970 in the whole country: sinistral and dextral shear occurs along (E)NE–(W)SW (e.g., the Balaton-  
971 Tóalmás-, Balatonfő-, Kapos-, Bácsszentgyörgy-Tompa, Derecske fault zones), and (W)NW–  
972 (E)SE oriented (e.g., Szulok-Sellye-Cún or southeast Danube basin) fault zones, respectively,  
973 while ca. N–S oriented structures usually exhibit normal faulting/pull apart nature and were  
974 often acted as transfer zones (e.g. Zagyva trough) between the various strike-slip shear zones  
975 (*Fig. 21*).



976

977 *Fig. 21. Kinematic interpretation of the mapped tectonic deformations. For the legend of the*

978

*mapped structures see Fig. 9.*

979 The map scale pattern of the individual fault branches, as well as the overall alignment and  
980 geometry of the various fault zones and morphological elements within the redefined Mid-  
981 Hungarian mobile belt, the Danube-Tisza interfluve and Eastern Hungary (Section 6.4.) are all  
982 compatible with the sinistral shear sense deduced from the detailed fault patterns mapped within  
983 the individual shear zones. This is in agreement with the results of earlier studies (e.g., Pogácsás  
984 et al., 1989; Detzky Lőrincz et al., 2002; Horváth et al., 2006a, 2009; Fodor et al., 2005a-b;  
985 Bada et al., 2006, 2007; Ruzsiczay-Rüdiger et al., 2007). Considering also the E–W trending  
986 neotectonic compression-related folds in the west (i.e., the Zala domain; see Section 6.2.) and  
987 similarly oriented transpression/compression-related reverse faults/imbricated structures in the  
988 south (i.e., at the northern and southern margins of the Mecsek Mts.; see e.g., Wein, 1961;  
989 Hámor, 1966; Wéber, 1977; Némedi Varga, 1983; Tari, 1992; Csontos et al., 2002; Wórum and  
990 Hámori, unpubl.; Konrád and Sebe, 2010; Kovács et al., 2018) a N–S oriented and eastward  
991 slightly rotating maximum horizontal stress axis ( $\sigma_1$ ) can be envisaged on a basin scale during  
992 the neotectonic phase (*Fig. 21*). The mapped deformation pattern clearly shows a dominant  
993 strike-slip stress regime associated with an E–W to ESE–WNW oriented horizontal minimum  
994 stress axis ( $\sigma_3$ ) except for the westernmost part of the country, where a compressional stress  
995 regime associated with E–W oriented folding prevailed. This regional (paleo)stress pattern,  
996 inferred from the mapped fault pattern directly related to the stress field during neotectonic fault  
997 genesis, explains well the observed neotectonic features and, in basic tendencies, shows  
998 similarities with the recent stress field orientation (Bada 1999, Bada et al., 1999, 2007). One of  
999 the main differences is that a significantly smaller rotation of the maximum horizontal stress  
1000 axis was inferred towards the northeast compared to the recent stress pattern, which (being  
1001 parallel to it) cannot explain adequately the sinistral fault reactivations, for example along the  
1002 Derecske fault zone. The deduced general stress field orientation fits basically well to the  
1003 reported neotectonic stress field orientations varying between (N)NW–(S)SE and (N)NE–

1004 (S)SW determined either for the entire Pannonian basin (Bada, 1999; Fodor et al., 1999; Gerner  
1005 et al., 1999), or at local scale within the basin (Bergerat and Csontos, 1988; Pogácsás et al.,  
1006 1989; Tari, 1992; Csontos and Bergerat, 1993; Detzky Lőrincz, 1997; Tomljenović and  
1007 Csontos, 2001; Detzky Lőrincz et al., 2002; Fodor et al., 2002, 2008; Márton et al., 2002;  
1008 Csontos et al., 2002, 2005; Konrád and Sebe, 2010; Skorday, unpubl.; Bodor, unpubl.;  
1009 Várkonyi, unpubl.; Várkonyi et al., 2013; Visnovitz et al., 2015; Petrik, unpubl.; Kovács et al.,  
1010 2018; Beke et al., 2019; Budai, 2019; Héja, unpubl.).

1011 There are only few efforts published in the past estimating the magnitude of displacement  
1012 occurred along the various neotectonic strike-slip fault zones in the country. Early estimations  
1013 using 2D seismic data provided a sinistral offset of approximately 5–10 kilometers along  
1014 various segments (Kiskőrös, Szolnok) of the Kapos fault zone for the Late Miocene–Quaternary  
1015 interval (Pogácsás et al., 1989; Detzky Lőrincz, 1997). Along the Derecske fault zone a total  
1016 sinistral offset of 4.5–6 km was estimated based on a sequence stratigraphic approach  
1017 (Lemberkovics et al., 2005), whereas a typical offset range of several hundreds of meters was  
1018 inferred for the individual fault segments. Horizontal displacement along the Balatonfő fault  
1019 (below Lake Balaton) amounts several hundreds of meters based on the analysis of ultra-high  
1020 resolution water seismic data (Visnovitz et al., 2015). Using former results deriving from 3D  
1021 seismic data (Várkonyi et al., 2013) the left-lateral horizontal offset in the Late Miocene–  
1022 Pliocene strata was estimated about 1.0–1.5 km along the 3–4 km wide Balaton fault zone in  
1023 the Buzsák area (Visnovitz et al., 2015).

1024 The drawback of these estimations that they are usually based on correlation of various linear  
1025 elements identified within the Late Miocene–Pliocene sequence thought to be interconnected  
1026 originally on the opposite sides of a fault zone. On one hand this method is highly uncertain in  
1027 our opinion, and on the other it does not take into account that significant displacement needs  
1028 to occur along a deep-seated PDZ until the first shear deformations (i.e., Riedel shears) appear

1029 near the surface (i.e., Hatem et al., 2017). Following the strike-slip faulting stage classification  
1030 used by Hatem et al. (2017) and Crider and Peacock (2004) majority of the strike-slip  
1031 deformation developed in Hungary reached Stages I and II only (development of en-echelon  
1032 faults, and their subsequent interaction and propagation). The best, textbook examples of these  
1033 stages of deformation are represented by the Derecske, Sellye and Balaton fault systems. Stage  
1034 III deformation (slip along a through-going fault) in our view occurred only along the Tóalmás  
1035 fault near the municipality of Gyömrő, along the Kapos-east fault North of Kalocsa and perhaps  
1036 along the Bácszentgyörgy-Tompa fault near Tompa, based purely on analysis of the  
1037 nearsurface neotectonic fault pattern.

1038 An effort was made to estimate possible displacement along typical neotectonic faults in  
1039 Hungary using the modelling results and scaling factors of Hatem et al. (2017). Using wet  
1040 kaolin claybox models calibrated and scaled to the strength and length of the crust (10 mm in  
1041 the claybox is equivalent to 500–1200 m of continental crust) these authors investigated the  
1042 relationship between the amount of displacement along PDZ-s buried at various depths and the  
1043 style as well as the evolution of near surface faulting above the PDZ. It was determined how  
1044 much cumulative slip along the buried PDZ was required in order to develop the characteristic  
1045 fault patterns of the well-distinguished deformation stages (0-III) at the surface. Considering a  
1046 typical PDZ depth of 1.5–3km in the Pannonian basin (corresponding to the ULS model of  
1047 Hatem et al. 2017) a 1000–2500m and 1200–3000m of displacement is required along the PDZ  
1048 in the basement to develop a Stage II Riedel system seen along the eastern Derecske fault and  
1049 a Stage III deformation seen along the Tóalmás fault, respectively (20 and 25 mm of  
1050 displacement in Fig. 5a of Hatem et al., 2017). It needs to be emphasized, that these estimations  
1051 are referring to displacement along the PDZ in the basement and not along fault planes  
1052 developed in the Late Miocene–Pliocene sequence, indicating that displacement estimation



1053 methods using Late Miocene–Pliocene features significantly overestimate the real  
1054 displacement.

1055 In summary, we think that neotectonic displacement magnitudes along the major fault zones  
1056 are probably less than previously anticipated and are in the order of maximum 2–3 kilometers  
1057 along their PDZ-s, even along the most prominent neotectonic shear zones during the  
1058 neotectonic phase. Comparing to recent active strike-slip zones in the world the neotectonic  
1059 deformation phase in Hungary can be considered as a rather weak tectonic event caused  
1060 primarily by the continuous northward indentation of the Adriatic microplate (“Adria-push”;  
1061 Bada et al., 2007) affecting a completely landlocked basin.

## 1062 *7. Conclusions*

1063 1. The new map of young geological deformations in Hungary presented in this paper provides  
1064 a detailed and significantly more accurate definition (actual position, extension and geometry)  
1065 of young deformations compared to previous studies. Based on nearly 2900 2D seismic profiles  
1066 and 70 3D seismic volumes, as well as the results of former regional neotectonic syntheses and  
1067 many local studies, the new map includes all important deformation structures (faults and folds,  
1068 both tectonic and atectonic) related to the neotectonic evolutionary phase of the Pannonian  
1069 basin, except for large-wavelength, drape-over folds formed due to the differential compaction  
1070 of the young sedimentary pile. Beside near surface structures the new map also displays the  
1071 pre-Pannonian root zones of the neotectonic faults, aiding the better understanding of the  
1072 geometric and genetic relationships between the shallow and deep-seated structures.

1073 2. The new map allowed the identification of several neotectonic domains with markedly  
1074 different deformation patterns. In all domains the neotectonic fault pattern clearly reflects the  
1075 control of identically oriented pre-Pannonian (mostly synrift) fault systems during the  
1076 neotectonic phase. Markedly different orientations of neotectonic structures indicate important  
1077 differences in the overall orientation of the underlying tectonic fabric. These observations

1078 clearly demonstrate that neotectonic activity is predominantly due to the reactivation of pre-  
1079 existing structures all over the Pannonian basin, as also indicated by previous studies.

1080 3. Despite experiencing the largest Middle- to Late Miocene extension and the formation of the  
1081 deepest depocenters in the whole Pannonian basin, SE Hungary practically lacks any observable  
1082 neotectonic activity, which is a striking, but still poorly understood feature. Unfavorable fault  
1083 orientations or the combination of thick sedimentary cover and insufficient displacements along  
1084 the major PDZs are speculated behind this phenomena.

1085 4. Fault segment geometries in neotectonic fault zones indicates a consistent regional  
1086 displacement pattern: sinistral shear along (E)NE–(W)SW oriented, and dextral shear along  
1087 (W)NW–(E)SE oriented fault zones, respectively. These observations — together with the E–  
1088 W trending contractional/transpressional structures (folds, reverse faults, imbricates) occurring  
1089 locally in western and southern Hungary — indicate a dominantly strike-slip stress regime with  
1090 a laterally slightly rotating (from N–S to NNE–SSW) maximum horizontal stress axis ( $\sigma_1$ )  
1091 during the neotectonic phase.

1092 5. Regarding its magnitude, the neotectonic phase within Pannonian Basin can be considered  
1093 as a weak tectonic event compared to active tectonic movements related to plate boundaries.  
1094 Maximum 2–3km of lateral displacement is envisaged along the PDZ-s of major neotectonic  
1095 faults zones in the basin, which is less than that estimated by other authors based mainly on the  
1096 correlation of geological features on the opposite sides of the deformation zones.

#### 1097 ***Acknowledgements***

1098 This work is dedicated to the memory of our unforgettable Colleague, Friend and Mentor, late  
1099 Prof. Dr. Frank Horváth, who initiated this new mapping project and guided it in its initial  
1100 phase. The research project was supported by the National Research, Development and

1101 Innovation Office of Hungary (2018-1.2.1-NKP-2018-00007), that is gratefully thanked here  
1102 enabling the construction of the new map in the first phase of the project.

1103 Special thanks to our industrial partners, Mol Plc. and O&G Development Ltd., who offered  
1104 publicly not yet available 3D seismic data for the purpose of this project.

### 1105 *Data Availability*

1106 The digital map constructed during this study can be found at  
1107 <http://dx.doi.org/10.17632/dnjt9cmj87.1> hosted at Mendeley Data (Status: Draft, Version 1)  
1108 and [www.geomega.hu](http://www.geomega.hu) (Wórum et al., 2020).

### 1109 *References*

1110 Bada, G., 1999. Cenozoic stress field evolution in the Pannonian basin and surrounding orogens:  
1111 inferences from kinematic indicators and finite element modelling. PhD Thesis, Vrije University,  
1112 Amsterdam. NSG Publication No. 990101, ISBN 90-9012374-1, 204 p.

1113 Bada, G., Horváth, F., Fejes, I., Gerner, P., 1999. Review of the present day geodynamics of the  
1114 Pannonian basin: progress and problems. *Journal of Geodynamics* 27, 501– 527.

1115 Bada, G., Fodor, L., Windhoffer, G., Ruzkiczay-Rüdiger, Zs., Sacchi, M., Dunai, T., Tóth, L.,  
1116 Cloetingh, S., Horváth, F., 2003a. Lithosphere dynamics and present-day deformation pattern in the  
1117 Pannonian basin. *Geophysical Research Abstracts* 5, 05772 (Nice, France).

1118 Bada, G., Mónus, P., Szafián, P., Szeidovitz, Gy., Tóth, L., Windhoffer, G., Zsíros, T., 2003b. A  
1119 létesítmény és környezete geofizikai, szeizmológiai és szeizmotektonikai jellemzői (Geophysical,  
1120 seismological and seismotectonic characteristics of the facility and its surroundings). In: Schweitzer F.,  
1121 Tiner T., Bérczi, K., (Eds.), *A püspökszilágyi RHFT környezet- és sugárbiztonsága*. MTA  
1122 Földrajztudományi Kutatóintézet, Budapest, pp. 57–90.

1123 Bada, G., Horváth, F., Tóth, L., Fodor, L., Timár, G., Cloetingh, S., 2006. Societal aspects of ongoing  
1124 deformation in the Pannonian region. In: Pintér, N., Grenerczy, Gy., Weber, J., Medak, D., Stein, S.

- 1125 (Eds.), *The Adria microplate: GPS Geodesy, Tectonics, and Hazards*. NATO ARW Series. Kluwer  
1126 Academic Publishers, pp. 385–402.
- 1127 Bada, G., Horváth, F., Dövényi, P., Szafián, P., Windhoffer, G., Cloetingh, S., 2007. Present-day stress  
1128 field and tectonic inversion in the Pannonian basin. *Global and Planetary Change* 58, 165–180.
- 1129 Bada, G., Szafián, P., Vincze, O., Tóth, T., Fodor, L., Volkhard, S., Horváth, F., 2010. Neotektonikai  
1130 viszonyok a Balaton keleti medencéjében és tágabb környezetében nagyfelbontású szeizmikus mérések  
1131 alapján (The neotectonic habitat of the eastern part of Lake Balaton and its broader environs: inferences  
1132 from high resolution seismic profiling). *Földtani Közlöny* 140, 367–390.
- 1133 Balázs, A., Matenco, L., Magyar, I., Horváth, F., Cloetingh, S., 2016. The link between tectonics and  
1134 sedimentation in back-arc basins: New genetic constraints from the analysis of the Pannonian Basin.  
1135 *Tectonics*, 35, 1526–1559, DOI: 10.1002/2015TC004109.
- 1136 Balázs, A., Magyar, I., Matenco, L., Sztanó, O., Tőkés, L., Horváth, F., 2018. Morphology of a large  
1137 paleo-lake: Analysis of compaction in the Miocene-Quaternary Pannonian Basin. *Global and Planetary*  
1138 *Change* 171, 134–147. DOI: 10.1016/j.gloplacha.2017.10.012
- 1139 Balla, Z., 1984. The Carpathian loop and the Pannonian basin: A kinematic analysis. *Geophysical*  
1140 *Transactions* 30, 313–353.
- 1141 Balla, Z., 1988. On the Origin of the structural pattern of Hungary. *Acta Geologica Hungarica* 31, 53–  
1142 63.
- 1143 Balla, Z., 1989. Reevaluation of the Diósjenő dislocation zone. *Annual Report of the Eötvös Loránd*  
1144 *Geophysical Institute of Hungary* 1987, 45–57. (in Hungarian)
- 1145 Balla, Z., Dudko, A., Tátrai, M., 1987. A Közép-Dunántúl fiatal tektonikája földtani és geofizikai adatok  
1146 alapján (The young tectonics of Middle Transdanubia based on geological and geophysical data).  
1147 *Annual report of Eötvös Loránd Geophysical Institute of Hungary* 1986, 74–94. (in Hungarian)
- 1148 Bally, A. W., Snelson, S., 1980. Realms of subsidence. *Can. Soc. Petrol. Geol. Memoir* 6, 9–94.

1149 Beke, B., Fodor, L., Millar, L., Petrik, A., 2019. Deformation band formation as a function of  
1150 progressive burial: Depth calibration and mechanism change in the Pannonian Basin (Hungary). *Marine*  
1151 *and Petroleum Geology* 105, 1–16. <https://doi.org/10.1016/j.marpetgeo.2019.04.006>

1152 Benkovics, L., Unpublished results. A Zagyva-árokban végzett mikrotektonikai vizsgálatok és  
1153 szeizmikus szelvényekkel való kapcsolata (Microtectonic investigations in the Zagyva trough and its  
1154 relationship to seismic sections). MSc thesis, 1991. Eötvös University, Dept. Regional Geology, 92 p.  
1155 (In Hungarian with English summary)

1156 Bérczi, I., 1988. Preliminary sedimentological investigation of a Neogene depression in the Great  
1157 Hungarian Plain. In: Royden, L.H., Horváth, F. (Eds.), *The Pannonian Basin*. AAPG Memoir 45, 107–  
1158 116.

1159 Bergerat, F., Csontos, L., 1988. Brittle tectonics and paleostress field in the Mecsek and Villány Mts.  
1160 (Hungary): Correlation with the opening mechanism of the Pannonian Basin. *Acta Geologica Hungarica*  
1161 31, 81–100.

1162 Bodor, B., Unpublished results. A Hernád-árok szerkezetföldtani vizsgálata (Structural investigation of  
1163 the Hernád graben). MSc thesis, 2011. Eötvös University, Dept. Regional Geology, 99 p. (In Hungarian  
1164 with English summary)

1165 Brezsnayánszky, K., Síkhegyi, F., 1987. Neotectonic interpretation of Hungarian lineaments in the light  
1166 of satellite imagery. *Journal of Geodynamics* 8, 123–203.

1167 Budai, T., Császár, G., Csillag, G., Fodor, L., Gál, N., Kerckmár, Zs., Kordos, L., Pálfalvi, S., Selmeczi,  
1168 I., 2008. *Geology of the Vértes Hills*. Explanatory book to the Geological Map of the Vértes Hills (1:50  
1169 000). Geological Institute of Hungary, Budapest, 368 p.

1170 Budai, S., Sebe, K., Nagy, G., Magyar, I., Sztanó, O., 2019. Interplay of sediment supply and lake-level  
1171 changes on the margin of an intrabasinal basement high in the Late Miocene Lake Pannon (Mecsek  
1172 Mts., Hungary). *International Journal of Earth Sciences* 108, 2001–2019.  
1173 <https://doi.org/10.1007/s00531-019-01745-3>

- 1174 Cloetingh, S., Burov, E., Poliakov, A., 1999. Lithosphere folding: Primary response to compression?  
1175 (from central Asia to Paris basin). *Tectonics* 18, 1064–1083.
- 1176 Crider, J.G., Peacock, D.C.P., 2004. Initiation of brittle faults in the upper crust: a review of field  
1177 observations. *Journal of Structural Geology* 26, 691–707.
- 1178 Czakó, T., Zelenka, T. 1981. New data about the neotectonics of Mátra Mountains, Northern Hungary.  
1179 *Advances in Space Research* 1, 289–298. DOI: 10.1016/0273-1177(81)90406-3
- 1180 Csalagovits, I., Juhász, Á., Szepesházy, K., Császár, G., Radócz, Gy., 1967. Magyarország paleozóos  
1181 és mezozóos képződményeinek fedetlen földtani térképe, 1:500 000 (Pre-Cenozoic geological map of  
1182 the Palaeozoic and Mesozoic formations of Hungary, 1:500 000). Geological Institute of Hungary,  
1183 Budapest.
- 1184 Cserny, T., Corrada, R., 1990. A Balaton aljzatának szedimentológiai térképe (Sedimentary maps of the  
1185 basement of the Lake Balaton). Annual report of Geological Institute of Hungary 1988, 169–176. (in  
1186 Hungarian with English abstract)
- 1187 Csontos, L., 1995. Tertiary tectonic evolution of the Intra-Carpathian area: a review. *Acta Vulcanologica*  
1188 7, 1–13.
- 1189 Csontos, L., Bergerat, F., 1993. Reevaluation of the Neogene brittle tectonics of the Mecsek–Villány  
1190 area (SW Hungary). *Annales Universitatis Scientiarum Budapestinensis de Rolando Eötvös Nominatae,*  
1191 *Sectio Geologica* 29, 3–12.
- 1192 Csontos, L., Nagymarosy, A., 1998. The Mid-Hungarian line: a zone of repeated tectonic inversions.  
1193 *Tectonophysics* 297, 51–71.
- 1194 Csontos, L., Nagymarosy, A., Horváth, F., Kovác, M., 1992. Cenozoic evolution of the Intra-Carpathian  
1195 area: a model. *Tectonophysics* 208, 221–241.
- 1196 Csontos, L., Benkovics, L., Bergerat, F., Mansy, J-L., Wórum, G., 2002. Tertiary deformation history  
1197 from seismic section study and fault analysis in a former European Tethyan margin (the Mecsek–Villány  
1198 area, SW Hungary). *Tectonophysics* 357, 81–102. DOI: 10.1016/S0040-1951(02)00363-3.

- 1199 Csontos, L., Vörös, A., 2004. Mesozoic plate tectonic reconstruction of the Carpathian region.  
1200 *Palaeogeogr. Palaeoclimatol. Palaeoecol.* 210, 1–56.
- 1201 Csontos, L., Magyarai, Á., Van Vliet-Lanoe, B., Musitz, B., 2005. Neotectonics of the Somogy Hills  
1202 (Part II): evidence from seismic sections. *Tectonophysics* 410, 63–80.  
1203 <https://doi.org/10.1016/j.tecto.2005.05.049>
- 1204 Dank, V., 1962. A Dél-Zalai-medence mélyföldtani vázlat (Sketch of the deep geological structure of  
1205 the south Zala Basin). *Földtani Közlöny* 92, 150–159. (in Hungarian with English summary)
- 1206 Dank, V., Fülöp, J., (Eds.), 1990. Magyarország szerkezetföldtani térképe, 1:500 000 (Structural-  
1207 geological map of Hungary, 1:500 000). Geological Institute of Hungary, Budapest.
- 1208 Detzky Lőrinc, K., 1997. Feszültségtér történet meghatározása szeizmikus szelvényeken azonosított  
1209 többfázisú tektonizmus alapján, a Szolnoki flis öv nyugati peremén (Determination of stress-field  
1210 history on the basis of multiphase tectonism identified in the seismic profiles, in the western part of the  
1211 Szolnok flysch belt). *Magyar Geofizika* 37, 228–246. (in Hungarian with English abstract)
- 1212 Detzky Lőrinc, K., Horváth, F., Detzky, G., 2002. Neotectonics and its relation to the Mid-Hungarian  
1213 Mobile Belt. In: Cloetingh, S., Horváth, F., Bada, G., Lankreijer, A., (Eds.), *Neotectonics and surface  
1214 processes: the Pannonian basin and Alpine/Carpathian system*. EGU St. Mueller Spec. Publ. Series 3,  
1215 247–266.
- 1216 Dombrádi, E., Sokoutis, D., Bada, G., Cloetingh, S., Horváth, H., 2010. Modelling recent deformation  
1217 of the Pannonian lithosphere: lithospheric folding and tectonic topography. *Tectonophysics* 484, 103–  
1218 118.
- 1219 Dudás, Á.. Unpublished results. Felső-miocén vetők és redők vizsgálata 2D szeizmikus vonalak alapján  
1220 a Duna-Tisza köze északi és középső részén (Study of Late Miocene faults and folds in the northern and  
1221 middle portion of the Danube-Tisza interfluvium based on 2D seismic profiles). MSc thesis, 2011. Eötvös  
1222 University, Dept. General and Applied Geology, 73 p.
- 1223 Dudko, A., 1988. A Balatonfő-velencei terület szerkezetalakulása. *Földtani Közlöny* 118, 207–218.

- 1224 Dudko, A., 1997. Neogene tectonics of the Mezőföld. Annual Report of the Geological Institute of  
1225 Hungary 1996/II, 213–223.
- 1226 Fodor, L., Unpublished results. Mesozoic-Cenozoic stress fields and fault patterns in the northwestern  
1227 part of the Pannonian Basin — methodology and structural analysis. DSc thesis, 2010. Hungarian  
1228 Academy of Sciences, 129 p. (in Hungarian)
- 1229 Fodor, L., Magyari, Á., Fogarasi, A., Palotás, K., 1994. Tercier szerkezetfejlődés és késő paleogén  
1230 üledékképződés a Budai-hegységben. A Budai-vonal új értelmezése (Tertiary tectonics and Late  
1231 Palaeogene sedimentation in the Buda Hills, Hungary. A new interpretation of the Buda Line). Földtani  
1232 Közlöny 124, 129–305. (In Hungarian with extended English abstract)
- 1233 Fodor, L., Jelen, B., Márton, E., Skaberne, D., Čar, J., & Vrabec, M., 1998. Miocene-Pliocene tectonic  
1234 evolution of the Slovenian Periadriatic Line and surrounding area – implication for Alpine-Carpathian  
1235 extrusion models. *Tectonics*, 17, 690–709.
- 1236 Fodor, L., Csontos, L., Bada, G., Györfi, I., Benkovics, L., 1999. Tertiary tectonic evolution of the  
1237 Pannonian basin system and neighbouring orogens: a new synthesis of paleostress data. In: Durand, B.,  
1238 Jolivet, L., Horváth, F., Séranne, M. (Eds.), *The Mediterranean Basins: Tertiary Extension within the*  
1239 *Alpine Orogen. Special Publications*, 156. Geological Society, London, pp. 295–334. DOI:  
1240 10.1144/gsl.sp.1999.156.01.15
- 1241 Fodor, L., Jelen, B., Márton, E., Rifelj, H., Kraljić, M., Kevrić, R., Márton, P., Koroknai, B., Bádi-Beke,  
1242 M., 2002. Miocene to Quaternary deformation, stratigraphy and paleogeography in Northeastern  
1243 Slovenia and Southwestern Hungary. *Geologija* 45, 103–114.  
1244 <https://doi.org/10.5474/geologija.2002.009>
- 1245 Fodor, L., Bada, G., Csillag, G., Horváth, E., Ruzkiczay-Rüdiger, Z., Palotás, K., Síkhegyi, F., Timár,  
1246 G., Cloetingh, S., 2005a. An outline of neotectonic structures and morphotectonics of the western and  
1247 central Pannonian Basin. *Tectonophysics* 410, 15–41.



- 1248 Fodor, L., Bada, G., Csillag, G., Horváth, E., Ruzsáczay-Rüdiger, Zs., Síkhegyi, F., 2005b. New data  
1249 on neotectonic structures and morphotectonics of the western and central Pannonian Basin. In: Fodor,  
1250 L., Brezsnayánszky, K., (Ed.), Application of GPS in plate tectonics, in research on fossil energy  
1251 resources and in earthquake hazard assessment. Occasional Papers of the Geological Institute of  
1252 Hungary 204, 35–44.
- 1253 Fodor, L., Radócz, Gy., Sztanó, O., Koroknai, B., Csontos, L., Harangi, Sz., 2005c. Post-Conference  
1254 Excursion: Tectonics, sedimentation and magmatism along the Darnó Zone. Geolines 19, 142–162.
- 1255 Fodor, L. I., Gerdes, A., Dunkl, I., Koroknai, B., Pécskay, Z., Trajanova, M., Horváth, P., Vrabc, M.,  
1256 Jelen, B., Balogh, K., Frisch, W., 2008. Miocene emplacement and rapid cooling of the Pohorje pluton  
1257 at the Alpine–Pannonian–Dinaric junction: a geochronological and structural study. Swiss Journal of  
1258 Earth Sciences 101, Supplement 1, 255–271. <https://doi.org/10.1007/s00015-008-1286-9>
- 1259 Fodor, L., Uhrin, A., Palotás, K., Selmeczi, I., Tóth-Makk, Á., Riznar, I., Trajanova, M., Rifelj, H.,  
1260 Bogomir, J., Budai, T., Koroknai, B., Mozetič, S., Nádor, A., Lapanje, A., 2013. A Mura-Zala-medence  
1261 vízföldtani elemzést szolgáló földtani-szerkezetföldtani modellje (Geological and structural model of  
1262 the Mura–Zala Basin and its rims as a basis for hydrogeological analysis). Annual Report of the  
1263 Geological Institute of Hungary 2011, 47–91.
- 1264 Fülöp, J., Dank, V., (Eds.), 1987. Magyarország földtani térképe a kainozóikum elhagyásával, 1: 500  
1265 000 (Geological map of Hungary without Cenozoic, 1:500 000). Geological Institute of Hungary,  
1266 Budapest.
- 1267 Gerner, P., Bada, G., Dövényi, P., Müller, B., Oncescu, M.C., Cloetingh, S., Horváth, F., 1999. Recent  
1268 tectonic stress and crustal deformation in and around the Pannonian basin: data and models. In: Durand,  
1269 B., Jolivet, L., Horváth, F., Séranne, M., (Eds.), The Mediterranean Basins: Tertiary Extension within  
1270 the Alpine Orogen. Blackwell Geol. Soc. London Spec. Publ., vol. 156, pp. 269–294.  
1271 10.1144/GSL.SP.1999.156.01.14
- 1272 Gyalog, L., Síkhegyi, F., (Eds.), 2005. Magyarország földtani térképe, M=1:100 000 (Geological map  
1273 of Hungary, 1:100 000). Geological Institute of Hungary, Budapest. <https://map.mbfisz.gov.hu/fdt100/>

- 1274 Györfi, I., Csontos, L., Nagymarosy, A., 1999. Early Tertiary structural evolution of the border zone  
1275 between the Pannonian and Transylvanian basins. In: Durand, B., Jolivet, L., Horváth, F., Séranne, M.  
1276 (Eds.), *The Mediterranean Basins: Tertiary extension within the Alpine Orogen*. Geological Society  
1277 Special Publications 156, 251–267.
- 1278 Haas, J., Péró, Cs., 2004. Mesozoic evolution of the Tisza Mega-unit. *Int. J. Earth Sci.* 93, 297–313.  
1279 DOI: 10.1007/s00531-004-0384-9.
- 1280 Haas, J., Budai, T., Csontos, L., Fodor, L., Konrád, Gy., (Eds.), 2010. Magyarország prekainozoos  
1281 földtani térképe 1:500 000 (Pre-Cenozoic geological map of Hungary, 1:500 000). Geological Institute  
1282 of Hungary, Budapest. <https://map.mbfisz.gov.hu/preterc500/>
- 1283 Halouzka, R., Schäffer, G., Kaiser, M., Molnár, P., Scharek, P., Pristās, J., 1998. Neotectonic map,  
1284 1:200000. Danube region environmental geology programme, DANREG. Geological Institute of  
1285 Hungary, Budapest.
- 1286 Harangi, Sz., Lenkey, L., 2007. Genesis of the Neogene to Quaternary volcanism in the Carpathian-  
1287 Pannonian region: role of subduction, extension, and mantle plume. In: Beccaluva, L., Bianchini, G.,  
1288 Wilson, M., (Eds.), *Cenozoic Volcanism in the Mediterranean Area*. Geological Society of America  
1289 Special Paper, New York. Geological Society of America, pp. 67–92.
- 1290 Hardy, S., 2011. Cover deformation above steep, basement normal faults: Insights from 2D discrete  
1291 element modeling. *Marine and Petroleum Geology* 28, 966–972. DOI:10.1016/j.marpetgeo.2010.11.005
- 1292 Hatem, A. E., Cooke, M. L., Toeneboehn, K., 2017. Strain localization and evolving kinematic  
1293 efficiency of initiating strike-slip faults within wet kaolin experiments. *Journal of Structural Geology*  
1294 101, 96–108. doi:10.1016/j.jsg.2017.06.011
- 1295 Hámor, G., 1966. Újabb adatok a Mecsek hegység szerkezetföldtani felépítéséhez (New data on the  
1296 structure of the Mecsek Mts). *Annual Report of the Geological Institute of Hungary 1964*, 193–206.
- 1297 Hetényi, R., Hámor, G., Földi, M., Nagy, I., Nagy, E., Bilik, I., 1982. A Keleti-Mecsek földtani térképe  
1298 (Geological map of the Eastern Mecsek). Geological Institute of Hungary, Budapest.

- 1299 Héja, G., Kövér, Sz., Németh, A., Csillag, G., Fodor, L. 2018. Evidences for pre-orogenic passive-  
1300 margin extension in a Cretaceous fold-and-thrust belt on the basis of combined seismic and field data,  
1301 (western Transdanubian Range, Hungary). *International Journal of Earth Sciences* 107, 2955–2973.  
1302 <https://doi.org/10.1007/s00531-018-1637-3>
- 1303 Héja, G., Unpublished results. Mesozoic deformations of the western part of the Transdanubian Range.  
1304 PhD Thesis, 2019. Eötvös University, Dept. Physical and Applied Geology.
- 1305 Horváth, F., 1993. Towards a mechanical model for the formation of the Pannonian basin.  
1306 *Tectonophysics*, 226, 333–357.
- 1307 Horváth, F., 1995. Phases of compression during the evolution of the Pannonian Basin and its bearing  
1308 on hydrocarbon exploration. *Marine and Petroleum Geology* 12, 837–844. [https://doi.org/10.1016/0264-](https://doi.org/10.1016/0264-8172(95)98851-u)  
1309 [8172\(95\)98851-u](https://doi.org/10.1016/0264-8172(95)98851-u)
- 1310 Horváth, F., Royden, L., 1981. Mechanism for the formation of the Intra-Carpathian Basins: a review.  
1311 *Earth Evolution Sciences* 3, 307–316.
- 1312 Horváth, F., Rumpler, J. 1984. The Pannonian basement: extension and subsidence of an alpine orogene.  
1313 *Acta Geologica Hungarica* 27, 229–235.
- 1314 Horváth, F., Tari, G., Unpublished results. Role of Neogene tectonic evolution and structural elements  
1315 in the migration and trapping of hydrocarbons. Exploration report, 1988. Kőolajkutató Vállalat,  
1316 Budapest, 155 p. (in Hungarian)
- 1317 Horváth, F., Cloetingh, S., 1996. Stress-induced late-stage subsidence anomalies in the Pannonian basin.  
1318 *Tectonophysics* 266, 287–300.
- 1319 Horváth, F., Tóth, T., Szafián, P., Bada, G., Vida, R., Benkovics, L., Csontos, L. és Dövényi, P.,  
1320 Unpublished results. A tervezett magasaktivitású radioaktív hulladéktároló tektonikai  
1321 veszélyeztetettségének analízise a Dunán végrehajtott speciális szeizmikus szelvényezés alapján  
1322 (Analysis of tectonic hazards of the planned repository site of high-level radioactive waste based on the

1323 special water seismic survey on the river Danube). Research report for the Paks Nuclear Power Plant  
1324 Plc., 1997. Budapest, 1–46. (In Hungarian)

1325 Horváth, F., Bada, G., Windhoffer, G., Csontos, L., Dombrádi, E., Dövényi, P., Fodor, L., Grenczy, G.,  
1326 Síkhegyi, F., Szafián, P., Székely, B., Timár, G., Tóth, L., Tóth, T., 2006a. Atlas of the present-day  
1327 geodynamics of the Pannonian basin: Euroconform maps with explanatory text (A Pannon-medence  
1328 jelenkori geodinamikájának atlasza: Eurokonform térképsorozat és magyarázó). Magyar Geofizika 47,  
1329 133–137. (in Hungarian with English abstract); [http://geophysics.elte.hu/atlas/geodin\\_atlas.htm](http://geophysics.elte.hu/atlas/geodin_atlas.htm)

1330 Horváth, F., Bada, G., Szafián, P., Tari, G., Ádám, A., Cloetingh, S., 2006b. Formation and deformation  
1331 of the Pannonian basin: Constraints from observational data. In: Gee, D.G., Stephenson, R.A., (Eds.),  
1332 European Lithosphere Dynamics, Geol. Soc., London, Mem. 32, 191–206.

1333 Horváth, F., Dombrádi, E., Tóth, L., 2009. Natural conditions, Geophysics. In: Kocsis, K., Schweitzer,  
1334 F. (Eds.), Hungary in Maps. Geographical Research Institute, Hungarian Academy of Sciences,  
1335 Budapest, 29–33.

1336 Horváth, F., Musitz, B., Balázs, A., Végh, A., Uhrin, A., Nádor, A., Koroknai, B., Pap, N., Tóth, T.,  
1337 Wórum, G., 2015. Evolution of the Pannonian basin and its geothermal resources. Geothermics, 53,  
1338 328–352.

1339 Horváth, F., Dulić, I., Vranković, A., Koroknai, B., Tóth, T., Wórum, G., Kovács, G., 2018. Overview  
1340 of geologic evolution and hydrocarbon generation of the Pannonian Basin. Interpretation 6, SB111–  
1341 SB122. DOI: 10.1190/int-2017-0100.1

1342 Horváth, F., Koroknai, B., Tóth, T., Wórum, G., Konrád, Gy., Kádi, Z., Kudó, I., Hámori, Z., Filipzski,  
1343 P., Németh, V., Szántó, É., Bíró, A., Koroknai, Zs., Földvári, K., Kovács, G., 2019. A „Kapos-vonal”  
1344 középső szakaszának szerkezeti-mélyföldtani viszonyai és neotektonikai jellegei a legújabb geofizikai  
1345 vizsgálatok tükrében (Structural-geological and neotectonic features of the middle portion of the Kapos  
1346 line based on the results of latest geophysical research). Földtani Közlemény 149, 327–350. (in Hungarian  
1347 with English abstract); DOI: 10.23928/foldt.kozl.2019.149.4.327

- 1348 Horváth, I., Darida-Tichy, M., Dudko, A., Gyalog, L., Ódor, L., 2004. Geology of the Velence Hills and  
1349 the Balatonfő. Explanatory Book of the Geological Map of the Velence Hills (1:25 000) and the  
1350 Geological Map of Pre-Sarmatian Surface of the Balatonfő–Velence Area (1:100 000). Geological  
1351 Institute of Hungary, Budapest, 316 p.
- 1352 Juhász, Gy., 1991. Lithostratigraphical and sedimentological framework of the Pannonian (s.l.)  
1353 sedimentary sequence in the Hungarian Plain (Alföld), Eastern Hungary. *Acta Geol. Hung.* 34, 53–72.
- 1354 Juhász, Gy., 1992. A pannóniai s.l. formációk térképezése az Alföldön: elterjedés, fácies és üledékes  
1355 környezetek (Pannonian s.l. formations in the Hungarian Plain: distribution, facies and sedimentary  
1356 environments.). *Földtani Közlöny* 122, 133–165. (Both in Hungarian and in English)
- 1357 Juhász, Gy., Pogácsás, G., Magyar, I., 2007. Óriáskanyon-rendszer szeli át a pannóniai üledékeket? (A  
1358 giant canyon system incised into the Late-Neogene (Pannonian s.l.) sediments?). *Földtani Közlöny* 137,  
1359 307–326. (in Hungarian with English abstract)
- 1360 Juhász, Gy., Pogácsás, Gy., Magyar, I., Hatalyák, P., 2013. The Alpar canyon system in the Pannonian  
1361 Basin, Hungary – its morphology, infill and development. *Global Planetary Change* 103, 174–192. DOI:  
1362 10.1016/j.gloplacha.2012.10.003
- 1363 Kázmér, M., Kovács, S., 1985. Permian-Palaeogene palaeogeography along the eastern part of the  
1364 Insubric-Periadriatic lineament system: Evidence for continental escape of the Bakony-Drauzug unit.  
1365 *Acta Geologica Hungarica*, 28, 71–84.
- 1366 Kiss, A., Gellért, B., Fodor, L. 2001. Structural history of the Porva Basin in the Northern Bakony Mts.  
1367 (Western Hungary): Implications for the Mesozoic and Tertiary tectonic evolution of the Transdanubian  
1368 Range and Pannonian Basin. *Geologica Carpathica* 52, 183–190.
- 1369 Kiss, J., 2006. Magyarország gravitációs Bouguer-anomália térképe, M=1:500 000 (Gravity Bouguer  
1370 anomaly map of Hungary, 1:500 000). *Geophysical Transactions* 45, 99–104.  
1371 [https://map.mbfisz.gov.hu/gravitacios\\_anomalia/](https://map.mbfisz.gov.hu/gravitacios_anomalia/)

- 1372 Kiss, J., Gulyás, Á., 2006. Magyarország mágneses  $\Delta Z$ -anomália térképe, M=1:500 000 (Magnetic  $\Delta Z$   
1373 anomaly map of Hungary, 1:500 000). Eötvös Lóránd Geophysical Institute of Hungary, Budapest.  
1374 [https://map.mbfsz.gov.hu/magneszes\\_anomalia/](https://map.mbfsz.gov.hu/magneszes_anomalia/)
- 1375 Konrád, Gy., Sebe, K., 2010. Fiatal tektonikai jelenségek új észlelései a Nyugati-Mecsekben és  
1376 környezetében (New details of young tectonic phenomena in the Western Mecsek Mts and their  
1377 surroundings). *Földtani Közlöny* 140, 135–162. (in Hungarian with English abstract)
- 1378 Korpás, L., Fodor, L., Magyar, Á., Dénes, Gy., Oravecz, J., 2002. A Gellért-hegy földtana, karszt- és  
1379 szerkezetfejlődése (Geology, karst system and structural evolution of the Gellért Hill, Budapest,  
1380 Hungary). *Karszt és Barlang* 1998–1999/I–II, 57–93. (in Hungarian with English abstract)
- 1381 Kovács, Á., Sebe, K., Magyar, I., Szurominé Korecz, A., Kovács, E., 2018. Upper Miocene  
1382 sedimentation and tectonics in the Northern Imbricate Zone (Eastern Mecsek Mts, SW Hungary).  
1383 *Földtani Közlöny* 148, 327–340. (in Hungarian with English abstract)  
1384 <https://doi.org/10.23928/foldt.kozl.2018.148.4.327>
- 1385 Kovács, G., Fodor, L., Kövér, Sz., Molnár, G., Raáb, D., Telbisz, T., Timár, G., 2015. Verification of  
1386 late Miocene to Quaternary structural control on landforms: A case study with comprehensive  
1387 methodology from a low hilly area (Western Pannonian basin). *Austrian Journal of Earth Sciences* 108,  
1388 82–104. <https://doi.org/10.17738/AJES.2015.0015>
- 1389 Kovács, G., Telbisz, T., Székely, B., Koma, Zs. 2014. Tectonic geomorphometric studies in the  
1390 surroundings of Rechnitz tectonic window, Eastern Alps. *Geologia Sudetica* 42, 188–189.
- 1391 Kovács, S., Haas, J., Császár, G., Szederkényi, T., Buda, Gy., Nagymarosy, A. 2000.  
1392 Tectonostratigraphic terranes in the pre-Neogene basement of the Hungarian part of the Pannonian area.  
1393 *Acta Geol Hung* 43, 225–328.
- 1394 Kováč, M., Bielik, M., Hók, J., Kováč, P., Kronome, B., Labák, P., Mozco, P., Plašienka, D.; Šefara, J.,  
1395 Šujan, M., 2002. Seismic activity and neotectonic evolution of the Western Carpathians (Slovakia).  
1396 EGU Stephan Mueller Special Publication Series 3, 167–184.

- 1397 Lemberkovics, V., Bárány, Á., Gajdos, I., Vincze, M., 2005. A szekvencia-sztratigráfiai események és  
1398 a tektonika kapcsolata a Derecskei-árok pannóniai rétegsorában (Connection of sequence stratigraphy  
1399 and tectonics in the Pannonian strata of the Derecske Trough). *Földtani Kutatás* 42, 16–24.
- 1400 Loisl, J., Tari, G., Draganits, E., Zámolyi, A., Gjerazi, I., 2018. High-resolution seismic reflection data  
1401 acquisition and interpretation, Lake Neusiedl, Austria, northwest Pannonian Basin. *Interpretation* 6,  
1402 SB77–SB97. doi:10.1190/int-2017-0086.1
- 1403 Lopes Cardozo, G., Bada, G., Lankreijer, A., Nieuwland, D., 2002. Analogue modelling of a prograding  
1404 strike-slip fault: Case study of the Balatonfő fault, western Hungary. In: Cloetingh, S., Horváth, F.,  
1405 Bada, G., Lankreijer, A., (Eds.), *Neotectonics and surface processes: the Pannonian basin and*  
1406 *Alpine/Carpathian system*. EGU St. Mueller Special Publication Series 3, 217–226.
- 1407 Lukács, R., Harangi, Sz., Guillong, M., Bachmann, O., Fodor, L., Buret, Y., Dunkl, I., Sliwinski, J., von  
1408 Quadt, A., Peytcheva, I., Zimmerer, M. 2018. Early to Mid-Miocene syn-extensional massive silicic  
1409 volcanism in the Pannonian Basin (East-Central Europe): Eruption chronology and geodynamic  
1410 relations. *Earth-Science Reviews* 179, 1–19.
- 1411 Magyar, I., 2010. A Pannon-medence ösföldrajza és környezeti viszonyai a késő miocénben őslénytani  
1412 és szeizmikus rétegtani adatok alapján (The paleogeography and environmental conditions of the  
1413 Pannonian basin in the Late Miocene based on paleontological and seismic data). *GeoLitera*, Szeged,  
1414 1–140.
- 1415 Magyar, I., Geary, D.H., Müller, P., 1999. Paleogeographic evolution of the Late Miocene Lake Pannon  
1416 in Central Europe. *Palaeogeogr. Palaeoclimatol. Palaeoecol.* 147, 151–167.
- 1417 Magyar, I., Radivojevic, D., Sztanó, O., Synak, R., Ujszászi, K., Pócsik, M., 2013. Progradation of the  
1418 paleo-Danube shelf margin across the Pannonian Basin during the Late Miocene and Early Pliocene.  
1419 *Glob. Planet. Chang.* 103, 168–173.
- 1420 Magyar, I., Sztanó, O., Sebe, K., Katona, L., Csoma, V., Görög, Á., Tóth, E., Szuromi-Korecz, A., Šujan,  
1421 M., Braucher, R., Ruszkiczay-Rüdiger, Zs., Koroknai, B., Wórum, G., Sant, K., Kelder, N., Krijgsman,

1422 W., 2019. A paksi fúrómagok szerepe a pannóniai emelet nagy felbontású időrétegtanának és  
1423 geokronológiájának kifejlesztésében (Towards a high-resolution chronostratigraphy and geochronology  
1424 for the Pannonian Stage: Significance of the Paks cores (Central Pannonian Basin)). *Földtani Közlöny*  
1425 149, 351–370. <https://doi.org/10.23928/foldt.kozl.2019.149.4.351>

1426 Magyari, Á., Musitz, B., Csontos, L., Van Vliet-Lanoë, B., 2005. Quaternary neotectonics of the  
1427 Somogy Hills, Hungary (part I): Evidence from field observations. *Tectonophysics* 410, 43–62. DOI:  
1428 10.1016/j.tecto.2005.05.044

1429 Maillard, A., Gaullier, V., Vendeville, B. C., Odonne, F., 2003. Influence of differential compaction  
1430 above basement steps on salt tectonics in the Ligurian-Provençal Basin, northwest Mediterranean.  
1431 *Marine and Petroleum Geology* 20, 13–27. DOI:10.1016/s0264-8172(03)00022-9

1432 Matenco, L., Radivojevic, D., 2012. On the formation and evolution of the Pannonian Basin: Constraints  
1433 derived from the structure of the junction area between the Carpathians and Dinarides: *Tectonics* 31, 1–  
1434 31. DOI: 10.1029/2012TC003206.

1435 Matura, A., Weselly, G., Kröll, A., Császár, G., Vozár, J., 1998. Map of the pre-Tertiary basement  
1436 (including Paleogene in the Australpine-Carpathian belt), 1:200 000. Danube region environmental  
1437 geology programme, DANREG. Geological Institute of Hungary, Budapest.

1438 Márton, E., Fodor, L., Jelen, B., Márton, P., Rifelj, H., Kevrić, R. 2002. Miocene to Quaternary  
1439 deformation in NE Slovenia: complex paleomagnetic and structural study. *Journal of Geodynamics* 34,  
1440 627–651. DOI: 10.1016/s0264-3707(02)00036-4

1441 Misra, A. A., 2018. Normal Faulting Related to Differential Compaction on the 85°E Ridge in the Bay  
1442 of Bengal, India. *Atlas of Structural Geological Interpretation from Seismic Images*, 107–111.  
1443 DOI:10.1002/9781119158332.ch19

1444 Nádor, A., Sztanó, O., 2011. Lateral and vertical variability of channel belt stacking density as a function  
1445 of subsidence and sediment supply: field evidence from the intramontaine Körös Basin, Hungary.  
1446 *SEPM Spec. Publ.* 97, 375–392.



- 1447 Nádor, A., Thamó-Bozsó, E., Magyar, Á., Babinszki, E., 2007. Fluvial responses to tectonics and  
1448 climate change during the Late Weichselian in the eastern part of the Pannonian Basin (Hungary).  
1449 *Sedimentary Geology* 202, 174–192.
- 1450 Némedi Varga, Z., 1977. A Kapos-vonal (The Kapos line). *Földtani Közlöny* 107, 313–328. (in  
1451 Hungarian with English abstract)
- 1452 Némedi Varga, Z., 1983. A Mecsek hegység szerkezetalakulása az alpi hegységképződési ciklusban  
1453 (Structural evolution of the Mecsek mountains in the Alpine orogenic cycle). *Annual Report of the*  
1454 *Geological Institute of Hungary* 1981, 467–484. (in Hungarian with English abstract)
- 1455 Oláh, P., Fodor, L., Tóth, T., Deák, A., Drijkoningen, G., Horváth, F., 2014. A Szentendrei-sziget  
1456 környéki vízi szeizmikus szelvényezések eredményei (Geological results of the seismic surveys around  
1457 Szentendre Island, Danube River, North Hungary). *Földtani Közlöny* 144, 359–380. (in Hungarian with  
1458 English abstract)
- 1459 Nollet, S., Kleine Vennekate, G. J., Giese, S., Vrolijk, P., Urai, J. L., Ziegler, M., 2012. Localization  
1460 patterns in sandbox-scale numerical experiments above a normal fault in basement. *Journal of Structural*  
1461 *Geology*, 39, 199–209. DOI:10.1016/j.jsg.2012.02.011
- 1462 Palotai, M., Unpublished results. Oligocene–Miocene Tectonic Evolution of the Central Part of the Mid-  
1463 Hungarian Shear Zone. PhD thesis, 2013. Eötvös Loránd University, Dept. General and Historical  
1464 *Geology*, 147 p.
- 1465 Palotai, M., Csontos, L., 2010. Strike-slip reactivation of a Paleogene to Miocene fold and thrust belt  
1466 along the central part of the Mid-Hungarian Shear Zone. *Geologica Carpathica* 61, 483–493.  
1467 <https://doi.org/10.2478/v10096-010-0030-3>
- 1468 Palotai, M., Mindszenty, A., Kopecskó, K., Poros, Zs., 2012. Az Ínség-kő geológiája (The Ínség-kő:  
1469 Danube bedrock geology at Gellért Hill, Budapest). *Földtani Közlöny* 142, 243–250. (in Hungarian with  
1470 English abstract)

- 1471 Pávai Vajna, F., 1925. Über die jüngsten tektonischen Bewegungen der Erdgebirge. *Földtani Közlöny*  
1472 55, 282–297. (in Hungarian)
- 1473 Pécskay, Z., Lexa, J., Szakács, A., Seghedi, I., Balogh, K., Konečný, V., Zelenka, T., Kovács, M., Póka,  
1474 T., Fülöp, A., Márton, E., Panaiotu, C., Cvetković, V., 2006. Geochronology of Neogene magmatism in  
1475 the Carpathian arc and intra-Carpathian area. *Geologica Carpathica* 57, 511–530.
- 1476 Petrik, A. B., Unpublished results. Structural evolution of the southern Bükk foreland. PhD thesis, 2016.  
1477 Eötvös University, Dept. of Physical and Applied Geology, 208 p. (in Hungarian with English abstract)
- 1478 Petrik, A., Fodor, L., Bereczki, L., Klembala, Zs., Lukács, R., Baranyi, V., Beke, B., Harangi, Sz., 2018.  
1479 Variation in style of magmatism and emplacement mechanism induced by changes in basin  
1480 environments and stress fields (Pannonian Basin, Central Europe). *Basin Research* 31, 380–404. DOI:  
1481 10.1111/bre.12326
- 1482 Pogácsás, G., Lakatos, L., Barvitz, A., Vakarcs, G., Farkas, C., 1989. Pliocén kvarter oldaleltolódások  
1483 a Nagyalföldön (Pliocene–Quaternary strike-slip faults in the Great Hungarian Plain, Hungary).  
1484 *Általános Földtani Szemle* 24, 149–169. (in Hungarian with English abstract)
- 1485 Rónai, A., 1974. Size of Quaternary movements in Hungary's area. *Acta Geol. Hungarica* 18, 39–44.
- 1486 Rónai, A., 1987. Quaternary vertical movements of the Earth's surface in East-Central Europe. *Journal*  
1487 *of Geodynamics* 8, 263–274.
- 1488 Royden, L.H., Horváth, F., Nagymarosy, A., Stegena, F., 1983. Evolution of the Pannonian Basin  
1489 System: 2. Subsidence and thermal history. *Tectonics* 2, 91–137.
- 1490 Royden, L.H., 1988. Late Cenozoic tectonics of the Pannonian basin system. In: Royden, L.H., Horváth,  
1491 F., (Eds), *The Pannonian basin*. *Am. Ass. Petr. Geol. Mem.*, 45, 27–48.
- 1492 Ruzkiczay-Rüdiger, Zs., Fodor, L. I., Horváth, E. 2007. Neotectonics and Quaternary landscape  
1493 evolution of the Gödöllő Hills, Central Pannonian Basin, Hungary. *Global and Planetary Change* 58,  
1494 181–196. <https://doi.org/10.1016/j.gloplacha.2007.02.010>

1495 Ruszkiczay-Rüdiger, Zs., Balázs, A., Csillag, G., Drijkoningen, G., Fodor, L. 2020. Uplift of the  
1496 Transdanubian Range, Pannonian Basin: How fast and why? *Global and Planetary Change*, 103263.  
1497 doi:10.1016/j.gloplacha.2020.103263

1498 Sacchi, M., Horváth, F., Magyar, O., 1999. Role of unconformity-bounded units in the stratigraphy of  
1499 the continental record: a case study from the late Miocene of the western Pannonian Basin, Hungary.  
1500 In: Durand, B., Jolivet, L., Horváth, F., Seranne M., (Eds.), *The Mediterranean Basins: extension within*  
1501 *the Alpine Orogen*, *Geol. Soc. Spec. Publ.* 156, 357–390.

1502 Saftić, B., Velić, J., Sztanó, O., Juhász, Gy., Ivković, Z., 2003. Tertiary subsurface facies, source rocks  
1503 and hydrocarbon reservoirs in the SW Part of the Pannonian Basin (Northern Croatia and South-Western  
1504 Hungary). *Geologia Croatica* 56, 101–122.

1505 Schmid, S.M., Bernoulli, D., Fügenschuh, B., Matenco, L., Schefer, S., Schuster, R., Tischler, M.,  
1506 Ustaszewski, K., 2008. The Alpine-Carpathian-Dinaridic orogenic system: correlation and evolution of  
1507 tectonic units. *Swiss J. Geosci.* 101, 139–183.

1508 Síkhegyi, F., 2002. Active structural evolution of the western and central part of the Pannonian basin:  
1509 A geomorphologic approach. In: Cloetingh, S., Horváth, F., Bada, G., Lankreijer, A., (Eds.),  
1510 *Neotectonics and surface processes: the Pannonian basin and Alpine/Carpathian system*. EGU St.  
1511 *Mueller Spec. Publ. Series* 3, 203–216.

1512 Síkhegyi, F., Unpublished results. Neotectonics of Somogy- and Zala Hills - morphostructural studies.  
1513 PhD thesis, 2008. University of West Hungary, Sopron, 150 p.

1514 Skorday, E., Unpublished results. Az Ortaháza-kilimáni-gerinc és északi előterének szerkezete (The  
1515 structure of the Ortaháza-kilimán ridge and its northern foreland). MSc thesis, 2010. Eötvös University,  
1516 Dept. General and Applied Geology, 88 p.

1517 Soós, B., Unpublished results. A Zagyva-árok extenziójának szerkezete és mértéke (Structure and  
1518 quantification of extension in the Zagyva graben). MSc thesis, 2017. Eötvös University, Dept. General  
1519 and Applied Geology, 123 p.

- 1520 Székely, B., Zámolyi, A., Draganits, E., Briese, C., 2009. Geomorphic expression of neotectonic activity  
1521 in a low relief area in an Airborne Laser Scanning DTM: a case study of the Little Hungarian Plain  
1522 (Pannonian Basin). *Tectonophysics* 474, 353–366.
- 1523 Sztanó, O., Magyar, I., Szónoky, M., Lantos, M., Müller, P., Lenkey, L., Katona, L., Csillag, G., 2013a:  
1524 Tihany Formation in the surroundings of Lake Balaton: Type locality, depositional setting and  
1525 stratigraphy. *Földtani Közlöny* 143, 73–98. (in Hungarian with English abstract)
- 1526 Sztanó, O., Szafián, P., Magyar, I., Horányi, A., Bada, G., Hughes, D.W., Hoyer, D.L., Wallis, R.J.,  
1527 2013b. Aggradation and progradation controlled clinothems and deepwater sand delivery model in the  
1528 Neogene Lake Pannon, Makó Trough, Pannonian Basin, SE Hungary. *Global Planetary Change* 103,  
1529 149–167.
- 1530 Sztanó, O., Kováč, M., Magyar, I., Šujan, M., Fodor, L., Uhrin, A., Rybár, S., csillag, G., Tóké, L.,  
1531 2016. Late Miocene sedimentary record of the Danube/Kisalföld Basin: Interregional correlation of  
1532 depositional systems, stratigraphy and structural evolution. *Geologica Carpathica*, 67, 525–542.  
1533 <https://doi.org/10.1515/geoca-2016-0033>
- 1534 Tari, G., 1992. Late Neogene transpression in the Northern Thrust zone Mecsek Mts. Hungary. *Annales*  
1535 *of the Eötvös University Budapest. Section of Geology* 29, 165–187.
- 1536 Tari, G., Unpublished results. Alpine tectonics of the Pannonian Basin. PhD thesis, 1994. Rice  
1537 University, Houston, Texas, 501 p.
- 1538 Tari, G., 1996. Extreme crustal extension in the Rába River extensional corridor (Austria/Hungary).  
1539 *Mitteil. Ges. Geol. Bergbaust. Österreich* 41, 1–17.
- 1540 Tari, G., Horváth, F., 2010. Eo-Alpine evolution of the Transdanubian Range in the nappe system of the  
1541 Eastern Alps: revival of a 15 years tectonic model. *Földtani Közlöny* 140, 483–510. (in Hungarian with  
1542 English abstract)
- 1543 Tari, G., Horváth, F., Rumpler, J., 1992. Styles of extension in the Pannonian Basin. *Tectonophysics*  
1544 208, 203–219.

- 1545 Tari, G., Dövényi, P., Dunkl, I., Horváth, F., Lenkey, L., Stefanescu, M., Szafián, P., Tóth, T., 1999.  
1546 Lithosphere structure of the Pannonian basin derived from seismic, gravity and geothermal data. In:  
1547 Durand, B., Jolivet, L., Horváth, F., Séranne, M. (Eds.), Geological Society London Special  
1548 Publications, 156, 215–250.
- 1549 ter Borgh, M., Vasiliev, I., Stoica, M., Knezevic, S., Matenco, L., Krijgsman, W., Rundic, Lj., Cloetingh,  
1550 S., 2013. The isolation of the Pannonian basin (Central Paratethys): new constraints from  
1551 magnetostratigraphy and biostratigraphy. *Global Planet. Change* 103, 99–118.  
1552 <http://dx.doi.org/10.1016/j.gloplacha.2012.10.001>
- 1553 Tischler, M., Gröger, H.R., Fügenschuh, B. & Schmid, S.M., 2007. Miocene tectonics of the Maramures  
1554 area (Northern Romania): implications for the Mid-Hungarian fault zone. *Int. J. Earth Sci.* 96, 473–496.
- 1555 Tomljenović, B., Csontos, L., 2001. Neogene-Quaternary structures in the border zone between Alps,  
1556 Dinarides and Pannonian basin (Hrvatsko zagorje and Karlovac basin, Croatia). *International Journal of*  
1557 *Earth Sciences* 90, 560–578. <https://doi.org/10.1007/s005310000176>
- 1558 Tóth, L., Mónus, P., Kiszely, M., Trosits, D., 2020. Magyarországi földrengések évkönyve – 2019  
1559 (Hungarian Earthquake Bulletin – 2019). *GeoRisk*, Budapest, 242 p. DOI:10.7914/SN/HM
- 1560 Tóth, T., Unpublished results. Folyóvízi szeizmikus mérések (Seismic survey on rivers). PhD Thesis,  
1561 2003. Eötvös University, Dept. of Geophysics, Budapest, 141 p.
- 1562 Tóth, T., Horváth, F., 1997. Neotektonikus vizsgálatok nagyfelbontású szeizmikus szelvényezéssel  
1563 (Neotectonic investigations using high-resolution seismic profiling). In: Marosi, S., Meskó, A., (Eds.),  
1564 A paksi atomerőmű földrengésbiztonsága. Akadémiai Kiadó, Budapest, pp. 123–152.
- 1565 Uhrin, A., Magyar, I., Sztanó, O., 2009. Effect of basement deformation on the Pannonian sedimentation  
1566 of the Zala Basin, SW Hungary. *Földtani Közlöny* 139, 273–282. (in Hungarian, with English abstract)
- 1567 Várkonyi, A., Unpublished results. Late Cenozoic deformation and sedimentation based on seismic and  
1568 borehole data in North Somogy (south-western Hungary). MSc thesis, 2012. Eötvös University, Depts.

1569 Regional Geology, Physical and Applied Geology & MTA-ELTE Geological, Geophysical and Space  
1570 Science Research Group, 97 p.

1571 Várkonyi, A., Törő, B., Sztanó, O., Fodor, L., 2013. Late Cenozoic deformation and tectonically  
1572 controlled sedimentation near the Balaton zone (central Pannonian basin, Hungary). In: Occasional  
1573 Papers of the Geological and Geophysical Institute of Hungary, 72–73 (ISSN 2064-0293, ISBN 978-  
1574 963-671-294-5).

1575 Visnovitz, F., Horváth, F., Fekete, N., Spiess, V., 2015. Strike-slip tectonics in the Pannonian Basin  
1576 based on seismic surveys at Lake Balaton. *Int. J. Earth Sci.* 104, 2273–2285.

1577 Wein, Gy., 1961. A szerkezet alakulás mozzanatai és jellegei a Keleti-Mecsekben (Phases and  
1578 characteristics of the structural evolution in the East Mecsek Mts.). *Annales of the Geological Institute  
1579 of Hungary* 49, 759–768.

1580 Wéber, B., 1977. Nagyszerkezeti szelvényvázlat a Ny-Mecsekből (Structural profile across the western  
1581 Mecsek Mts.). *Földtani Közlöny* 107, 27–37.

1582 Williams, S. R. J., 1987. Faulting in abyssal-plain sediments, Great Meteor East, Madeira Abyssal Plain.  
1583 Geological Society, London, Special Publications 31, 87–104. DOI:10.1144/gsl.sp.1987.031.01.08

1584 Windhoffer, G., Bada, G., 2005. Formation and deformation of the Derecske Trough, Pannonian Basin:  
1585 Insights from analog modeling. *Acta Geologica Hungarica* 48, 351–369.

1586 Windhoffer, G., Bada, G., Nieuwland, D., Wórum, G., Horváth, F., Cloetingh, S., 2005. On the  
1587 mechanics of basin formation in the Pannonian basin: inferences from analogue and numerical  
1588 modelling. *Tectonophysics* 410, 389–415.

1589 Wórum, G., Unpublished results. A Mecsek-Villányi térség szerkezete és fejlődéstörténeti eseményei  
1590 szeizmikus szelvények alapján (The structure and evolutionary events of the Mecsek-Villány region  
1591 based on the analysis of seismic profiles). MSc thesis, 1999. Eötvös Univ., Dept. Geophysics. 117 p.

1592 Wórum, G., Hámori, Z. Unpublished results. A BAF kutatás szempontjából releváns a MOL Rt. által  
1593 készített archív szeizmikus szelvények újrafeldolgozása (The reprocessing of the archive seismic

- 1594 profiles of MOL Plc. relevant for the research of the BAF). Research report 2004. Geomega Ltd.  
1595 Budapest, 39 p.
- 1596 Xu, S., Hao, F., Xu, C., Wang, Y., Zou, H., Gong, C., 2015. Differential compaction faults and their  
1597 implications for fluid expulsion in the northern Bozhong Subbasin, Bohai Bay Basin, China. *Marine and*  
1598 *Petroleum Geology* 63, 1–16. DOI:10.1016/j.marpetgeo.2015.02.013
- 1599 Zámolyi, A., Székely, B., Draganits, E., Timár, G., 2010. Neotectonic control on river sinuosity at the  
1600 western margin of the Little Hungarian Plain. *Geomorphology* 122, 231–243.